ORGANIC MATTER BIOGEOCHEMICAL CHARACTERISTICS IN LAKE SUPERIOR: INSIGHTS INTO COMPOSITION, SOURCE AND REACTIVITY

A DISSERTATION

SUBMITTED TO THE FACULTY OF THE

UNIVERSITY OF MINNESOTA

BY

HONGYU LI

IN PARTIAL FULTILMENT OF THE REQUIREMENTS FOR

THE DEGREE OFDOCTOR OF PHILOSOPHY

ADVISOR: ELIZABETH C. MINOR

AUGUST2014

ACKNOWLEDGEMENTS

I would like to thank to my PhD advisor, Professor Elizabeth C Austin-Minor, for her support, patience, accessibility, andencouragement during these past five years. Liz is one of the smartest people I know and is my best role model for a scientist, mentor, and mother. She has given me the guidance and freedomto pursue various projects as my interests develop. Her scientific advice and insightful discussion helped improve this work in every possible way. Her enthusiasm and love for science is contagious and made me want to be as lively, enthusiastic, and energetic as Liz. I also have to thank the members of my PhD committee, Professors Steve Colman, Thomas Johnson,Josef Werne and James Cotner for their scientific advice. They all are brilliant scientists,but friendly, accessible and supportive to my career development. My gratitude goes to other faculty members at the LargeLakes Observatory and UMD including JayAustin, Sergei Katsev, RobertHecky, Erick Brown, Nigel Wattrus and Randall Hick for their best possible education in the science of limnology and oceanography. I thank Sarah Grosshuesch for helping with stable isotope analysis and other instrument-related issues. I also want to thank Yvonne Chan who has been solving every single non-research, otherwise, work-related issues I have had in the past five years. I thank Captain Mike King, JasonAgnich, and the other crew of R/V Blue Heron. I appreciate all the sampling assistancefrom Minor's lab group, especially Prosper Zigah and Bruce Mattson. I am grateful for the support and fun times with myfriends: Jiying, Prosper, Xiuji, Martijn, Betsy, Meg,Messias, Rozhan and Brittany.

I thank Elizabeth B. Kujawinski, Melissa C. Kido Soule and KristaLongnecker at the WHOI FT-MS facility for FT-ICR-MS analyses. The research was supported by NSF GrantOCE-0825600 (to E. C. M). Appreciation also goes to University of Minnesota Water Resources Science graduate program and Swenson College of Science and Engineering for their travel funds which allowed me topresent my research to a wide

audience in national and international meetings. I thank the Department ofChemistry and Biochemistry, University of Minnesota Duluth for awarding me teachingassistantship positions.

A special thanks to my family, words cannot express how grateful I am to my mother-in-law, father-in-law, my mother, and father for all of the sacrifices that they've made on my behalf. I would also like to thank to my beloved husband, Gai Geng for supporting me, for everything. I can't thank you enough for encouraging me throughout this experience. To my beloved daughter Emily X. Geng, for being such a good girl, always cheering me up.

Dedication

I dedicate this thesis to

my family, my husband, Gai, and my beloved daughter XiXi

for their constant support and love.

I love you all dearly.

Abstract

Organic matter (OM) composition and its relationship with OM source and dynamics in Lake Superior were investigated with the combination of advanced spectroscopic techniques and multiple-geochemical signatures. Studies of water-column dissolved, water-column particulate, and sedimentary organic matter (DOM, POM, and SOM, respectively) were performed. The composition of DOM obtained with two different solid phase extraction resins (C18 vs SDB-XC) was investigated using Uv-visible spectrometry and negative-ion electrospray Fourier transform ion cyclotron resonance mass spectrometry (ESI FT-ICR MS). Lake Superior raw offshore water was found to be very clear; its DOM is low in aromaticity, with primarily non-humic, hydrophilic and low molecular weight materials. Radiocarbon signatures reveal the primarily modern (post-bomb) nature of Lake Superior DOM. With such Lake Superior water, we found SDB-XC disks to outperform C18 disks in the isolation of DOC in terms of both higher recovery and less degree of fractionation to the initial DOM composition. Extracts of the same samples obtained with the different extraction disks share 70% of compounds, which were dominated by lignin-CRAM-like material but also include a variety of other functional groups including lipids, proteins, carbohydrates and condensed hydrocarbon. To assess settling particulate organic matter seasonality and availability to the benthic community, settling particulate matter was studied in terms of mass fluxes and main biochemical characteristics and composition at two Lake Superior offshore sites over the course of a year. Increase in sinking flux was variably associated with sediment resuspension and enhanced surface production. The combination of PCHO-C%, THAA and Fourier transform infrared spectroscopy (FTIR) data revealed that the relative bioavailability and nutritional values of POM to benthic microbes should be lower in spring than summer, although both periods exhibited high sinking fluxes. Isotopic and elemental analyses, FTIR, principal components analysis (PCA), and two dimensional (2D) correlation analysis, where core depth was used as perturbation, were used to study the diagenesis of organic

matter (OM) in Lake Superior sediments. Depth-related changes among sites were found to be similar, leading to an increased contribution from inorganic (and possibly refractory aromatic organic) components at each site, and a loss of contribution from other organic components. Synchronous spectra reveal that aliphatic esters and carbohydrates degrade significantly with increasing depth, leading to an increased contribution from clays/ biogenic silica/ inactive carbohydrates. Asynchronous spectra show that, generally, carboxyl groups, including aliphatic ester and amide/protein, degrade first, followed by a group of carbohydrates, and then aromatic compounds and/ or the Si-O framework in clays and biogenic silica.

Table of Contents

ACKNOWLEDGEMENTS i

Dedication iii

Abstract iv

List of Tables ix

List of Figures x

Chapter 1 Introduction 1

1.1 Dissolved organic matter (DOM) in aquatic system: sources and composition 1

1.2 Particulate organic matter (POM) in aquatic systems: sources and seasonal variation 5

1.3 Sedimentary organic matter and its diagenetic changes 7

1.4 Stable Carbon Isotopes and ^{14}C Age of Organic Matter: to trace source and time 9

1.5 Spectroscopic Techniques: FTIR and FT-ICR-MS 12

1.6 The Study System: Lake Superior 15

1.7 Objectives and organization of this dissertation 17

Chapter 2 Dissolved Organic Matter in Lake Superior: Insights into the effects of extraction methods on chemical composition 19

Summary ..... **Ошибка! Закладка не определена.**

2.1. Introduction 20

2.2 Material and Methods 24

2.2.1 Sites and Sampling 24

2.2.2 DOC analysis 25

2.2.3 UV/Visible spectroscopic analysis 26

2.2.4 Isotopic Analyses on Bulk DOM 27

2.2.5 FT-ICR-MS analysis 28

2.2.6 Cluster Analysis and Principle Component Analysis (PCA) 28

2.3. Results and Discussion 29

2.3.1. TOC analysis, stable ($\delta^{13}C$) and radiocarbon ($\Delta^{14}C$) signatures of 'init' DOM 29

2.3.2 Disk Performance Comparison Based on TOC analysis and UV/Visible Spectrometry 30

2.3.3. FT-ICR-MS Analysis 33

2.3.4 Comparison of the FT-ICR-MS spectral features (elemental ratios, DBE, etc) 36

2.3.5 Comparison of the FT-ICR-MS with Multivariate analysis 39

2.4. Conclusions 40

Chapter 3 Biochemical characteristics of settling particulate organic matter in Lake Superior: a seasonal comparison 49

Summary ..... **Ошибка! Закладка не определена.**

3.1. Introduction 50

3.2 Material and methods 52

3.2.1 Study site and sampling details 52

3.2.2 Elemental and isotopic analysis 53

3.2.3 FTIR spectra Measurement and Pre-processing 54

3.2.4 MBTH Total Carbohydrates Analysis 54

3.2.5 Total Amino Acid Analysis: OPA/MPA Derivitization 55

3.3 Results and discussion 58

3.3.1 Mass fluxes, organic carbon fluxes and stable carbon isotope analysis 58

3.3.2. Carbohydrate and Amino acid distributions 61

3.3.3 Compositional variation of POM as seen by FTIR 63

3.3.3.1. Infrared absorbance of POM and its 2nd derivative spectra 63

3.3.3.2 Seasonal variations of settling POM based on PCA and FTIR 66

3.4. CONCLUSIONS 68

Chapter 4 Diagenetic changes in Lake Superior sediments as seen by FTIR and 2D correlation spectroscopy 79

Summary ..... **Ошибка! Закладка не определена.**

4.1 Introduction 79

4.2 Materials and methods 81

4.2.1 Study site and sampling 81

4.2.2 Elemental and isotopic analysis 82

4.2.3 FTIR spectral measurement and pre-processing 83

4.2.4 2D correlation and PCA 83

4.3 Results and discussion 84

4.3.1 Elemental and isotopic analysis of Lake Superior sediments 84

4.3.2 Insights into sediment OM composition based on 1D FTIR spectroscopy and 2nd derivative spectra 85

4.3.3 PCA of the FTIR data 86

4.3.4 Diagenetic changes with depth as revealed by 2D correlation FTIR 88

4.3.4.1 2D FTIR synchronous map 88

4.3.4.2. 2D FTIR asynchronous map 94

4.4 Conclusions 98

Chapter 5: Summary of conclusions and future work 110

REFERENCES 115

Appendix 144

List of Tables

Table 2-1, Sampling information, DOC concentration, stable carbon ($\delta^{13}C$) and radiocarbon signatures of 'init' DOM, CDOM and DOC recoveries (% CDOM and % DOC of 'eR' to 'init' samples) and UV-Visible spectrophotometry indices for 'init' and 'eR' samples of both C18 and SDB-XC extractions.----------42

Table 2-2, Elemental data from formula assignments. The subscript w indicates magnitude-averaged values; the subscript n indicates number-averaged values as described in Minor et al. 2012.----------43

Table 3-1, Organic carbon percentage (OC%), organic nitrogen percentage (ON%), molar carbon/nitrogen ratio (C/N ratio), concentration of THAA, THAA-C percentage, THAA-N percentage, and Mol% composition of the 17 THAAs in the selected 10 sediment trap samples covering both sites (EM vs WM) and seasons (winter vs summer). The sampling date listed is the middle day of the entire 11-12 days for each collection of the sample.---------- ----70

Table 4-1, $\Delta^{14}C$ and corresponding age (in radiocarbon years) of sedimentary particulate matter with porewater removed by centrifuging before freeze-drying. Precisions are based on error of standards or multiple analyses.---------- 100

Table 4-2, Bands used for compound identification of Lake Superior sediment samples (surface layer) with FTIR 2nd derivative spectra. ----------101

Table 4-3, Compound class correlation relationship (varying with depth) as indicated by 2D synchronous FTIR cross-peaks.----------102

List of Figures

Fig. 2-1, Lake Superior. Stars indicate open-lake stations and circles indicate near-shore stations.---------- 44

Fig. 2-2. Protocol used for sampling and extraction, including naming conventions followed in the text.----------44

Fig. 2-3, Principle component analysis results based on A) normalized absorption coefficients from 200 to 800cm^{-1}; B) spectrophotometry indices including E2/E3, SUVA254 and spectral slope of all samples. Black filled squares represent <GFF 'init' samples; gray filled circles represent SDB-XC SPE DOM samples; triangles represent C18 SPE DOM samples.---------- 45

Fig. 2-4, Negative ion mode FTICRMS of a) WM surface SDB-XC SPE DOM with the enlargement of m/z 310 to 313 on the right, b) WM surface SDB-C18 SPE DOM with the enlargement of m/z 310 to 313 on the right.---------- 46

Fig. 2-5, Van Krevelen diagram of a) formulae (m/z) found in both C18 and SDB-XC SPE DOM for surface sample at BR site; b) formulae (m/z) found in both C18 and SDB-XC SPE DOM for surface sample at WM site; c) unique compounds from SDB-XC SPE DOM at BR; d) unique compounds from SDB-XC SPE DOM at WM; e) unique compounds from C18 SPE DOM at BR; f) unique compounds from C18 SPE DOM at WM; CHO and CH compounds (black) are overlaid with CHON (blue) compounds on top of which any CHONP compounds (cyan) are placed. Any CHOP compounds (red) are on the top. The van Krevelen spaces are divided into seven discrete regions, modified from the diagrams proposed by Hockaday et al. 2009, Kim 2003; Sleighter and Hatcher 2007. The percentage of peaks from each region over total number of peaks in the sample is shown in brackets.---------- 47

Fig. 2-6, Comparison of C18 SPE DOM and XC SPE DOM based on peak absence/presence of FT-ICR-MS. A) Cluster diagram of the samples based on original Bray-Curtis distance. The samples with lower information content (lower x-values) are more similar than those which occur farther apart; B) Principle component analysis results. ---------- 48

Fig. 3-1, Lake Superior. Stars indicate sampling sites. ---------- 71

Fig. 3-2, Seasonality of A) total particulate mass fluxes and B) POC mass fluxes in the fall 2009- spring 2010 period in Lake Superior. 3-4 continuous summer trap samples (after June 17th 2010) were averaged to obtain the same resolution as winter trap samples (10-11 days). Black dashed lines indicate onset of fall mixing event (12-10-09) and summer stratification (06-10-10) based upon thermistor data from the EM mooring.---------- 72

Fig. 3-3, Seasonality of A) Carbon contents in total settling material; B) Stable carbon isotope values; C) Nitrogen contents in total settling material; D) Stable nitrogen isotope values; E) molar ratio of carbon vs nitrogen. 3 to 4 continuous summer trap samples, which represent settling POM of 3-4 days, were mixed and measured as one sample to match the sampling durations at other seasons. Black dashed lines indicate onsite of spring mixing event (12-10-09) and summer stratification (06-10-10).----- 73

Fig 3-4, A, Seasonal variation of carbohydrate carbon percent in total POC; B, PCHO flux in the fall 2009- spring 2010 period in Lake Superior. Every 3-4 continuous summer trap samples, which represent settling POM of 3-4 days, were mixed and measured as one sample. Black dashed lines indicates onsite of spring mixing event (12-10-09) and summer stratification (06-10-10).---------- 74

Fig. 3-5, Concentration of THAA, THAA-C percentage, THAA-N percentage of the 5 selected samples from both A) EM and B) WM. Black dashed lines indicates onsite of

spring mixing event (12-10-09) and summer stratification (06-10-10).---------- 75

Fig 3-6, PCA projection based on Mol % composition of the 17 THAAs in the selected 10 sediment trap samples. EM samples are shown with filled black squares and WM samples are shown with filled dark gray stars. The sampling dates are indicated in the figure, and represent the middle day of the entire 11-12 days for each collection of the sample. The data matrixes were z-scored and variance scaled before the PCA analysis was performed.---------- 75

Fig. 3-7, 1D FTIR spectra of all settling particulate matter samples collected at different time of the year at A) EM site, B) WM site. The colors indicate different samples. Each spectrum was normalized via total area before comparison to reduce variation from sample loading/processing.---------- 76

Fig. 3-8, The FTIR spectrum and its 2nd derivative for sinking particulate samples from A. winter (Jan 10th to 21th, 2010) and B. summer (Aug 10th to 15th, 2010) at WM.---------- 77

Fig 3-9, PCA projection of normalized FTIR data for A) EM, B) WM.---------- 77

Fig. 3-10, Seasonality of POM compound class distributions in Lake Superior at EM (gray) and WM (black) sites based on normalized absorbance intensity (to total sample absorbance) changes at wavelengths of A) 1651cm^{-1} representing Amide I C=O stretching, B) 1540 cm^{-1} representing Amide II C=O stretching, C) 3410 cm^{-1} representing O-H stretching of carboxylic acid and carbohydrate, D) 1736cm^{-1} representing aliphatic ester C=O stretching, E) 1097 cm^{-1} representing overlap of carbohydrate, biogenic silica/silicate minerals, F), 1005 cm^{-1} representing overlap of carbohydrate, biogenic silica/silicate minerals. Each spectrum was normalized via total area before comparison to reduce variation from sample loading/processing.

Black dashed lines indicate onsite of the spring mixing event (12-10-09) and summer stratification (06-10-10).---------- 78

Fig. 4-1, Map of Lake Superior. Sampling sites (CM, EM, NM, SM and WM) are shown with stars. Sedimentation rates from previous studies are included for reference: Down triangles were obtained with the ^{210}Pb method and are from Evans (1981); up triangles are from Kemp et al. (1978) using the pollen method; circles are from Bruland et al. (1975) and were obtained from ^{210}Pb and pollen methods.---------- 103

Fig. 4-2, Elemental and isotopic analysis results from Lake Superior sediments, showing down core trends in a) C% (wt./wt.), b) N% (wt./wt.), c) δ^{13}C and d) atomic C/N ratio. ---------- 104

Fig. 4-3, 1D FTIR spectra of sediments at different depths at a) CM and b) WM stations. Each spectrum was normalized via total area as described in text before comparison to reduce variations from sample loading/processing. ---------- 105

Fig. 4-4, 1D FTIR spectrum and 2nd derivative for the top 2cm of the a) bulk sediment and b) combusted sediment samples at the CM station. The combustion condition of 400℃, 8 hours as suggested by Ball, 1964; Ben-Dor and Banin, 1989 was applied to minimize the loss of structural water and ensure the complete removal of OC. ----- 106

Fig. 4-5, PCA projection (a) and corresponding PC1 loading plot (b) for normalized FTIR data. For Fig. 5a, samples are named as the first station letter (see Table 4-1) plus a number indicating depth within the sediment core: 1, 0-2 cm; 2, 2-4 cm; 3, 4-6 cm; 4, 6-8 cm; 5, 8-10 cm. Deepest layers are shown with bold italic font and underlining. ---------- 107

Fig. 4-6, Synchronous 2D correlation spectrum down-core for CM station. The

spectral data set was constructed sorting from the shallowest depth to the deepest. The data set was normalized and PCA reconstructed before 2D correlation analysis (see text for further details). For ease of identification of peaks the slice through auto-peak diagonal is plotted to the right of each 2D correlation spectrum. White indicates positive correlation; black indicates negative correlation.---------- 108

Fig. 4-7, Asynchronous 2D correlation spectrum for a) CM and b) WM. Each spectral data set was constructed sorting from the shallowest depth to the deepest. The data set was normalized and PCA reconstructed before 2D correlation analysis. For ease in identification of peaks, horizontal slices (y is constant) across the region of interest are plotted below each 2D correlation spectrum.---------- 109

Chapter 1 Introduction

Organic matter in aquatic environments is a major reactive reservoir of Earth's carbon cycle (Hedges et al, 1997). It is derived from *in situ* primary production (autochthonous) by phytoplankton, microphytobenthos and chemoautotrophs, or allochthonous sources including riverine input, terrestrial plant debris and anthropogenic runoff (Hedges et al, 1997). The relative importance of these sources varies, and is related to surface area, size of drainage basin and nutrient availability within the system. For lakes, the influence on OM composition from terrestrial OM could be much more significant because of the relative large drainage basin area/ surface area ratio in lakes as compared to the ocean. Lake Superior has a low drainage basin area/surface area ratio relative to most lakes, but high compared to oceans, and so is an intermediate case. Higher terrestrial OM inputs allow aquatic systems to be net heterotrophic (Urban et al., 2005; Kritzberg et al., 2005); and the amount of non-autochthonous carbon incorporated into zooplankton biomass has been shown to be correlate to basin area/surface area ratios (Zigah et al., 2012). OM occurs as a continuum of particulate organic matter (POM), colloidal material and dissolved organic matter (DOM) in aquatic systems. Post-production alteration and remineralization occurs to OM, especially affecting POM during its transit from the surface to deep ocean/lake; only a small fraction of POM is able to evade remineralization and get sequestered in the sediments (Burdige, 2007). Although organic matter is present in low concentrations in sediments (usually lower than 1% in the ocean), sequestration of organic matter in sediments is an important control on atmospheric carbon dioxide (CO_2) levels (Burdige, 2007).

1.1 Dissolved organic matter (DOM) in aquatic system: sources and composition

DOM in aquatic systems is operationally defined as materials passing through a filter (previously 0.7 or 0.45 μm, more commonly today a 0.1 or 0.2 μm filter). It is the major form of OM in most aquatic environments, especially in oligotrophic

ecosystems such as oceans and large lakes, where the contribution of suspended particles is low (Benner, 2002; Davis and Benner. 2005; Zigah et al 2012). DOM can originate from a number of autochthonous as well as allochthonous sources (Duce and Duursma, 1977; Whittle, 1977). The autochthonous sources are associated with processes such as excretion of aquatic organisms, autolysis of dead organisms and microbial decomposition. Allochthonous DOM includes organic compounds from the land, rivers and marshes as well as atmospheric deposition of DOM to surface waters. Indications exist that a fraction of riverine DOM is removed by flocculation, precipitation and adsorption to particles and then deposited close to shore (Gearing et al., 1977; Hedges and Mann, 1979), thus reducing the impact of riverine OM to the ocean carbon cycle. On the other hand, studies have shown that terrestrial DOM can behave more conservatively (e.g. Mantoura and Woodward, 1983), suggesting a more significant contribution of riverine OM to oceanic OM than is often assumed.

DOM can influence natural aquatic systems by: 1) fueling the microbial loop and supporting heterotrophic activity (Williams 2000); 2) affecting the penetration of light and exchange of heat at the sea/lake surface (Blough and Del Vecchio, 2002); 3) maintaining pH through organic acid buffering; 4) affecting the redox chemistry of trace metals; and 5) acting as a strong ligand for many elements (Warnken et al., 2007). DOM also occurs as one of the earth's largest active C pools, thus even minor changes in DOM reservoir size and dynamics can potentially impact many aspects of the biogeochemical cycles of aquatic systems and the global C cycle. Thus, further detailed understanding of DOM composition, fate, and reaction mechanisms in aquatic systems is needed to build upon our improved understanding of the origin, function, and cycling of aquatic DOM acquired in recent decades (Benner, 2002).

DOM chemistry and composition is poorly understood, in part, because it has been difficult to isolate in an unbiased manner sufficient amounts of representative material for analysis. The very low concentration of organic matter (~1 to 2 mg C/l) in the

oceans and oligotrophic lakes (Carlson et al., 1994; Wetzel, 2001; Raimbault et al., 2008) challenges most analytical techniques, especially for marine systems which contain large amounts of inorganic salts. Through isolation of DOM, highly concentrated organic samples with low salt content can be obtained, and different analytical techniques can then be performed on these concentrates. Such isolation approaches fall into three main categories: solid phase extraction (SPE), ultrafiltration, and reverse osmosis and reverse osmosis/electrodialysis (RO/ED). The SPE approach for the isolation of DOM using one or a combination of XAD resins was established in the late 1970s and has been applied to many studies as the classic extraction approach (e.g., Dittmar et al. 2001). Very different recoveries were obtained for different aquatic systems, e.g., a total recovery of 16-21% for sea water (Druffel et al. 1992) and 50 to 80% recoveries for "colored water" with high contents of humic substances (Thurman and Malcolm 1981). This is possibly due to a selective isolation of different fractions of DOM with these resins. Recently, much DOM isolation has employed other resins such as C18 (hydrocarbon chains bonded to a silica structure, Sleighter and Hatcher, 2008) and PPL resins (modified styrene divinyl benzene polymer, Dittmar et al. 2008). C18 resins are made of a silica matrix bonded to octadecyl (C18) functional groups, which act as sites for non-polar interactions. A comparison of SPE sorbents in cartridge form by Dittmar et al. (2008) found that C18 resins (with 39 ± 4% recovery) were the most efficient silica-based sorbent, and PPL resin which is based upon styrene divinyl benzene polymers produced the highest DOM recoveries of up to 62% ± 6% recovery. In addition, all SPE resins were found to selectively isolate certain fractions of compounds in DOM, particularly humic substances with high aromacity (Dittmar et al., 2008). The SPE approach also has other problems such as the time required to process larger-volume samples and the possibility of chemical changes to the nature of DOM due to pH alteration during extraction. Ultrafiltration, which isolates DOM fractions based on molecular size (primarily with a 1-kDa membrane), is another widely recognized method for the extraction of DOM (ultrafiltered DOM, or UDOM), and the one most favored by

isotope geochemists. It isolates up to 30% of marine DOM (e.g., Benner et al. 1997) and larger percentages of the initial DOC in colored waters, such as most lakes and rivers, which have larger terrestrial impact and higher average molecular weight DOM (e.g., Stephens and Minor 2010). The combination of reverse osmosis and electrodialysis allows isolation of much larger fractions of aquatic DOM as compared to other techniques, with DOC recovery ranging 60% to 95% (Vetter et al. 2007, Koprivnjak et al., 2009). However, the RO/ED technique requires access to expensive equipment that can be prohibitive in many cases especially in the field, and due to large membrane surface areas, may contribute significantly to organic carbon blanks.

Advanced spectroscopic techniques together with molecular analyses and degradative techniques have been employed to identify the composition of DOM in raw water and concentrates. Measurements of DOC, C:N ratios, bulk stable and radiocarbon and N isotopic compositions, colored DOM, and fluorescent DOM provide different ways to evaluate the bulk properties of each DOM sample. Degradative and extractive techniques combined with analyses of the resulting material have been applied to detect and quantify specific carbohydrates, lignins, amino acids, sugars, proteins, nucleic acids, lipids and other biomolecules in DOM in many aquatic systems, but these compounds only account for a small fraction of dissolved organic carbon (DOC) (<11% of oceanic DOC, Benner, 2002). With the aid of high resolution spectroscopic techniques, some more complex groups of compounds have been identified. Heteropolysaccharides (HPS) have been found to be the major constituents of marine ultrafiltered DOM (UDOM) (Benner et al., 1992; Aluwihare et al., 1997). HPS are believed to be a rapidly cycling component of DOM in the upper ocean. In 2006, Hertkorn et al characterized refractory carboxyl-rich alicyclic molecules (CRAM) in marine DOM with nuclear magnetic resonance spectroscopy and ultrahigh resolution mass spectrometry. CRAM is found throughout the water column and is the most abundant component of deep ocean DOM ever characterized. CRAM is comprised of a complex mixture of carboxylated and fused alicyclic structures with a

carboxyl-C:aliphatic-C ratio of 1:2 to 1:7.

1.2 Particulate organic matter (POM) in aquatic systems: sources and seasonal variation

POM in aquatic ecosystems, operationally defined as materials retained on a 0.7 or 0.45 μm (or, more recently, a 0.1 or 0.2 μm) filter, also plays significant roles in the global carbon cycle through biological, chemical and physical pathways. POM is also heterogeneous, consisting of living and dead cells, fecal pellets, aggregates, organically coated mineral grains, marine snow and other materials, all of which could originate from autochthonous primary production and terrestrial input (Minor and Nallathamby, 2004). Autotrophic phytoplankton and bacteria as well as metazoan heterotrophic organisms in aquatic ecosystems are included within the POM pool. In oceanic environments and many oligotrophic lakes, POM is mostly derived from phytoplankton (Deuser et al., 1981). Conversely, POM in the coastal and shelf waters is influenced by the inputs of terrestrial organic matter discharged by rivers and re-suspension of bottom sediments (Degens and Ittekkot, 1985).

POM serves as an important source of food for heterotrophic organisms and transports organic matter produced in the euphotic zone to the sediments. During its transport, POM undergoes extensive biogeochemical changes including uptake by biota, remineralization, and exchange with DOM. The portion that survives water column transport and travel through the surface sediments (another degradation hotspot) is buried in the sediments, thereby influencing the cycles of global carbon, nutrients, trace metals as well as anthropogenic pollutants (Eppley and Peterson, 1979, Sholkovitz and Copland, 1981, Baker and Eisenreich, 1989; Baker et al., 1991). Marine and lacustrine sediment-trap studies show that only 1 to 35% of the organic carbon synthesized in the photic zone reaches the sediment surface, mainly varying with water-column depth, trophic state of the system and seasonality (Charlton and Lean, 1987; Eadie et al., 1984; Bloesch and Uehlinger, 1990; Hernes et al., 2001).

POM rain rates decrease with depth in the water column due to remineralization (Wakeham et al., 1997; Hedges at al., 2000), while the molecularly uncharacterized component (MUC), mainly in the nonliving POM pool, is found to constitute an increasing proportion of POM with increasing water column depth. Evidence suggests that the major components of the nonliving POM pool could be remnants of biomacromolecules (see review by Hedges *et al*., 2000). Detrital POM is thought to consist of biomacromolecules that survived short time-scale remineralization and it is the first step in the sequential flow of organic matter originally from organisms to POM in water column and eventually to sediment. According to this point of view, molecular-level characterization of detrital POM as well as its variation is necessary not only for investigating the source and dynamics of POM but also for a better understanding of degradation and selective preservation of the macromolecules in POM as well as the mechanistic processes behind these. On the other hand, because the refractory fraction of settling POM cannot easily be utilized by benthic invertebrates (Plante & Jumars, 1992; Plante & Shriver, 1998; Grey and Jones, 2001; Davis and Benner, 2005), the study of temporal and spatial changes in labile portions, i.e., potential food items (such as protein, lipids) in POM is also a key step in understanding the dynamics of benthic communities.

Detailed characterization of POM is important but difficult as a result of POM being heterogeneous (Ostrom et al. 1998; Minor and Nallathamby, 2004). Different POM components may have different temporal and spatial variations in chemical composition, as well as different cycling times and ultimate fates in aquatic ecosystems.There have been some studies on identification and characterization of living cells vs. nonliving POM (or detritus) to explore the composition and fate of these materials (Minor and Nallathamby, 2004). Detailed chemical characterizations of detritus within natural POM have been performed using flow cytometry in conjunction with fluorochrome staining to identify the presence of particular compounds (Moreira-Turcq and Martin, 1998; Kerner et al., 2003). Flow cytometric

sorting coupled with analysis by mass spectromety (Minor et al 1999; Minor and Nallathamby, 2004) has also been found to be a promising method for looking at detrital vs living POM. All of the above methods require separation of living and detritial POM for variation studies, which is time consuming, and a major problem of these methods is the ambiguity of defining 'detrital'. Thus, in term of POM characterization, this study characterizes bulk POM as a function of temporal and spatial variations with Fourier transform infrared spectrometry (FT-IR), which is a simple and non-destructive technique, as discussed in section 1.4 and Chapter 3.

1.3 Sedimentary organic matter and its diagenetic changes

Organic matter is a quantitatively minor but highly dynamic and important fraction of ocean and lake sediments, especially at the surface layers. It is comprised of variable amounts of identifiable biomolecules such as carbohydrates, proteins, and lipids (Kemp and Johnston, 1979; Lewis et al, 1993; Repeta et al, 2002) and other biochemicals originally from the tissues of living benthic micro-organisms and the detritus of organisms formerly living in the ocean/lake and its watershed (Mannino and Harvey 2000a,b; Repeta et al, 2002) which have survived decomposition in the water column (Meyers and Eadie, 1993). Organic matter deposited at the sea-floor and lake bottom is usually subject to additional (often rapid) diagenetic changes with increasing depth within the sediments, leading to burial of only an estimated <0.5% of the global net marine primary production (e.g., Berner, 1989; Henrichs 1992; Hedges et al. 1992; Meyers et al. 1995; Burdige 2007). Understanding the composition of OM, as well as its changes during diagenesis, is important because the organic matter in lake sediments participates in a variety of biogeochemical processes. First of all, organic matter diagenesis in sediment is an important part of local and global C cycles (Cole et al. 1994; Cotner et al. 2004; Urban et al. 2005); what is buried long-term in the sediments or is altered to increase OM's refractory nature and thus promote carbon burial is sequestered OM, which is removed from active exchange with atmospheric carbon dioxide. Second, organic matter is the most important food source

of benthic animals and microbes. Dissolved oxygen concentrations are usually lowered when organic matter is degraded by aerobic bacteria, and anoxic or hypoxic conditions may develop under stratified conditions (Pedersen & Ishiwatari, 1990). So, the amount of oxidizable organic matter below the sediment/water interface can act as a control on dissolved oxygen concentrations in sediment pore water and sometimes overlying water as well. The presence or absence of anoxia affects not only C but also the biogeochemical cycles of N, P, S, Si and some trace metals (e.g., Fe) in aquatic systems and their underlying sediments (Meyers and Ishiwatari, 1993; Thunell et al. 2004; Gälman et al 2008) through shifts in both chemical and biologically mediated redox reactions (Putschew et al. 1996; Burdige, 2007). Last but not least, organic matter also forms part of the paleolimnologic and paleoceanographic record preserved in lake and ocean sediments and is used for interpreting past changes in biogeochemical cycles, ocean circulation and climate. Thus, identifying the compositional alteration of organic matter in sediments is fundamental to the understanding of the sources and cycling of OM, global C, N, P and S cycles and to the discovery and application of paleo-proxies (Meyers and Ishiwatari, 1993; Herbert, 2001; Talbot and Laerdal 2001; Lehmann, et al. 2002).

Down core diagenetic alteration of some important paleo-proxies including stable carbon isotopic, stable nitrogen isotopic and C /N ratios of organic matter, and the concentration of humic substances and some important lipid biomarkers in the Great Lakes sediments have been studied (see review by Meyers and Ishiwatari, 1993). Also, in 1979, Kemp and Johnston used wet-chemistry analysis to investigate diagenesis of some extractable organic matter in the sediments of Lake Ontario, Erie, and Huron. They found out that trophic state and water depth were the two most important controls on the degree of diagenesis of modern sedimentary organic matter; and that the decomposition rates of sedimentary organic matter are in the following order: amino acids>>amino sugars>carbohydrates>humic compounds>lipids. Although there have been studies of the individual paleo-proxies or some extractable fractions like

amino acids, amino sugars and carbohydrates, little is known about the composition and transformation of the high molecular weight entities: the proteins, the polysaccharides, the lipids and the humic compounds. Investigations are required to determine the diagenetic variation and reactivity of different functional groups including those within the portion of OM that is less extractable.

1.4 Stable Carbon Isotopes and ^{14}C Age of Organic Matter: to trace source and time

OM from different sources could have significantly different composition and dynamics, thus playing significantly different roles in biogeochemical cycles. For most aquatic systems whose OMflux and transformation pathways are difficult to constrain, identification of the source and age of organic matter and how it changes through time can be especially important when characterizing OM. Natural abundance stable isotopes have proven useful for identifying sources andbiogeochemical processes occurring in aquatic environments (Hedges et al. 1988). Stable isotope ratios are commonly reported using delta notation (δ). This notation compares the ratio of the heavier isotope to the lighter isotope in a sample to that of a standard. Because the variations are small, we multiply by 1000 and the resulting delta value is therefore in permil (‰). Delta values are defined as follows:

$$\delta = \left(\frac{R_{sample}}{R_{standard}} - 1 \right) \times 1000$$

equation (1.1)

Isotope fractionations occur during biogeochemical processes such as nutrient and CO_2 assimilation, nitrification and nitrate reduction. These fractionations can be very different within different environments, thus impacting the average carbon and nitrogen isotope ratios. Two major carbon isotopic groups of plants depending on their photosynthetic pathways are: C4 plants, using the C4 or Hatch-Slack photosynthetic

pathway, and C3 plants, using the C3 or Calvin photosynthetic pathway (Deines 1980; Farquhar et al. 1989). As a result of different isotopic fractionation of different photosynthesis pathways, C4 plants have $\delta^{13}C$ values between −9 to −17‰, average at –13‰, whereas C3 plants have $\delta^{13}C$ values ranging from −23 to −34‰, average at −27‰ (Deines 1980). The $\delta^{13}C$ of consumers closely resembles that of their diet, typically within +0.5‰ (Vander Zanden and Rasmussen 2001). Thus, the stable carbon isotope ratio ($\delta^{13}C$) of bulk OM samples is dependent primarily on the proportions of OM inputs from aquatic and terrestrial sources (e.g., Sweeney and Kaplan, 1980; Voß and Struck, 1997), and can be very useful tracers of organic substances in systems where potential sources have distinct isotopic signatures.

The nitrogen isotope ratio ($\delta^{15}N$) is affected by N sources, and by nitrogen transformation pathways.. For example, biological N_2 fixation introduces ^{15}N-depleted nitrogen to OM from atmospheric N_2 (Saino and Hattori, 1980), while denitrification increases the $\delta^{15}N$ of remaining nitrate by preferential reduction of the ^{15}N-depleted nitrate to N_2 or N_2O (e.g., Cline and Kaplan, 1975). For nitrogen isotopes, consumers are enriched, on average, +3.4‰ compared to their prey (Vander Zanden and Rasmussen 2001), thus $\delta^{15}N$ has been effectively used in research to evaluate trophic levels and food web structures in ecosystems. The combination of $\delta^{13}C$ and $\delta^{15}N$ values has been widely used to determine sources and cycling of OM in oceans/lakes (e.g., Farquhar et al. (1989); Murphy et al. (1989); Aravena and Wassenaar, 1993). However because of the small dynamic rangeof OM $\delta^{13}C$ and $\delta^{15}N$ values (Dittmar et al., 2001; Gonneea et al., 2004; Wakeham et al. 2006), and theconsiderable overlapping of $\delta^{13}C$ values from multiple OM sources in many lake and river systems, its use for inferringOM sources can be difficult.

OM in aquatic systems, due to its complex nature, consists of a labile fraction with a high turnover rate and a refractory aged fraction. The labile fraction is a possible source of nutrition for the microbial loop (Kirchman et al., 1991). The turnover rate of

marine DOC is highly variable. It varies from less than a day up to more than 1000 years. Natural abundance radiocarbon($\Delta^{14}C$, with a half life of 5730 years) can be used to distinguish relatively labile and refractory OM (on decadal to millennial timescales) in aquatic systems, and is defined as following:

$$\Delta^{14}C=[Fm\times e^{\lambda(1950-Yc)}-1]\times 1000 \qquad \text{equation (1.2)}$$

$$Fm=\left[\frac{\left[\frac{^{14}C}{^{12}C}\right]_{sample,-25}}{0.95\left[\frac{^{14}C}{^{12}C}\right]_{OX1,-19}}\right] \qquad \text{equation (1.3)}$$

Where lambda is 1/(true mean-life) of radiocarbon = 1/8267 = 0.00012097 and Y_c is year of collection. Fraction Modern (Fm) is a measurement of deviation of the $^{14}C/^{12}C$ ratio of a sample from "Modern." Modern is defined as 95% of the radiocarbon activity (in AD 1950) of NBS Oxalic Acid I normalized to $\delta^{13}C_{VPDB}$=-19 per mil.

Using radiocarbon data, Williams and Druffel (1987) calculated that in the central North Pacific Ocean upper mixed layer water, 56% of the DOC was less than 30 years old, and the remaining 44% was older than 6000 years. The mean average age of oceanic dissolved organic carbon (DOC) is over 1000 years (Kirchman et al., 1991).Thus the refractory fraction probably consists mainly of selectively preserved constituents in the water column. In terms of DOM and POM from rivers and lakes, radiocarbon (^{14}C) studies indicate that DOM and POM in rivers and estuaries range from modern to thousands of years in age also (Masiello and Druffel 2001; Raymond and Bauer 2001, Loh et al. 2006). However, the short cycling time of a portion of riverine OM may result in even older, more refractory forms of organic matter in

some rivers and estuaries and ultimately being exported to the coastal ocean or large lakes. From this point of view, the natural abundance radiocarbon($\Delta^{14}C$) signature (ranging from -1000 to ~+200‰), which describes the average radiocarbon age of OM samples, can also act as a robustsource proxy besides indicating the relative maturity of a sample (Petsch et al. 2001; McCallisteret al. 2004; Wakeham et al. 2006). Combining such data with other source proxies such as the biomolecular, elemental and chemicalcompositions of OM, biogeochemists have been able to successfully identify and constrain sources of organic matter and biogeochemical processes occurring in aquatic environments (e.g. Hedges et al. 1986; Williams et al. 1992; Druffel et al. 1992). In this study, the combination of compositional differences of OM with radiocarbon ages, stable carbon and nitrogen signatures, will be used to infer source differences and diagenetic pathways of OM in Lake Superior.

1.5 Spectroscopic Techniques: FTIR and FT-ICR-MS

The complexity of natural OM requires high resolution techniques to provide definitive structural or functional information. Fourier transform ion cyclotron mass spectrometry (FT-ICR-MS) and Fourier transform infrared spectrometry (FT-IR) involving multidimensional techniques, which are among the most promising analytical techniques for the characterization of aquatic OM, are used in this study.

FT-ICR-MS was developed about three decades ago, stemming from advances in the area of proteomics. It is a very sophisticated tool with the power to bring a major fraction of aquatic DOM within our analytical window. Electrospray Ionization (ESI) is a low-fragmentation ionization technique which ionizes the macromolecules, while leaving them mostly intact; the resulting ions can be analyzed by a high resolution mass spectrometer. ESI is an optimal ionization method for the study of DOM because it can ionize both acidic and basic functional groups (depending upon ESI settings and sample solution pH) at atmospheric pressure. A wide range of molecules in DOM can be detected by applying both positive and negative ionization modes, although sodiated complexes may occur and be problematic in positive mode

(Kujawinski et al., 2006). FT-ICR-MS is an ultrahigh resolution (resolving power >80,000~400,000) and accuracy (<1ppm) mass spectrometry technique based on the detection of the ion cyclotron frequency of different ions within a strong magnetic field. The combination of ESI and FT-ICR-MS allows exact molecular formula determination for many peaks within a DOM sample, which represents a significant advance in the identification of compounds within DOM. However, quantitative aspects of ESI-FT-ICR-MS should be used with caution because of ion suppression issues which vary as a function of sample concentration and matrix effects that are not well understood in complex mixtures. The mass spectra resulting from analysis of DOM samples by ESI FT-ICR-MS are composed of up to 6,000 unique peaks, depending upon samples (Sleighter and Hatcher, 2007). Once formulas are assigned, other data mining methods can be used to explore compositional similarity and difference among sample sets. The commonly used data mining methods include Van Krevelen analysis (Wu et al. 2004), Kendrick mass analysis (Hughey et al, 2001) and carbon number versus molecular mass plot. A new statistical method that has also been employed on FT-ICR-MS data is two-dimensional (2D) correlation analysis. It was applied to FT-ICR-MS of 20 ultrafiltered dissolved organic matter samples from a salinity transect and used to investigate the chemical changes in the dissolved organic matter pool at the molecular level (Abdulla et al. 2013). The combination of mass spectrometry with other spectroscopic techniques including nuclear magnetic resonance spectroscopy (NMR) and Fourier transform infrared spectroscopy (FTIR) and with separations approaches is a promising path, which, however, needs further exploration(e.g., review by Mopper et al., 2007).

FTIR, one of the most available and widely used techniques for structural characterization of molecules, can provide an overview of compound class or functional group composition in complex mixtures of organic matter (e.g., Abdulla et al. 2009; Abdulla et al., 2010). It is based on the fact that vibrations of different covalent bonds in organic functional groups absorb infrared radiation at different wavenumbers resulting in an IR spectrum that can be used for structural characterization of molecules. Although originally used for small, relatively simple organic compounds, FTIR has gained popularity as a method for OM characterization (Mecozzi and Pietrantonio, 2006; Minor and Stephens, 2008; Abdulla et al., 2010). With the application of 2D-correlation approaches to FTIR data (Abdulla et al., 2010a and b), more structural information can be extracted from FTIR spectra of complex compound mixtures such as those present in sediments. Noda (1993) developed the new concept of generalized perturbation based two dimensional correlation spectroscopy, which works by spreading the spectral intensity changes within a data set collected across a perturbation (ages, temperature, depth) across a second dimension as a function of the perturbation. The main advantages of 2D correlation spectroscopy lie in the following points: (i) enhancement of spectral resolution by spreading peaks over the second dimension; (ii) strengthening of functional group assignments through correlation of related IR bands; (iii) probing the specific sequential order of spectral intensity changes taking place through a data set or the value of a controlling variable affecting the spectrum through asynchronous analysis. The use of 2D-spectroscopy will and is resolving many ambiguities especially in natural complex mixtures of compounds with many overlapping peaks (Noda& Ozaki, 2004; Mecozzi et al. 2009 (a,b); Popescu et al. 2010; Abdulla et al., 2010b). Comparing 2D FTIR with multivariate statistical methods (such as discriminant

analysis, principal component analyses and cluster analysis) can help to confirm trends within an FTIR data set and provide additional complementary insights into the distribution of sample compositions.

1.6 The Study System: Lake Superior

Lake Superior is the Earth's largest lake by surface area (82,100 km^2), with a maximum depth of over 400 m, mean depth of 150 m, water residence time of 180 years, and is dimictic, mixing twice annually (Herdendorf, 1990; Urban et al., 2005). It is an oligotrophic system with many features similar to the oligotrophic oceans, such as low nutrient availabilities and with primary production by in-lake phytoplankton, with picoplankton photosynthesis being the dominant source of reduced organic matter (Sterner 2010). In the Lake Superior system, distinct carbon isotope ratio signatures for organisms collected in wetlands and from offshore waters are found. Compared to offshore organisms, the wetland food web is depleted in ^{13}C; nitrogen isotope ratio signatures are found to be enriched in ^{15}N by ~3‰ at each succeeding trophic level in both wetland and lake (Keough et al, 1996). Differences between wetland and lake phytoplankton may be explained by the isotopic signatures of their dissolved inorganic carbon sources. The ^{13}Cdepletion in wetland phytoplankton could be caused by using DIC derived from decomposing detritus (Keough et al, 1998). Average rates of primary production in Lake Superior are low, likely due to the cold water temperatures and low nutrient concentrations in the lake (Sterner et al. 2004). There are allochthonous riverine organic carbon inputs but these constitute only about 10 percent of the overall annual primary production (Cotner et al. 2004, Sterner et al., 2004). The dissolved organic carbon and particulate organic carbon concentration ranges from 89-208μM and 2.3 to16.5 μM, respectively (Zigah et. al. 2012) and carbon is estimated to account for half the molecular weight of DOM. DOM comprised 94% of the water-column organic carbon in Lake Superior (Urban et al., 2005). Urban et al. (2005) found that the lake's DOM is primarily terrestrial, due

to much longer turnover times for the terrestrially-derived material as compared to autochthonous DOM in the lake. In Lake Superior, the most important sink for organic matter is respiration by heterotrophic bacteria (Cotner et al., 2004). The other important loss in the lake is through burial. Organic carbon deposition in Lake Superior sediments is about 0.48×10^{12} g C yr^{-1} (McManus et al., 2003) to 1.5×10^{12} g C yr^{-1} (Johnson et al., 1982; Klump et al., 1989). Baker et al. (1991) also found that less than 5% of organic carbon in surface POC is transported to the bottom and accumulates in sediment based on a sediment trap study. The carbon cycle for Lake Superior is not very well understood; e.g. Cotner et al. (2004) indicates an unbalanced C budget in terms of input and output of C, while a new estimate for whole-lake annual primary production, 9.73 Tg y−1, which was derived by in situ incubations combined with a statistical model, brings the organic carbon cycle of Lake Superior closer to being balanced (Sterner 2010).

Radiocarbon and stable carbon isotopic study on the carbon sources and cycling of Lake Superior reveals that in the open lake distinct processes operating in the surface (e.g., photosynthesis) and deep waters (sediment resuspension and pore-water intrusion) control the relative contribution of modern and old DOC and POC in the water column (Zigah et al 2011). Molecular characterization of DOM within Lake Superior and its tributaries by UV–visible spectroscopy, FTIR, direct temperature resolved mass spectrometry (Minor and Stephens, 2008) and FT-ICR-MS (Steinbring, 2010) reveals that Lake Superior has a very different DOM composition from its tributaries, which was attributed in part to the process of photodegradation of terrestrially-derived material. These studies show a shift from higher molecular weight organic matter enriched in protein and lignin at the tributary sites toward compositionally different material in the open lake (Minor and Stephens, 2008). Lake Superior’s unique formulae are found primarily in the lignin-like and reduced hydrocarbon regions of Van Krevelen space, though electrospray amenable Lake Superior DOM is also shown to have a higher proportion of heteroatom (N and S) containing formulae than DOM from the tributaries (Minor et al., 2012).

1.7 Objectives and organization of this dissertation

The primary goal of this thesis is to investigate the OM composition in Lake Superior and to look at its relationship with organic matter source and dynamics. To do this advanced spectroscopic techniques were combined with multiple geochemical signatures to investigate the biogeochemical variations of DOM, POM, and sedimentary OM in Lake Superior at a range of temporal and spatial scales. The specific objectives of each chapter are:

Chapter 2. To investigate the chemical composition of solid phase extracted DOM from Lake Superior with ESI FT-ICR-MS and Uv-vis Spectrometry. The goal is to examine the influence of extraction resins (C18 vs XC) on the composition of DOM concentrates. We developed appropriate strategies to extract DOM compositional information on a molecular level from the spectroscopic data and to make comparisons of samples isolated with different extraction resins and from nearshore and offshore sites. The results are compared with the stable carbon isotope and radiocarbon signatures of bulk samples.

Chapter 3. To characterize POM as a function of season, sources and bioreactivity in Lake Superior by combining FTIR with hydrolysis, extraction, and derivatization approaches. The comparison of molecular derivatization techniques (for carbohydrates and amino acids) and FTIR provides insights into the validity of the FTIR approach, which is quick and easy, on POM characterization. The POM compositional information on a functional group level, in conjunction with seasonal mass fluxes, C, N and stable carbon isotope signatures reveals POM degradation and selective preservation mechanisms in Lake Superior.

Chapter 4. To study the early diagenesis of OM in Lake Superior sediments with FTIR and 2D correlation analysis. The goal is to characterize sedimentary organic matter in terms of the functional groups of the principal building blocks of living aquatic organisms (e.g. proteins, carbohydrates, and lipids). 2D correlation analysis with

depth as perturbation is then applied to determine the OM compositional changes at five lake stations over a depth range of 0 to 10 cm, thus revealing early diagenetic trends in sediments from Lake Superior. This chapter has been published in Organic Geochemistry (Li et al 2013). The research concept, the experiment design, the sample and data analysis as well as paper composing was carried out by me. Elizabeth C. Minor participated in all the above processes and contributed to the paper by providing intellectual discussion and comments which substantially improved the quality of the research. Prosper Zigah helped with stable and radiocarbon isotope analysis, and provided comments which improved the paper.

Chapter 5 includes the summary of conclusions and suggestions for future work.

Chapter 2 Dissolved Organic Matter in Lake Superior: Insights into the effects of extraction methods on chemical composition

Summary

In this study, the composition of solid phase extracted dissolved organic matter (DOM) from Lake Superior, obtained with two different solid phase extraction (SPE) resins (C18 vs SDB-XC), was investigated using UV-visible spectrometry and negative-ion electrospray Fourier transform ion cyclotron resonance mass spectrometry (ESI FT-ICR MS). The performance of the two SPE disks and their influences on the molecular chemical composition of the extracted retentates were studied. DOC results and UV-visible spectrometry parameters indicate that Lake Superior raw offshore water is very clear; its DOM is low in aromaticity, with primarily non-humic, hydrophilic and low molecular weight materials. Radiocarbon signatures reveal the primarily modern (post-bomb) nature of Lake Superior DOM. With such Lake Superior water, we found SDB-XC disks to outperform C18 disks in the isolation of DOC in terms of both higher recovery and less degree of fractionation relative to the initial DOM composition, as determined by DOC analysis and UV-visible spectrometry. However, both extraction disks introduce considerable contamination to extracts, thus method blank samples are suggested to be analyzed together with samples to identify blank-associated components. FT-ICR MS and multivariate analyses were used to detect individual molecules within the samples, to determine their elemental compositions, and to investigate molecular-level variations in DOM obtained with different SPE resins and at different sites (nearshore vs offshore). Surface samples from one nearshore site (BR) and one offshore site (WM) were used to compare the two SPE resins. Extracts of the same samples obtained with the different extraction disks (SDB-XC vs C18) share 70% of compounds, which were dominated by lignin-CRAM-like material but also include a variety of other functional groups including lipids, proteins, carbohydrates and condensed hydrocarbons. Compounds exclusive to the SDB-XC extractions were found to follow the distribution of the shared compounds, however, they were somewhat more heteroatom-rich and aromatic. The C18 exclusive compounds were found to have

somewhat higher H/C ratios and to contain a large proportion of compounds containing oxygen and nitrogen (CHON). Cluster analysis and principle component analysis confirms that sample location is the main driver of the composition of extracted samples but does show some fractionation of the samples based upon the type of resin.

2.1. Introduction

Dissolved organic matter (DOM) is ubiquitous in aquatic systems, and it constitutes one of the largest dynamic reservoirs of organic carbon on Earth (Hedges et al, 1997). Its variable molar masses and chemical structures help to determine its roles in the natural environment, including acting as a food and nutrient source to aquatic organisms, as a photosensitizer for anthropogenic compounds, and as a chelator of trace metals. Identifying the molecular composition of DOM, especially the molecularly uncharacterized fraction (Benner, 2002) is fundamental to the understanding of the sources, reactivity and cycling of DOM as well as global C. However, the very low concentration of organic matter (~1 to 2 mg C/l) in the oceans and oligotrophic lakes (Carlson et al., 1994; Wetzel, 2001; Raimbault et al., 2008) challenges most analytical techniques, especially for marine water which contains large amounts of inorganic salts.

A major focus of DOM research has been in the isolation and desalting of sufficient amounts of representative material for analysis that would provide more comprehensive structural information using analytical methods such as nuclear magnetic resonance (NMR), infrared spectroscopy and mass spectrometry. Such isolation approaches fall into the three main categories: solid phase extraction (SPE), ultrafiltration, and reverse osmosis and reverse osmosis/electrodialysis (RO/ED). The SPE approach for the isolation of DOM using one or a combination of XAD resins was established in the late 1970s and has been applied to many studies as the classic extraction approach (e.g., Dittmar et al. 2001). Very different recoveries were

obtained for different aquatic systems, e.g., a total recovery of 16-21% for sea water (Druffel et al. 1992) and 50 to 80% recoveries for "colored water" with a high contribution from humic substances (Thurman and Malcolm 1981). This is possibly due to a selective isolation of different fractions of DOM with these resins. Recently, much DOM isolation has employed other resins such as C18 (Sleighter and Hatcher, 2008) and PPL resins (Dittmar et al. 2008). C18 resins are made of a silica matrix bonded to octadecyl (C18) functional groups, which act as sites for non-polar interactions. A comparison of SPE sorbents in cartridge form by Dittmar et al. (2008) found that C18 resins (with 39 ± 4% recovery) were the most efficient silica-based sorbents, and PPL resin which is based upon styrene divinyl benzene polymers produced the highest DOM recoveries (up to 62% ± 6% recovery). In addition, all SPE resins were found to selectively isolate certain fractions of compounds in DOM, preferably humic substances with high aromacity (Dittmar et al., 2008). The SPE approach also has other problems such as the time required to process larger-volume samples and the possibility of chemical changes to the nature of DOM due to pH alteration during extraction. However, due to its simple setup and wide applicability in different working conditions, especially in remote field settings, SPE disks and cartridges have been widely applied in aquatic DOM studies for isolating DOM. Ultrafiltration, which isolates DOM fractions based on molecular size (primarily with a 1-kDa membrane), is another widely recognized method for the extraction of DOM (ultrafiltered DOM, or UDOM), and the one most favored by isotope geochemists. It isolates up to 30% of marine DOM (e.g., Benner et al. 1997) and larger percentages of the initial DOC in colored waters, such as most lakes and rivers which have larger terrestrial impact, and higher average molecular weight DOM (e.g., Stephens and Minor 2010). The combination of reverse osmosis and electrodialysis allows isolation of much larger proportions of aquatic DOM as compared to other techniques, with DOC recovery ranging 60% to 95% (Vetter et al. 2007, Koprivnjak et al., 2009). However, the RO/ED technique requires access to expensive equipment that can be prohibitive in many cases especially in the field, and due to large membrane surface

areas, may contribute significantly to organic carbon blanks.

Advanced spectroscopic techniques have been employed to identify the composition of DOM with both raw water and concentrates. Measurements of DOC and colored DOM (via UV-spectrometry) provide average evaluation of the bulk properties of each DOM sample. FT-ICR-MS, which has a high degree of mass accuracy and precision, can provide definitive structural or molecular information on the complex natural OM. Over the past two decades, FT-ICR-MS has been providing new insights into DOM in different aquatic systems (Kujawinski, 2002; Mead et. al. 2013; Nebbioso and Piccolo, 2013). FT-ICR-MS can detect ions over a wide range of m/z values at high accuracy; the assignment of exact molecular weights and subsequently molecular formulas to individual components within DOM can be achieved without the need for prior separation by chromatographic methods. Coupled with electrospray ionization (ESI), which ionizes both acidic and basic functional groups in DOM (depending upon ESI settings and sample solution pH) at atmospheric pressure, a wide range of molecules in DOM can be detected (Kujawinski et al., 2006). While a highly efficient qualitative characterization tool, ESI-FT-ICR-MS is at present only semi-quantitative; its signal intensities should be used with caution because of ion suppression issues, which vary as a function of sample concentration and matrix effects that are not well understood in complex mixtures (Kujawinski, 2002). An additional complication in the application of ESI-FT-ICR-MS to complex heterogeneous samples such as DOM is that even with the high levels of accuracy and precision currently available, the calculation of molecular formulae is not fully constrained; it requires the input of possible elements and elemental abundances, and at molecular formulae above m/z 500, the assumption that homologous series of compounds are most likely to occur in these samples (Kujawinski and Behn, 2006). A typical DOM mass spectrum results in a large matrix of thousands of molecular formulae and their signal intensities. Thus comparing multiple samples to understand environmental variations in DOM structure requires appropriate data visualization and

data mining approaches (e.g., Sleighter and Hatcher, 2008; Abdulla et. al. 2013).

Lake Superior is the Earth's largest lake by surface area (82,100 km^2) and is a dimictic, oligotrophic system (Herdendorf, 1990; Urban et al., 2005). Preliminary characterization of DOM within western Lake Superior and its tributaries by UV–visible spectroscopy, FTIR, direct temperature resolved mass spectrometry (Minor and Stephens, 2008) and FT-ICR-MS (Minor et. al., 2011) revealed that the western arm of Lake Superior has a very different DOM composition from that found in local tributaries, which was attributed in part to the process of photo-degradation of terrestrially-derived material. These studies showed a shift from higher molecular weight organic matter enriched in protein and lignin at the tributary sites toward compositionally different material which had a stronger aliphatic signature in the open lake. Lake Superior DOM was also shown to have a higher proportion of heteroatom (N, S, and P) containing formulae than DOM from the tributaries (Minor et al., 2011). Distinct processes operating in the surface (e.g., photosynthesis) and deep waters (sediment re-suspension and pore-water intrusion) in the open lake control the relative contribution of modern and old DOM in the water column as indicated by stable and radiocarbon isotopic studies (Zigah et. al. 2011). Bulk DOC across the entire lake (western through eastern basins) appears to be semilabile according to its average radiocarbon composition, which indicates an average turnover time of $\leq$60 years (Zigah et. al. 2012).

Within the past decade, in a study of SPE cartridge extraction, a modified styrene-divinylbenzene resin (in PPL cartridges) has been found to be efficient and to retain a more representative proportion of marine DOM than C18 resin (Dittmar et al. 2008). While extraction disks of different resin types have been applied for years to isolate marine and freshwater DOM, comparison of the retention characteristics of C18 and SDB-XC (poly-styrenedivinylbenzene) disks has not, to date, been performed. Therefore, in this study the performance of C18 and SDB-XC disks was compared using coastal and off-shore Lake Superior water. Dissolved organic carbon

(DOC) concentrations, stable ($\delta^{13}C$) and radiocarbon (^{14}C) signatures and UV-Visible analyses of bulk DOM samples were used to assess the nature of water samples from different sites and depths. DOC and UV-Visible analyses of raw water, filtrates and retentates (DOM isolates) were also used to evaluate disk performance, including both the quantity and quality of isolated DOM. The molecular level composition of the extracted DOM obtained using the different disk resins (C18 vs SDB-XC) from one offshore site (WM) and one nearshore site (BR) were investigated using negative-ion electrospray Fourier transform ion cyclotron resonance mass spectrometry (ESI FT-ICR MS). The ultimate goals were: 1) to compare the performance of the two SPE disk resins (C18 vs SDB-XC) on isolating DOM in Lake Superior, a temperate, oligotrophic fresh water large lake; 2) to investigate the influences of extraction method on the molecular-level chemical composition of DOM as measured by FT-ICR-MS; 3) and to compare DOM composition at nearshore and offshore sites in Lake Superior.

2.2 Material and Methods

2.2.1 Sites and Sampling

Surface and deep-water samples were taken from seven Lake Superior sites (Fig.2-1) in June 2010 when the water-column was well-mixed. The sampling sites were chosen to cover nearshore and open-lake regions, western to eastern basins in order to obtain a comprehensive view of the lake water composition. Water samples were collected via Niskin bottles from a CTD rosette at each site for DOC concentration and SPE processes.

The SPE resins applied for comparison were C18 and SDB-XC (3M Empore disks). Information on resin structure can be found on the 3M website. The Empore C18 disk (pore size being 60 Å) contains octadecyl bonded silica sorbent which acts as non-polar stationary phase. The SDB-XC disks (pore size 80Å), are made of a poly (styrenedivinylbenzene) copolymer and thus retain compounds based upon both aliphatic and aromatic interactions. Manufacturer protocols were used to obtain DOM extracts (“eR”) from 3 to 5 liters of filtered (<GF/F, nominally <0.7 μm) water samples (“init”), as shown in Fig. 2-2.

Briefly, each filtered sample was first acidified to pH 2 using hydrochloric acid (ACS Reagent grade). Aliquots of this acidified sample were added to the prepared SDB-XC disk (rinsed with HPLC grade acetone, pesticide grade isopropanol, Fisher Optima grade Methanol and MilliQ water) or the C18 disk (rinsed with Fisher Optima grade Methanol/MilliQ water (v/v, 9:1) one time, Fisher Optima grade Methanol two times and then MilliQ water), and then extracted under reduced pressure (around 300 mmHg). A 90:10(v/v) methanol:water solution was used to recover the DOM from each sample-containing disk. To monitor SPE performances, aliquots of 'init' sample were analyzed by UV-Visible spectrophotometer and total organic carbon (TOC) analyzer and aliquots of extraction filtrate ('eF', the portion of DOM that is not retained on the resin) were also analyzed by UV-Visible spectrophotometer. The 'eR' samples were stored in a freezer (-20ºC), transported to lab, dried in a vacuum oven at approximately 40°C and then stored at room temperature in the dark to await analysis via UV-Visible spectrophotometer and TOC analyzer (after dissolution in known aliquots of MilliQ water), and ESI FT-ICR-MS (after addition of 70:30(v/v) methanol: water). Method blanks were also prepared by extracting 5-L of Milli-Q water in the same manner as lake water samples. All glassware used was acid-washed and baked in a muffle furnace at 450^{o}C for four hours prior to use and plastics were acid-washed in 10% HCl and rinsed with copious amounts of deionized water prior to use.

2.2.2 DOC analysis

DOC concentrations of whole water, 'init' and 'eR' (aliquots dried and then reconstituted in MilliQ water) at each site, both surface and deep, were determined with a Shimadzu TOC_{VCSH} analyzer (Shimadzu Scientific Instruments, Inc., Columbia, MD, USA). Non-purgeable organic carbon in each sample (previously acidified to pH 2 with 6N ACS Reagent grade HCl) was analyzed after high temperature catalytic oxidation (HTCO). Potassium hydrogen phthalate (KHP) solutions were used for calibration. To assess the instrumental performance, deep sea standards (from the

DOC Consensus Reference Materials Program http://yyy.rsmas.miami.edu/groups/biogeochem/CRM.html), additional KHP standards and MilliQ blanks were analyzed as samples. Three injections were performed for each sample and two more injections were performed when the standard deviation of the first three injections was greater than 2.5%; in the latter case, the closest three of the five injections were averaged to yield sample concentration.

2.2.3 UV/Visible spectroscopic analysis

Scanning UV-Visible spectrophotometry was performed on whole water, 'init', 'eF', and 'eR' samples with a Genesys6 scanning spectrophotometer (Thermo Fisher Scientific Inc., Waltham, MA, USA). The samples were scanned from 800 to 200 nm using a 1 cm or 5 cm quartz cuvette (depending on estimated sample concentrations). The Naperian absorption coefficient, α, was obtained using the following equation after blank correction, backscatter correction and dilution correction of absorbance:

$$\alpha_\lambda = 2.303 A_\lambda * l^{-1} \quad \text{eq. (1)}$$

where A is absorbance; λ is wavelength; and *l* is the path length (cuvette size) in meters. UV-Visible spectra of milli-Q water were used for blank correction. The average absorbance over 700-800 nm of each sample was used to correct backscatter. The sum of the volume-normalized absorption coefficients in the range of 250 nm to 400 nm was used to calculate the chromophoric dissolved organic matter (CDOM) abundance. These CDOM abundance values were then used to calculate percent recoveries of each extraction including:

$$\%\ \text{recovery after initial filtration} = CDOM_{init}/CDOM_{whole} \times 100\% \quad \text{eq. (2)}$$

$$\%\ \text{eF recovery} = CDOM_{eF}/CDOM_{init} \times 100\% \quad \text{eq. (3)}$$

$$\%\ \text{eR recovery} = CDOM_{eR}/CDOM_{init} \times 100\% \quad \text{eq. (4)}$$

$$\%\ \text{mass balance} = \%\ \text{eF recovery} + \%\ \text{eR recovery} \quad \text{eq. (5)}$$

The following indexes were used to study the chemical properties of each sample:

E2/E3 ratio, which is the ratio of the volume normalized absorption coefficients at 250 nm (E2) and 365 nm (E3). This ratio is inversely related to molecular weight and inversely proportional to the amount of aromatic material in the sample (Peuravuori and Pihlaja 1997).

$SUVA_{254}$, which is the ratio of the ultraviolet light absorption coefficient at wavelength 254 nm to the sample DOM concentration, giving a quantitative measure of the aromatic content per unit of organic carbon concentration (Weishaar et al. 2003).

Spectral slope, S, which is determined by curve-fitting the absorption coefficient from 250 to 400 nm to a single exponential decay function using a reference wavelength of 250 nm (Stedmon et al., 2000). Calculations of S were performed in Excel 2003, where iteration was used to maximize R^2. This index is used to give an indication of terrestrial influence and water color (Helms et al. 2008).

2.2.4 Isotopic Analyses on Bulk DOM

Radiocarbon and stable carbon isotope measurements of 'init' DOM samples were performed at the National Ocean Sciences Accelerator Mass Spectrometry Facility (NOSAMS) at the Woods Hole Oceanographic Institution as described in Zigah et al. (2011). Briefly, the organic matter in <GF/F filtered water samples (acidified to pH 2) were first oxidized to CO_2 by ultraviolet (UV) oxidation. After removal of a subsample of the purified CO_2 for δ^{13}C-DOC measurement, the remainder of the purified CO_2 was reduced to graphite and then analyzed by accelerator mass spectrometry (AMS) to determine radiocarbon content. Radiocarbon values are reported as Δ^{14}C following Stuiver and Polach (1977).

2.2.5 FT-ICR-MS analysis

Surface SPE DOM samples extracted with both C18 and SDB-XC disks from BR and WM sites were selected for FT-ICR-MS analysis. This was performed on a Thermo Scientific 7 Tesla Electrospray Ionization Fourier Transform Ion Cyclotron Resonance Mass Spectrometer (LTQ FT Ultra hybrid mass spectrometer) at the Woods Hole Oceanographic Institution. A linear ion trap mass spectrometer (LTQ MS) served as the ion accumulation site for high resolution analysis in the ICR cell. A scan range of 200-1100 m/z and 200 scans per analysis were used for this study. Since negative ionization results in a larger range of chemical formulae for DOM samples than positive ionization (Hertkorn et al., 2008) and because problematic sodiated complexes may occur in positive mode (Kujawinski and Behn, 2006), all dried samples for this study were redissolved with 70:30(v/v) methanol:water solution and then directly injected in the ESI FT-ICR-MS system for scanning in negative mode. Peak detection was based on a signal-to-noise ratio (S/N) greater than 5, and the peak lists were internally calibrated with a list of calibrants (Appendix Table 2-1). Elemental formulae were assigned to the aligned peaks (m/z values) using the Compound Identification Algorithm (CIA) originally described by Kujawinski and Behn (2006), modified in Kujawinski et al. (2009).An assignment rate of 97.9 %±1.1% was achieved for all samples. Any statistical analyses applied in this study were based on all peaks with S/N >5, rather than just the peaks with assigned elemental formulas,

2.2.6 Cluster Analysis and Principle Component Analysis (PCA)

The Bray-Curtis dissimilarity measurementwas used to calculate the distance matrix of CA (code from Fathom toolbox, David Jones, University of Miami,http://www.rsmas.miami.edu/personal/djones/matlab/matlab.html) based on FT-ICR-MS data. This dissimilarity measurement has been found to be robust and reliable for expressing sample relationships in environmental sciences and has been widely applied to FT-ICR-MS data (Kujawinski et al. 2009; Schmidt et al. 2009;

Minor et al. 2012). The Bray-Curtis dissimilarity calculation only considers zero/nonzero abundance of species within the sample, thus is suitable for eliminating the influence of selective ionization suppression at different m/z caused by matrix-effects. Similarly, in applying PCA, the FT-ICR-MS data matrix consisting of only peak presence/absence information of samples from all sites, depths and season was used to minimize the influence of varying response factors. Prior to PCA, z-scoring and variance scaling was performed. PCA was also applied on UV-visible spectrometry data for all samples based on both normalized absorption coefficients from 200 to 800cm^{-1} and the calculated spectrophotometry indices including E2/E3, SUVA254 and spectral slope. Matlab 7.0 and in-house m-files were used for data processing and multivariate analyses.

2.3. Results and Discussion

2.3.1. TOC analysis, stable ($\delta^{13}C$) and radiocarbon ($\Delta^{14}C$) signatures of 'init' DOM

DOC analysis (Table 2-1) shows that the offshore sites and the nearshore BR site have similar DOC concentrations (range, 86.0-92.8 µM), while the nearshore ONT site exhibits higher DOC concentrations (108.6 µM), possibly due to the excess DOC input by spring snowmelt at ONT site. The surface and deep samples show no significant difference in DOC concentration based on a pairwise t-test (p= 0.6707). Our average offshore DOC concentration (88.2 ±1.50µM) is comparable to open-lake DOM values reported by Zigah et al. 2012 (88.3-94.2µM for samples from spring and summer 2009) and lower than nearer-shore values reported by Minor and Stephens 2008 (210 ±19 µM). Our average offshore DOC value is smaller than reported tributary DOC by a factor of 3 to 12 (Urban et al., 2005; Minor and Stephens 2008) and is somewhat higher than reported surface open ocean DOC values (65-75 µM, Hansell and Carlson, 2001). The $\delta^{13}C$ values (-26.5±0.1‰) of all samples do not exhibit considerable variation and are close to the previously reported Lake Superior

DOM $\delta^{13}C$ values (-26~-28‰) in 2009 (Zigah et al. 2012). The lake's "init" DOM is primarily modern (post-1950s) at all sites according to its positive $\Delta^{14}C$ values. An inclusion of smaller but variable amounts of pre-aged DOM from different sources may contribute to the variations of $\Delta^{14}C$ values among samples from different locations and depths.

2.3.2 Disk Performance Comparison Based on TOC analysis and UV/Visible Spectrometry

TOC analysis and UV-visible spectrometry were used to examine the performance of our SPE approach and to compare characteristics of 'init' DOM vs 'eR' from the SDB-XC vs C18 disks applied in this study. SPE method banks had low but measurable carbon levels. The 'eR' fractions of the blanks contained 2.86 μmol C and 1.67 μmol C per liter of MilliQ water that was processed through SDB-XC disk and C18 disk, respectively. These values correspond, respectively, to 13.1% and 11.0% of the average organic carbon recovered per liter of lake water . This indicates that extraction disks do introduce some contamination and that the processed blank has to be analyzed together with the samples via the same structural and compositional characterization technique (such as FT-ICR-MS in this study) to exclude the possibility of misinterpretations of sample content.

The percentage of in-situ CDOM recovered after initial filtration (<GF/F) was 94.4± 5.2%, indicating no significant contamination introduced by the initial filtration step. CDOM mass balance (eR% + eF%) averaged 94.2 ± 8.6% for SDB-XC disk SPE extraction and 85.1± 6.0% for C18 disk SPE extraction, indicating no significant CDOM contamination introduced by either resin.Comparison of recoveries from extractions of Lake Superior water (Table 2-1) shows that SDB-XC disks perform better than C18 disk in terms of both CDOM recoveries (31.0±3.80% relative to 24.4 ±3.9%) and DOC recoveries (25.8. ±9.20% relative to 18.4±6.4%). Both SDB-XC and C18 resin disks produce higher CDOM recoveries relative to DOC recoveries at

most sites with the exception of WM deep sample, suggesting preferential retention of CDOM relative to DOC. Our SPE DOC recoveries of Lake Superior water were much lower than most reported lake/river studies (Thurman and Malcolm 1981) and comparable to or lower than marine studies (Druffel et al. 1992, Sleighter and Hatcher, 2008; Dittmar et al. 2008). This is possibly due to a combination of selective retention by solid phase resins and the organic matter composition in oligotrophic, clear-water Lake Superior.

The indices obtained via UV-visible spectrophotometry (E2/E3 ratios, $SUVA_{254}$ and spectral slope) were used to characterize the 'init' CDOM at each site, to compare XDB-XC vs C18 resin disks and to examine if the SPE substantially isolated certain portions of the DOM pool. As shown in Table 2-1, the E2/E3 values of 'init' water range between 8.78 to 17.5 with the general trend being higher values in offshore lake samples relative to nearshore samples (except for SM_deep). This is consistent with previous nearshore to offshore studies in Lake Superior and in a Chesapeake Bay sub-estuary, which found that the E2:E3 ratio ranged from 5.40 to 15.29 for the Superior transect and from 4.42 to 10.28 for the Chesapeake transect; in both transects the ratios increased from marsh to riverine, estuarine, coastal and open lake/ocean sites (Stephens and Minor, 2010). DOM from Atlantic Ocean water was found to have E2/E3 ratios of 13.5±1.6 (Helms et al. 2008). The values indicate that Lake Superior water is generally light in color and low in DOM molecular weight, with open-lake values comparable to or even higher than ocean values. The E2/E3 values of recovered 'eR' fractions from both SDB-XC and C18 resin disks are lower and show less variation than the 'init' samples, indicating both extractions preferentially isolated higher molecular weight and/or more aromatic DOM. However, the SDB-XC extraction produces 'eR' E2/E3 values (8.7±0.7) closer to 'init' E2/E3 values (12.6±2.8) than does C18 extraction (7.0±0.5). This suggests that SPE with SDB-XC disk alters 'eR' molecular weight and/or aromatic DOM contents to a lesser degree than C18 extraction disk.

$SUVA_{254}$ of Lake Superior 'init' water ranges between 2.81 to 3.83 with most open-lake sample values around 3 and BR and ONT mixed season sample values at the high end of the range. Based on previous studies (Weishaar et al. 2003) of DOM from a variety of environments (marine to dark-water rivers), Lake Superior offshore waters ($SUVA_{254}$ values $\leq$3 L mg^{-1} m^{-1}) contain mainly non-humic, hydrophilic and low molecular weight materials. Our $SUVA_{254}$ values are consistent with previous work in Lake Superior, where $SUVA_{254}$ values ranged from 9.0 in the St. Louis River to 2.0 in the open lake (Stephens and Minor, 2010). Our $SUVA_{254}$ values also show that SPE extraction with both SDB-XC and C18 resins generally leads to preferential retention of more aromatic DOM components, as suggested by the higher $SUVA_{254}$ values of 'eR' than 'init' (except for WM_deep). The SDB-XC extraction produces 'eR' $SUVA_{254}$ values (3.53±0.75) somewhat closer to 'init' $SUVA_{254}$ values (3.11±0.29) as compared to those of C18 extractions(3.60±0.67), with the exception of samples from NM and the two nearshore sites. This indicates that SPE with SDB-XC alters 'eR' aromatic DOM contents to a lesser degree than C18 extraction, however, its performance is affected by 'init' DOM composition.

For samples from all sites, and extractions with both resin types, the 'eR' fractions have lower spectral slope values than 'init', with 'eR'-C18 showing a greater deviation from 'init' water. These indicate a shift toward greater molecular size and/or aromaticity within the 'eR' fractions and are therefore consistent with the other UV-visible proxies. Thus, the combination of the UV-visible spectrometry proxy information, with $SUVA_{254}$ and E2/E3 providing insight into aromaticity and the S providing a combined view of aromaticity and molecular weight, suggests that material with higher average molecular weight and aromaticity is preferentially concentrated within the 'eR' samples by both SPE resin types, with SDB-XC SPE providing less compositional alteration and deviation from 'init' water samples.

To further investigate the compositional variation of ‘eR’ samples with different SPE resin types, Principle Component Analysis (PCA, Kvalheim et al., 1985; Sanni et al., 2002) was performed on the UV-visible spectrometry data of both ‘init’ and ‘eR’ samples, using the following two data sets: A) the normalized absorption coefficients of the complete UV-visible spectra from 200 to 800cm^{-1} and B) calculated spectrophotometry indices, as seen in Fig. 2-3. Despite the possible compositional differences of ‘init’ DOM samples from different sites and depths, the SPE ’eR’ concentrates were separated from ‘init’ samples, with sample preparation as the main factor driving the PCA1 variation. Fig. 2-3b shows that ‘eR’ of SDB-XC extraction may have retained more similar compositional information relative to its ‘init’ as compared to C18 extraction; this is shown by the closer spacing of SDB-XC ‘eR’ samples to the <GFF ‘init’ samples.

In sum, the combination of DOC analyses and UV/visible spectrometry parameters on bulk organic matter indicates that Lake Superior offshore water is oligotrophic, low in dissolved organic carbon content, and very clear. The DOM is low in aromatic components, with primarily non-humic, hydrophilic and low molecular weight material. In comparison of the two types of SPE disks as applied to isolations of Lake Superior water, we found SDB-XC disks to outperform C18 disks in the isolation of DOC in terms of both higher recovery and a lower degree of fractionation relative to the initial DOM composition. Our blank and mass balance studies of SPE with both extraction disks show that they both introduce non-negligible contamination to ‘eR’ fractions, thus the interpretation of DOM structures based on the retentates has to be performed with care. Method blank samples have to be analyzed by whatever techniques are applied to other samples to identify blank-associated components.

2.3.3. FT-ICR-MS Analysis

Using extraction to isolate DOM may provide an imperfect view of the native DOM pool due to preferential recovery of certain compound types as suggested by our

UV-vis spectrometry data and reported by Dittmar et al. 2008 and Kruger et al. 2011. Therefore, ESI FT-ICR-MS has been applied to determine molecular differences between the samples from different sites (WM vs BR) and obtained with different extraction resins (SDB-XC vs C18). All samples were analyzed under negative ion mode, which has been shown to provide greater DOM response and suppressed blank contributions relative to positive ion mode (Hertkorn et al., 2008; Minor et al., 2012). High abundances of DOM peaks with high intensity ranging from m/z 250 to 600 (Fig. 2-4) were detected, which is consistent with previous spectra from Lake Superior and its tributaries (Minor et.al., 2012). DOM peaks in samples were singly charged as determined using the isotopic distribution of carbon (Stenson et al, 2002), which is again consistent with previous DOM studies, including that of Lake Superior and selected tributaries (Minor et al., 2012). Peaks identified in the method blank contributed 1147 to 1685 peaks to each sample, accounting for 11.8% to 15.9% of the total number of peaks in each sample, thus blank correction of the samples was performed. After blank correction, the number of peaks in samples (S/N >5) are 8691 (‘eR’ of SDB-XC) and 8908 (‘eR’ of C18) for BR surface samples and 8472 (‘eR’ of SDB-XC) and 8551 (‘eR’ of C18) for WM surface samples.

We also observed clear differences in the molecular characteristics between ‘eR’ of SDB-XC vs C18 extraction. The peak magnitudes of the SDB-XC samples are generally higher than those of the C18 extracted samples and different numbers of peaks can be seen within the same m/z ranges. As an example, the enlargement area of m/z 310 to 313 is shown in Fig. 2-4; 15 peaks exist in ‘eR’ of SDB-XC while only 10 peaks exist in ‘eR’ of C18 extracted WM surface samples.

To better visualize and compare such large amounts of molecular information (more than 8000 peaks per sample), statistical and visualization methods have been employed as shown in Fig. 2-5. For the same water sample (from BR surface or WM surface), the common formulae (m/z) and the unique formulae found in ‘eR’ obtained

with different resin disks (SDB-XC vs C18) are displayed using Van Krevelen diagrams (Fig. 2-5). The formulae (m/z) common to 'eR' from both extraction disks account for a very large percentage of each sample's total DOM formulae in both the offshore site (WM, 70.8% in SDB-XC 'eR' and 69.0% in C18 'eR') and nearshore site (BR, 70.3% in SDB-XC 'eR' and 69.7% in C18 'eR'), as seen in Fig.2-5a and b. The prevalence of these common formulae makes sense considering the same 'init' water sample was used for the extractions. The lignin-like fraction (a small fraction of which contains N and P) was found to be the major component at both sites and likely derives from terrestrial inputs. The Van Krevelen space of this fraction also overlaps with the section consistent with CRAM, the most abundant identified component of DOM in the deep ocean (Hertkorn et al. 2006). Observation that CRAM is a major structural component (17–25%) of isolatedHMW DOC in Lake Superior was reported by Zigah et al. (2014).Their estimated old age (2043 BP years)of CRAM in Lake Superior HMW DOM is consistent with its refractory nature reported for ocean(Hertkorn et al., 2006). CRAM, identified by a combination of NMR and FT-ICR-MS techniques, was also found to be a large contributor to DOM in freshwater Lake Ontario (Lam et al. 2007). The origin of CRAM has been widely discussed; CRAM could result from degradation of cell wall and membrane components in aquatic organisms or transformation of lignin-like material originally from terrestrial sources (Hertkorn et al. 2006). Most of the CRAM in HMW DOC from Lake Superior is believed to be terrigenous and/or from solubilized sedimentary OC released via pore water diffusion and sediment resuspension events (Zigah et al. 2014). Formulae in other functional groups including lipid, protein, amino-sugar, carbohydrate, and the condensed hydrocarbon region were also found, and a portion of these formulae contain N and P in addition to C, H, and O.

The percentage of peaks unique to the SDB-XC extraction 'eR' and the C18 extraction 'eR' at both sites are similar, and range from 29.1% to 30.9% of the total number of peaks in the original sample. The compounds unique to the SDB-XC

extraction ‘eR’ and the C18 extraction ‘eR’ were both found over the entire van Krevelen spaces including lipid, protein, amino-sugar, carbohydrate, condensed hydrocarbon and lignin-CRAM regions. However, the SDB-XC extraction ‘eR’ has unique compounds that somehow follow the distribution of its common peaks, with a lower percentage of lignin-CRAM-like compounds and enrichment of condensed hydrocarbon, tannins, aminosugar, lipids and carbohydrates. In contrast, the unique C18 extraction ‘eR’ compounds are densely located within a particular region, with an H/C ratio from 1 to 2 and an O/C ratio from 0.25 to 0.5, consistent with amino acid-like and lignin-like material. The percentage distribution of the compound classes (Fig.2-5e and 2-5f) reveals that the protein-like material is highly enriched in the unique C18 extraction ‘eR’ compounds. Such molecular-level distribution differences can explain the UV-visible data above, where SDB-XC ‘eR’ samples were more similar to the ‘init’ water sample as compared to C18 ‘eR’.

2.3.4 Comparison of the FT-ICR-MS spectral features (elemental ratios, DBE, etc)

Elemental ratios, double bond equivalences (DBE), elemental formula percentages, and elemental percentages (Table 2-2) were calculated as described in Minor et al. (2012) to provide an additional view of the chemical variations in samples from different sites, and extracted with different resins. The DBE (13.10-13.64) and DBE/C (0.40-0.46) values of ‘eR’ samples obtained with the different resins are similar. The exclusive compounds in SDB-XC ‘eR’ and the C18 ‘eR’ both have higher number-averaged DBE (17.63-19.07) as compared to the total formulae in each sample; however, when DBE is normalized to the total number of C atoms in a given molecule (DBE/C), exclusive compounds in C18 ‘eR’ have lower values (DBE/C) than the total formulae and the exclusive compounds in XC ‘eR’. This is probably a function of the larger average molecular size of the C18 ‘eR’ compounds (as shown in the UV Visible proxy data); the C18 ‘eR’ exclusive compounds contain a higher

number of rings and/or double bonds, but are, actually, a bit less unsaturated on a per C basis.

Small variations in terms of 'eR' elemental ratios are also found. The SDB-XC 'eR' compounds were found to have larger number-averaged and weight-averaged O/C and P/C ratios, smaller H/C ratios and similar N/C and S/C ratios relative to the C18 'eR' compounds. The preferential retention of heteroatom-containing compounds with SDB-XC disks is likely to result in such a distribution. For both SDB-XC and C18, the exclusive compounds have lower O/C ratios, and higher N/C ratios and somewhat higher P/C and S/C ratios. The SDB-XC exclusive compounds as compared to the C18 exclusive compounds have lower number-averaged and weight averaged H/C ratios and higher P/C ratios.

The percentages of formulae containing S (F_S) and P (F_P) are also higher in SDB-XC 'eR' relative to C18 'eR', while the percentages of formulae containing N (F_N) is slightly higher in the C18 'eR'. The exclusive compounds in both resin-type 'eRs' have considerably higher F_N, F_P and F_S values than the total formulae.

Combining the elemental data with the DBE numbers, the 'eR' from both SDB-XC and C18 extraction contains a large proportion of unsaturated,heteroatom-rich compounds such as aromatic compounds and oxygen-heteroatom-containing compounds. However, the SDB-XC resin appears to isolate DOM with slightly lower H/C ratios and slightly more double bonding; it also isolates a slightly higher percentage of formulae containing P than does the C18 resin.

Our O/C_w ratios for total formulae in the extracts (0.40~0.43) are slightly higher than previously reported values, including Lake Superior C_{18}-extracted DOM (0.38, Minor et al. 2012); whole water DOM from the Dismal Swamp in Virginia, USA (0.39,

Sleighter and Hatcher, 2008); SPE-extracted DOM from a Chesapeake Bay sub-estuary (0.33–0.35; Sleighter and Hatcher, 2008); and C_{18}- extracted DOM from Atlantic Ocean surface water (0.34–0.36; Kujawinski et al., 2009). H/C_w values for our samples (1.27 to 1.34) are also slightly higher than previously reported for C_{18}-extracted DOM from Lake Superior (1.22) and selected tributaries (1.08~1.28; Minor et al. 2012). They are comparable to reported Dismal Swamp whole water (Sleighter and Hatcher, 2008) and Chesapeake Bay C18 SPE-extracted DOM (1.25 and 1.29) H/C_w values, and values reported by Kujawinski et al. (2009) and Koch et al. (2008) for C_{18}-extracted DOM from Ocean surface water (1.3–1.39).

Compounds containing only carbon, hydrogen and oxygen (CHO) account for 45.6% to 46.7% of all DOM formulae in each extracted sample (Table 2-2). This percentage is significantly lower than reported for surface ocean, deep ocean and river C18-extracted DOM samples (72.2–93.7%; Kujawinski et al., 2009), and Lake Superior tributary C18-extracted DOM samples (Minor et al. 2012). DOM compounds with formulae of CHON account for 29.1%~32.7% (depending on sample) of all DOM formulae in each sample. These compounds are possibly in the amino-acid/protein family. The number of CHONP formulae ranges from 11.3% to 14.9% and these are likely to be nucleotides and DNA/RNA derivatives. With the above three types of compounds comprising over 95% of DOM formulae in each sample, compounds with formulae of CHOS, CHONS, CHOP and CHONSP are only minor species. Comparing ‘eR’ obtained with the 2 different extraction resins, SDB-XC ‘eR’ has a similar percentage of CHO compounds, a higher proportion of CHOS, CHONP, CHONSP compounds, and a lower proportion of CHON, CHONS and CHOP compounds. The exclusive compounds exaggerate these trends with a much lower percentage of CHO compounds and much higher percentage of heteroatom-containing compounds as seen in Table 2-2. The majority of the exclusive formulae for both resins are CHON compounds.

Our UV-Vis data and these FT-ICR-MS data show that the use of styrene divinylbenzene-based resins vs C18 resins leads to the isolation of somewhat different portions of the DOM pool. Thus comparisons of literature values obtained with different SPE protocols should be viewed with some caution.

2.3.5 Comparison of the FT-ICR-MS with Multivariate analysis

Cluster Analysis (CA) and PCA were performed on the FT-ICR-MS data to further investigate the variation among samples extracted at different sites (WM vs BR) and with different resin types (SDB-XC vs C18). Cluster analysis is a convenient tool to compare samples and to visualize their differences on the basis of multidimensional data such as mass spectra. The analysis is based on the peak presence/absence of all identified molecular formulas after blank correction in the different 'eR' samples. The x-axis represents the degree of similarity with Bray-Curtis distance. As seen in Fig. 2-6a, the variance between samples from different sites (WM vs BR) rather than different extraction techniques drives the grouping, which is an ideal result considering that we want an effective and representative isolation of DOC that represents the 'init' sample nature which is usually affected by sampling location, season and depth. PCA was also used to explore the compositional differences and similarities among samples. As seen in the PC1 vs PC2 plot (Fig. 2-6b), the grouping by PCA is similar to the results from cluster analysis. PC1, which accounts for 40.70% of the total variance, separated the BR samples (on the negative side) with WM samples (on the positive side); however, at the same time, PC2, which accounts for 31.93% of the total variance, separated the C18 samples (on the positive side) with the SDB-XC samples (on the negative side). This finding confirms some retention of sample nature by SPE even with different extraction resins, and the occurring of fractionation to the initial DOM composition, affected by the type of resins. Understanding the fractionation on a molecular level might be critical to the comparison of different DOM studies of different natural systems.

2.4. Conclusions

Combining DOC analysis, UV-Visible spectrometry, stable and radiocarbon signatures and FT-ICR-MS allows us to assess the nature of Lake Superior DOM and to investigate and compare the performance of different SPE resins (SDB-XC vs C18) on the isolation of DOC in terms of both recovery and 'eR' molecular features.

In the comparisons, we found that using XC disks leads to greater DOC and CDOM recoveries as well as less fractionation in composition relative to initial water samples as determined by DOC mass balances and UV-Visible spectrophotometry parameters. The UV-visible spectrometry proxies, with $SUVA_{254}$ and E2/E3 providing insight into aromaticity and average molecular weight, and spectral slope providing a combined view of aromaticity and molecular weight, suggest that higher molecular weight and aromaticity material is preferentially concentrated within the 'eR' samples by both SPE resin types, with SDB-XC SPE providing less compositional deviation from 'init' water samples. Method blanks indicate that both extraction disks introduce contamination of up to 10% of 'eR' carbon compositions in our oligotrophic, low-C water samples, thus the processed method blank has to be analyzed along with samples.

FT-ICR-MS data shows some molecular-level differences among 'eR' obtained from the same sample using different extraction disk resins. The peak magnitudes of the SDB-XC samples are generally higher than those of the C18 extracted samples and different numbers of peaks can be seen within the same m/z ranges. However, using the different extraction resins on aliquots of the same sterile-filtered sample also led to commonalities in the two extracts, which shared approximately 70% of peaks identified by FT-ICR-MS. The lignin-CRAM like fraction (a small fraction of which contains N and P) was found to be the major component at both WM and BR sites. Formulae in other functional groups including lipid, protein, amino-sugar,

carbohydrate, and condensed hydrocarbon regions were also found, and a portion of the formulae contain N and P in addition to C, H, and O.

There was preferential retention of unsaturated multiple-heteroatom-rich compounds with the SDB-XC resin as revealed by elemental ratios and P% and S% values of SDB-XC vs C18 of shared compounds and exclusive compounds. Comparing the two resin types, SDB-XC 'eR' has similar percentages of CHO compounds, a higher proportion of CHOS, CHONP, CHONSP compounds, and a lower proportion of CHON, CHONS and CHOP compounds than C18 'eR'.

CA and PCA analysis, which are commonly used statistical measurements of sample similarity, confirm that the greatest variance in the sample set is driven by sample location, rather than the difference in extraction techniques. However, significant fractionation relative to the initial DOM composition does occur, and the degree is affected by the type of resins. Understanding such fractionation on a molecular level might be critical to the comparison of different DOM studies in different natural systems.

Table 2-1

Sampling information, DOC concentration, stable carbon ($\delta^{13}C$) and radiocarbon signatures of 'init' DOM, CDOM and DOC recoveries (% CDOM and % DOC of 'eR' to 'init' samples) and UV-Visible spectrophotometry indices for 'init' and 'eR' samples of both C18 and SDB-XC extractions.

Sample		CM	CM	EM	EM	NM	NM	SM	SM	WM	WM	BR	ONT
Water depth m		258	258	248	240	213	216	398	386	171	171	19	20
Sample depth m		5	190	5	210	5	150	5	340	5	127	4	5
'init' DOC µM		86.5	89.5	89.8	87.8	88.2	87.8	87.8	86.0	87.8	91.0	92.8	108.6
'init' $\delta^{13}C$ ‰*		--	--	-26.1	-25.9	--	--	-25.9	-26.0	-26.0	-29.0	--	-28.2
'init' $\Delta^{14}C$ ‰*		--	--	44.6	49.5	--	--	40.0	47.5	57.4	156.9	--	-18.5
CDOM Recovery %	XC	30.9	25.5	28.0	31.6	31.4	34.0	30.8	24.0	35.6	34.2	28.8	36.4
	C18	19.0	27.0	24.2	26.2	26.6	24.2	22.5	19.9	19.1	28.5	23.7	31.8
DOC Recovery %	XC	23.1	22.9	21.6	22.5	22.2	22.3	22.2	23.1	23.2	54.8	26.0	25.7
	C18	11.8	20.1	15.8	17.5	18.2	17.7	14.7	17.1	11.0	36.3	21.3	19.6
E2/E3	'init'	15.5	12.2	12.2	17.5	12.3	12.7	10.2	8.80	15.5	15.2	9.08	9.91
	XC 'eR'	8.91	9.40	9.40	8.98	8.91	8.29	9.08	9.10	8.77	8.57	7.55	7.21
	C18 'eR'	7.13	7.24	7.25	7.28	7.28	7.41	7.44	7.13	7.12	6.61	6.14	5.82
SUVA254 L/(m*mg)	'init'	3.02	2.98	2.81	2.83	3.00	3.02	2.90	3.12	3.16	3.10	3.50	3.83
	XC 'eR'	3.55	3.01	3.38	3.47	3.81	4.07	3.73	3.26	4.02	1.66	3.63	4.83
	C18 'eR'	3.89	3.36	3.59	3.41	3.65	3.50	3.82	3.34	4.32	1.92	3.62	4.72
Spectral slope	'init'	0.022	0.022	0.022	0.023	0.022	0.021	0.021	0.022	0.022	0.022	0.019	0.019
	XC 'eR'	0.019	0.019	0.019	0.019	0.019	0.018	0.019	0.019	0.019	0.018	0.017	0.017
	C18 'eR'	0.017	0.017	0.017	0.017	0.017	0.017	0.017	0.017	0.017	0.017	0.016	0.014

* From Zigah 2012; -- No measurements

Table 2-2

Elemental data from formula assignments. The subscript w indicates magnitude-averaged values; the subscript n indicates number-averaged values as described in Minor et al. 2012.

	BR surf XC	BR surf C18	BR surf XC exclusive	BR surf C18 exclusive	WM surf XC	WM surf C18	WM surf XC exclusive	WM surf C18 exclusive
DBE*	13.22	13.10	18.44	17.63	13.40	13.64	18.46	19.08
DBE/C	0.42	0.40	0.43	0.36	0.45	0.44	0.46	0.40
H/C_n	1.314	1.353	1.263	1.394	1.273	1.304	1.206	1.309
O/C_n	0.413	0.398	0.386	0.338	0.419	0.412	0.381	0.361
N/C_n	0.156	0.159	0.222	0.226	0.166	0.162	0.222	0.207
P/C_n	0.009	0.007	0.015	0.009	0.013	0.009	0.022	0.010
S/C_n	0.003	0.003	0.007	0.005	0.003	0.003	0.008	0.006
H/C_w	1.299	1.343	1.271	1.418	1.273	1.298	1.214	1.311
O/C_w	0.431	0.403	0.387	0.335	0.424	0.419	0.366	0.360
N/C_w	0.094	0.106	0.219	0.230	0.128	0.106	0.231	0.205
P/C_w	0.006	0.005	0.015	0.009	0.013	0.007	0.028	0.012
S/C_w	0.002	0.002	0.007	0.005	0.001	0.001	0.008	0.005
FN	47.50	48.28	67.35	68.32	48.78	48.29	66.43	64.25
FP	14.68	13.28	20.36	15.38	17.98	14.97	26.53	16.35
FS	4.96	4.58	9.93	8.31	4.65	3.70	11.18	7.83
%CHO	46.15	45.60	18.27	18.69	45.83	46.66	19.73	23.25
%CHON	30.79	32.71	43.72	48.91	29.13	31.76	36.44	44.89
%CHOS	1.55	1.22	2.80	1.63	0.89	0.60	1.87	0.89
%CHONS	2.30	2.49	4.45	4.90	2.12	2.20	4.85	5.01
%CHOP	0.62	0.63	1.46	1.42	0.45	0.73	0.95	1.85
%CHONP	12.58	11.36	15.56	11.39	14.93	12.82	19.21	12.11
%CHONSP	0.55	0.36	1.42	0.73	0.76	0.36	2.07	0.73

*The equation DBE=(C+^{13}C)-H/2+N/2+1 was used to calculate the DBE of each molecule. Then these DBEs were number-averaged, i.e., were calculated by dividing the sum of the DBEs by the total number of assigned formulae, for the value reported here.

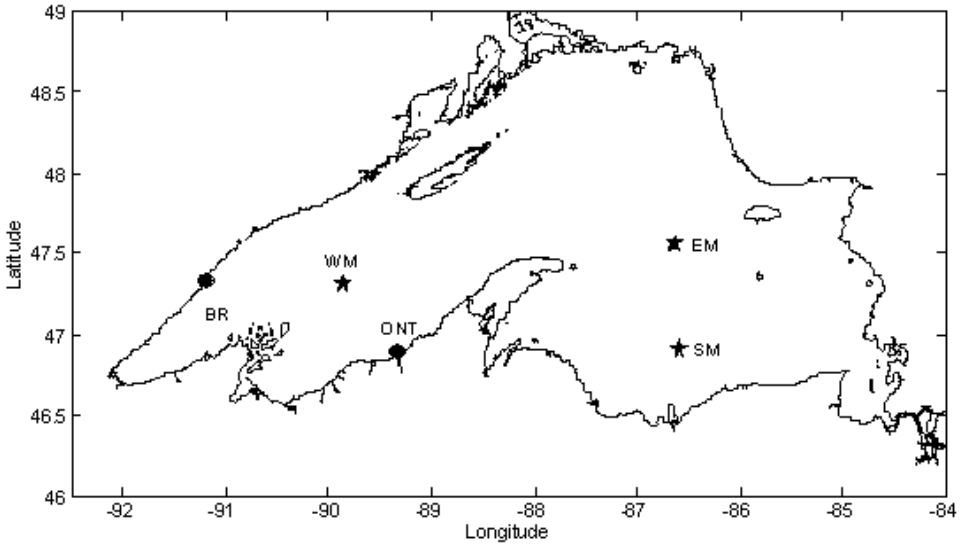

Fig. 2-1 Lake Superior. Stars indicate open-lake stations and circles indicate near-shore stations.

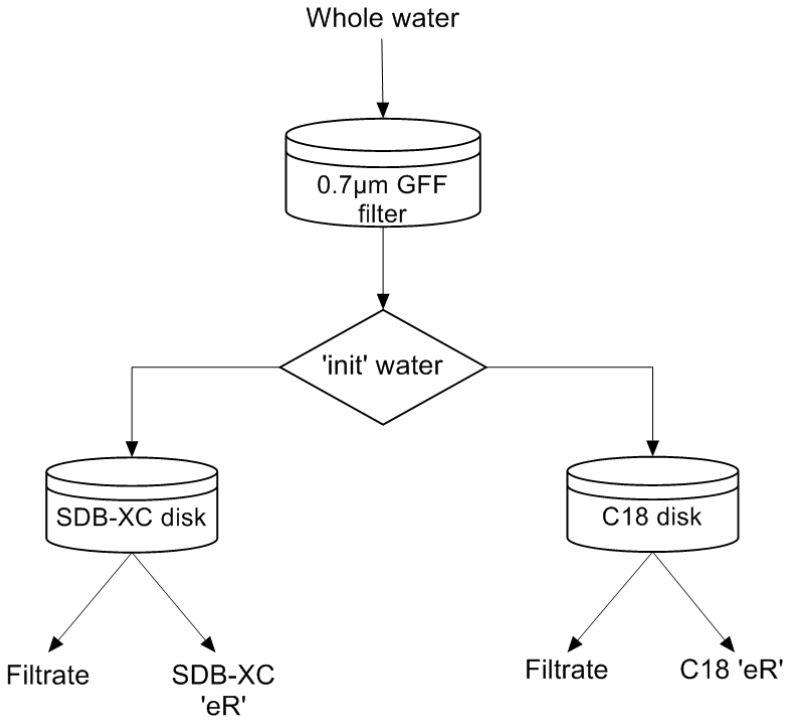

Fig. 2-2. Protocol used for sampling and extraction, including naming conventions followed in the text.

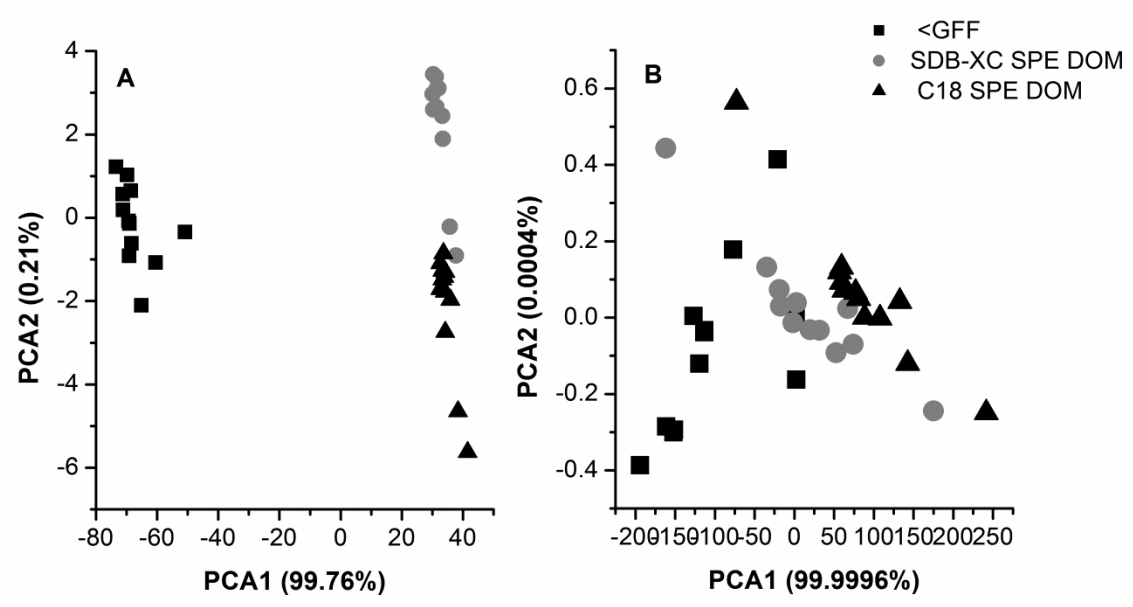

Fig. 2-3 Principle component analysis results based on A) normalized absorption coefficients from 200 to 800cm^{-1}; B) spectrophotometry indices including E2/E3, SUVA254 and spectral slope of all samples. Black filled squares represent <GFF 'init' samples; gray filled circles represent SDB-XC SPE DOM samples; triangles represent C18 SPE DOM samples.

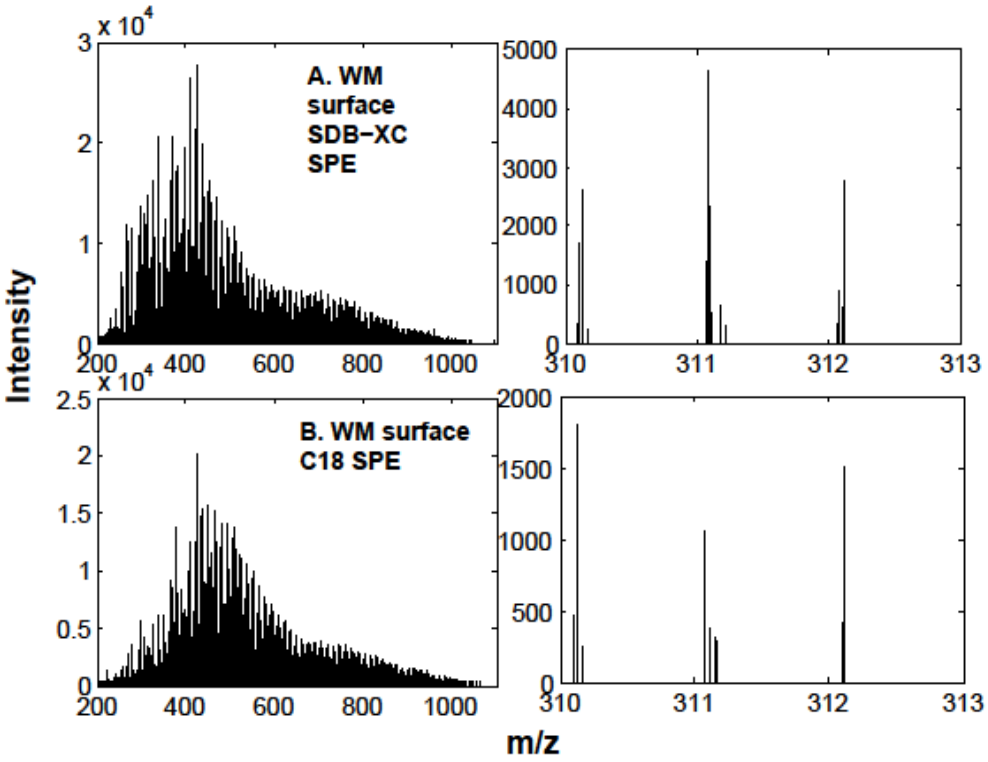

Fig. 2-4 Negative ion mode FTICRMS of a) WM surface SDB-XC SPE DOM with the enlargement of m/z 310 to 313 on the right, b) WM surface SDB-C18 SPE DOM with the enlargement of m/z 310 to 313 on the right.

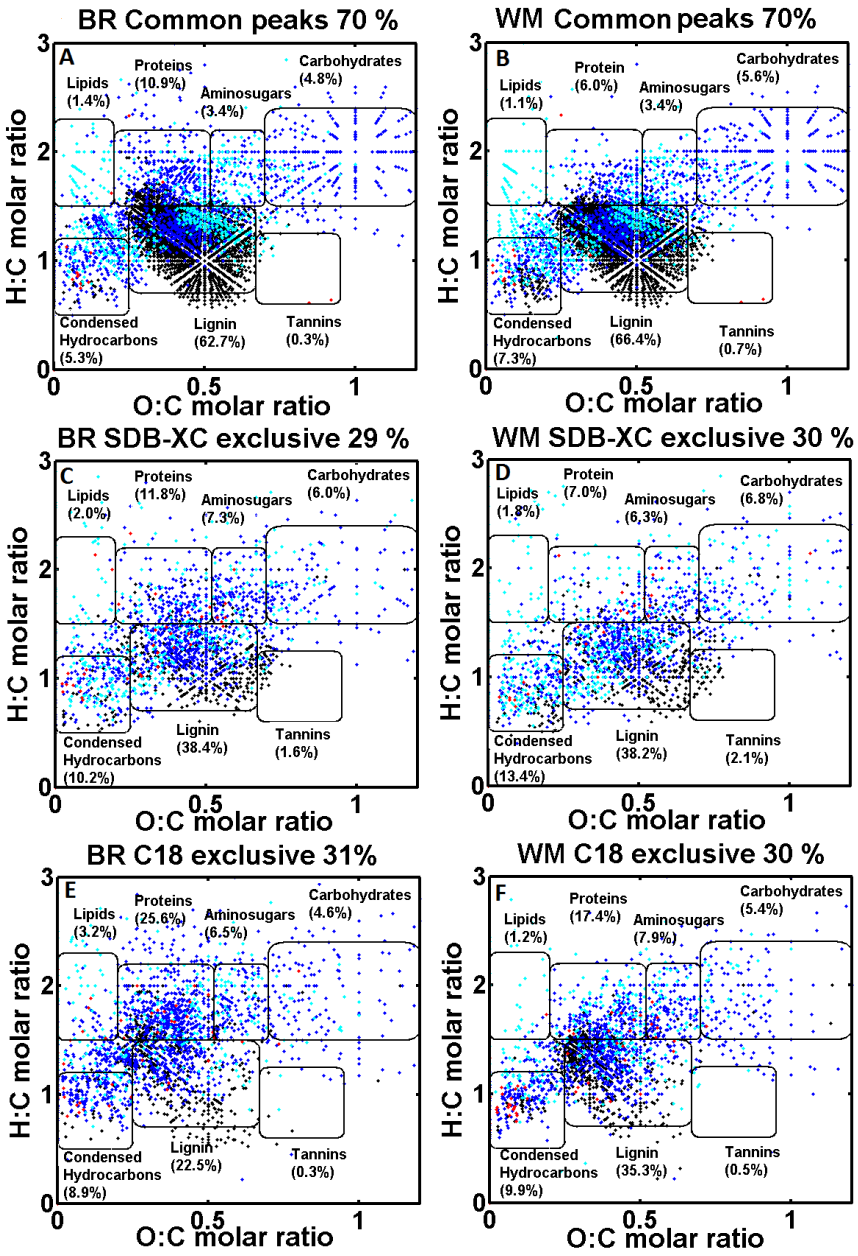

Fig. 2-5Van Krevelen diagram of a) formulae (m/z) found in both C18 and SDB-XC SPE DOM for surface sample at BR site; b) formulae (m/z) found in both C18 and SDB-XC SPE DOM for surface sample at WM site; c) unique compounds from SDB-XC SPE DOM at BR; d) unique compounds from SDB-XC SPE DOM at WM; e) unique compounds from C18 SPE DOM at BR; f) unique compounds from C18 SPE DOM at WM; CHO and CH compounds (black) are overlaid with CHON (blue) compounds on top of which any CHONP compounds (cyan) are placed. Any CHOP compounds (red) are on the top. The van Krevelen spaces are divided into seven discrete regions, modified from the diagrams proposed by Hockaday et al. 2009, Kim 2003; Sleighter and Hatcher 2007. The percentage of peaks from each region over total number of peaks in the sample is shown in brackets.

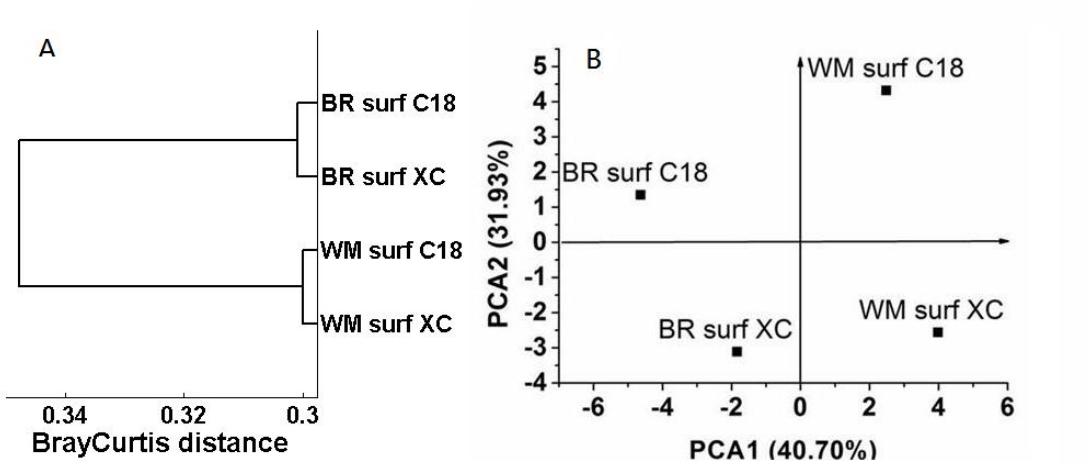

Fig. 2-6 Comparison of C18 SPE DOM and XC SPE DOM based on peak absence/presence of FT-ICR-MS. A) Cluster diagram of the samples based on original Bray-Curtis distance. The samples with lower information content (lower x-values) are more similar than those which occur farther apart; B) Principle component analysis results.

Chapter 3 Biochemical characteristics of settling particulate organic matter in Lake Superior: a seasonal comparison

Summary

To assess settling particulate organic matter (POM) seasonality and availability to the benthic community, settling particulate matter was studied in terms of mass fluxes and main biochemical characteristics (including organic carbon, nitrogen, and stable isotopic content) at two Lake Superior offshore sites over the course of a year. Fourier transform infrared spectroscopy (FTIR) and hydrolysis, extraction, and derivatization approaches were used to provide further compositional information. A similar seasonal pattern was observed at both sites. The C, N and stable isotope compositions show that the increase in sinking flux is variably associated with sediment resuspension and enhanced surface production. Elevation of particulate carbohydrate carbon normalized to POC (PCHO-C%) values, total hydrolysable amino acids per grams of dry sample weight (THAA), THAA normalized to POC (THAA-C%) and THAA normalized to PON (THAA-N%) values was seen at both sites corresponding to enhanced primary productivity in summer. However, distinct amino acid distributions at the two sites were revealed by PCA based on amino acid Mol % composition, possibly resulting from differences in OM sources and the degree of degradation occurring at the two sites. FTIR shows that spring particulate material has relatively strong inorganic clay mineral signals, indicating major sources from sediment resuspension and/or spring runoff. Summer particulate material has higher proportions of amide, carbohydrate and other organic functional groups indicating autochthonously derived material. The combination of PCHO-C%, THAA and FTIR data revealed that the relative bioavailability and nutritional values of POM to benthic microbes should be lower in spring than summer, although both periods exhibited high sinking fluxes. Due to sediment resuspension events and an oxic water column,

organic matter eventually buried in Lake Superior's sediments has probably experienced extensive alteration due to several trips through the water column and the highly bacterially active sediment-water interface.

3.1. Introduction

Particulate organic matter (POM) in aquatic ecosystems plays significant roles in the global carbon cycle by serving as a food source for heterotrophic organisms and by transporting organic matter produced in the euphotic zone to the sediments. During its transport, POM undergoes biogeochemical changes such as uptake by biota, solubilization, remineralization, and exchange with DOM, and a portion of it eventually reaches the surface sediments (Wakeham et al., 1997; Hedges at al., 2000, Burdige 2007). POM by its innate composition and its reactivity affects the cycles of global carbon, nutrients, and trace metals as well as anthropogenic pollutants (Eppley and Peterson, 1979, Sholkovitz and Copland, 1981, Baker and Eisenreich, 1989; Baker et al., 1991). Molecular level characterization of detrital POM as well as its variation is necessary not only for investigating the source and dynamics of POM but also for a better understanding of degradation and selective preservation of the macromolecules in POM. The study of temporal and spatial changes in potential food items in POM is also a key step in understanding the dynamics of benthic communities. Although detailed characterization of POM is important, it is difficult as a result of POM being heterogeneous, consisting of living and dead cells, fecal pellets, aggregates, organically coated mineral grains, and other materials.

Carbohydrate and protein are among the major biochemicals produced by photosynthetic processes in the euphotic zone. They represent a significant component of the particulate organic matter in the water column (Lee and Cronin 1982; Lee and Cronin 1984; Pakulski and Benner, 1992) and in sedimentary material. Particulate carbohydrates (PCHOs) were found to comprise 5–20% of the total sediment particulate organic carbon (POC) in marine sediments (Cowie and Hedges,

1992; Burdige et al. 2000). Amino acids, the building blocks of protein molecules, can comprise from less than 1% to as much as 50% of the organic carbon, and 10 to 100% of the organic nitrogen in oceanic deep water column POM and sediments (Lee and Cronin 1984; Lee 1988). The distribution of carbohydrates and amino acids in POM mainly depends on the source of the organic matter, the depositional rate and the water depth. It reflects the balance between biological production and biological consumption through the journey of those compounds to the bottom of the ocean/lake. Understanding the temporal and spatial changes in quantity and quality of carbohydrates and amino acids are very important to the study of benthic heterotrophic activities by microbes and macroorganisms. Wet chemical extraction and detection methods have been developed and applied as classic ways to quantify carbohydrates and amino acids in marine and fresh water POM samples. The MBTH (3-methyl-2-benzothiazolinone hydrazone hydrochloride) method of carbohydrate analysis (Johnson and Sieberth, 1977) and the precolumn o-phthalaldehyde (OPA)/ -mercaptopropionic acid (MPA) derivatization method of amino acids analysis are applied in this study. The MBTH method determines total carbohydrates within samples based on the spectrophotometric detection of formaldehyde produced from the periodic acid oxidation of monosaccharide-derived alditols with MBTH. With this method, the quantity of total carbohydrates (TCHO; free + combined monosaccharides) can be obtained with high precision (Pakulski and Benner, 1992). The precolumn OPA/MPA derivatization method is based on the separation of amino-acid derivatives by reverse-phase high-performance liquid chromatography (HPLC), followed by fluorescence detection.

Fourier transform infrared spectroscopy (FTIR) is one of the most available and widely used techniques for structural characterization of molecules. It is inexpensive, non-labor intensive and can quickly provide an overview of compound class or functional group composition in complex mixtures of organic matter based upon analysis of a small amount (~1mg) of raw dried sample (Abdulla et al., 2010). FTIR

analysis is based on the fact that vibrations of different covalent bonds in organic functional groups absorb infrared radiation at different wavenumbers resulting in an IR spectrum that can be used for structural characterization of molecules. However, as happens with DOM samples as well, the heterogeneity of POM samples acts to simplify their FTIR spectra, which exhibit broad bands resulting from overlap of multiple functional groups (Li and Minor, 2013). Thus, this study applies classic wet extraction and derivative molecular techniques for the analysis of carbohydrates and amino acids, and stable isotope analyses, along with FTIR characterization of sinking POM. Our main aims were to investigate the origin and biochemical composition of settling particulate organic matter (POM) in the open-water region of Lake Superior over seasonal scales and to assess POM nutritional values for benthic consumers, which are of considerable interest in biogeochemical studies.

3.2 Material and methods

3.2.1 Study site and sampling details

Lake Superior is the Earth's largest lake by surface area (82,100 km^2), with a maximum depth of over 400 m, mean depth of 150 m, water residence time of 180 years, and is dimictic, mixing twice annually, once in Spring (June/July) and once in Fall (December/January) (Herdendorf, 1990; Urban et al., 2005; Austin 2008). Lake Superior has low rates of primary production (Sterner et al. 2004). The dissolved organic carbon and particulate organic carbon concentrations range from 89 to208 μM and 2.3 to16.5 μM, respectively (Zigah et. al. 2012). Organic carbon deposition in Lake Superior sediments is about 0.48×10^{12} g C yr^{-1} (McManus et al., 2003) to 1.5×10^{12} g C yr^{-1} (Johnson et al., 1982; Klump et al., 1989).

McLane Parflux 21 cup sequential sediment traps with a diameter of 0.92 m^2 were deployed with moorings located in the eastern (EM, 125 m, total water depth 240 m) and western (WM, 150 m, total water depth 180 m) arms of the lake, as shown in Fig. 3-1, to obtain settling POM samples in the hypolimnion from October 2009 to

September 2010. On the same moorings, temperature loggers were deployed at a variety of depths from the surface to 150-200 m. The sample cups were programmed to rotate and collect descending particulate matter for 10/11 days during winter and 3/4 days during summer over an entire year period. Only deionized water was added to each cup and no other preservative was used. After removal from the lake (where *in situ* temperature was ~4°C) sediment trap samples were refrigerated at 4-5°C until further analysis. Material captured in the sediment traps was then equally split into 10 fractions with a McLane sediment trap splitter. Fractions of the captured material were freeze-dried and homogenized prior to further analysis for total carbon (C), total nitrogen (N), stable isotope ratios of C and N, total carbohydrates, total amino acids as well as FTIR.

3.2.2 Elemental and isotopic analysis

Acid fumigation (Harris et al., 2001) was used to remove carbonate carbon before elemental analysis (EA) and isotope ratio mass spectrometry (IR-MS). Weighed aliquots of sample were placed in clean Ag capsules and 50 ul MilliQ water was added to each aliquot. The samples were then fumed over 12M HCl (6-8 h), oven-dried (60°C, 4 h) and cooled. For more complete combustion, each sample (in the Ag capsule) was enclosed within a Sn capsule before %C, %N, $\delta^{13}C$ and $\delta^{15}N$ determination. One subset of samples was analyzed with a Costech CNS analyzer interfaced with a ThermoFinnigan Delta PlusXP stable isotope ratio mass spectrometer at the Large Lakes Observatory. The typical standard deviations for the instrumentation based on analyses of multiple external standards were 0.2‰ for $\delta^{13}C$ and 0.17‰ for $\delta^{15}N$. A second subset of samples was analyzed with a Micro Cube elemental analyzer interfaced to a PDZ Europa 20-20 isotope ratio mass spectrometer at the University of California Davis Stable Isotope Facility. The long term standard deviation for this instrumentation was reported to be 0.2‰ for $\delta^{13}C$ and 0.3‰ for $\delta^{15}N$. For both sets of sample measurements, replicates of at least two different laboratory standards (previously calibrated against NIST Standard Reference

Materials), which were selected to be compositionally similar to the samples, were interspersed with samples being analyzed. The stable isotope ratios are reported using delta notation (δ). This notation compares the ratio of the heavier isotope to the lighter isotope in a sample to the analogous ratio in a standard as defined with the following equation:

$$\delta = \left(\frac{R_{sample}}{R_{standard}} - 1 \right) \times 1000$$

equation (1.2)

The final delta values are expressed in permil (‰) relative to international standards V-PDB (Vienna PeeDee Belemnite) and Air for carbon and nitrogen.

3.2.3 FTIR spectra Measurement and Pre-processing

Spectra were obtained with a Nicolet Magna IR 560 FTIR ESP spectrometer equipped with purge gas generator unit by collecting 200 scans from 4000 to 400 cm^{-1} with a resolution of 2 cm^{-1} and using Happ-Genzel apodization. For expelling CO_2 contamination coming from air, 1 lag time (5 min) was employed between closing the analytical chamber and starting analysis. Freeze-dried, homogenized (but not acid-treated) samples were run as KBr pellets (1 mg sample, 150 mg KBr, homogenized in a mortar and pestle, 1500 psi). Each pellet was dried in a desiccator (>6 hrs) before analysis. A pure KBr pellet (KBr dried 2h at 105ºC prior to use, resulting pellet placed in desiccator overnight) was analyzed before each sample analysis as a background blank. Spectra were converted to absorbance units and baseline corrected. The second derivatives of these spectra were generated using Origin 7.0 and the 2nd order Savitzky-Golay method with 11 convolution points.

3.2.4 MBTH Total Carbohydrates Analysis

The MBTH method of carbohydrate analysis (Johnson and Sieberth, 1977) was applied to quantify total carbohydrates. The procedures applied in this study are adapted from Pakulski and Benner, 1992 and described briefly as following. A known

amount of each sample was first hydrolyzed with 12 M (72 wt. %) H_2SO_4 for two hours, diluted to 1.2M and then further hydrolyzed for 3h at 100°C. The diluted hydrolysate was neutralized with NaOH and reduced with freshly prepared ice-cold 10% KBH_4 to form formaldehyde. Then replicates of 2 ml aliquots of the resulting hydrolysate were taken for further oxidation with periodic acid (H_5IO_6). After reacting with MBTH, and a yellow-green color development, absorbance was recorded immediately at 635 nm with a spectrophotometer equipped with a 1 cm quartz cuvette. Dilution (5-10 fold) of the reduced and acidified hydrolysate was often necessary to obtain acceptable (less than 1.0) absorbances (e.g., 2.0 mg D-glucose hydrolysate needed to be diluted by a factor of 10). All chemicals used were ACS grade or ≥98% purity.

The amount of carbohydrate present in the samples was calculated by comparing the absorbance of the unknown samples with the absorbance of glucose standards using the relationship:

sample glucose wt. equivalent (mg)
= (sample absorbance) × (wt, glucose standard)/(glucose absorbance) eq. 3-1

Because glucose is 40% carbon by weight, the amount of glucose equivalent carbon in the sample was estimated as

sample carbohydrate carbon (mg C) = sample glucose equivalent (mg) × 0.4 eq. 3-2

3.2.5 Total Amino Acid Analysis: OPA/MPA Derivitization

Pre-column OPA/MPA derivatization combined with HPLC was employed to determined Total Hydrolysable Amino Acids (THAA) (adapted from Lindroth and Mopper, 1979; Mengerink et al. 2002; Frank and Powers, 2007), which were reported as THAA (mg) normalized to dry sample weight (g). Ten freeze-dried samples,

chosen to cover multiple seasons and both sites, were hydrolyzed with 3ml of 6N HCl under 110°C for 19hr (Lee and Cronin, 1982) and then dried in a vacuum oven to remove HCl. Each sample was then re-dissolved in 2ml of water and filtered through a pre-combusted Whatman glass microfiber filter (Grade GF/F 0.7μm, 25 mm) to remove particles. The combination of the hydrolysate and the washings of each sample was then dried in vacuum oven prior to derivatization and HPLC analysis.

The OPA/MPA derivatization reagent was prepared fresh each day by mixing, in order of listing, 6.25 mL methanolic OPA (2mg/mL in HPLC grade methanol), 10.0 mL borate buffer (0.2 M; pH=9.9) and 25 uL MPA solution. The final pH of the derivatization reagent was 9.36±0.05. Each dried hydrolysate sample was dissolved in 500 μl of MilliQ and filtered through a Whatman Puradisc 4mm Syringe Filter (0.2μm, PES membrane, polypropylene housing). No rinsing was applied prior to filtration of the samples; however, a method blank was collected and measured together with samples. Five μl aliquots of the filtered hydrolysate were then mixed with 500 ml of the borate buffer (0.2 M; pH=9.9) and derivatized with 40 μl of OPA/MPA reagent right before HPLC analysis.

The SHIMADZU HPLC system consisted of a LC-10A7 dual piston pump, a RF-10AXL fluorescence detector and a SIL-10A auto-sampler, all controlled by the SCL10A system controller for chromatographic analysis. PeakSimple 3.29 software was used for data collection. The separation of the amino acid derivatives was achieved on a Waters (Milford, MA) XBridge Shield RP18 column (100mm x 4.6mm i.d., 3.5μm particle size). The chromatographic separation was performed at a temperature of 30°C. The flow rate of the mobile phase was 1 ml/minute. Detection was performed fluorometrically with an excitation wavelength of 340 nm and an emission wavelength of 455 nm.

Gradient elution involving two mobile phases was employed. Mobile phase A consisted of 0.02 M sodium acetate buffer mixed with 0.3 % tetrahydrofuran (THF) adjusted to pH 7.2 with 6 M NaOH. Mobile phase B consisted of HPLC grade water and acetonitrile with a 1:1 ratio. All buffers were filtered through a 0.2μm filter and degassed with ultrapure helium. The total HPLC run time for the separation of the derivatized amino acids in a single sample or standard was 40 minutes. The gradient timetable was as follows:

Time (min)	%B
0	0
4	8
5	12
6	13
9	18
14	21
26	30
36	42
37	100
40	100
41	0
43	0

Stop time 43.01

HPLC grade methanol, acetonitrile and the Pierce Amino Acid Standard H with 17 amino acids were obtained from Fisher Scientific. Deionized water was processed through a Milli-Q purification system (Millipore, USA). All solid phase chemicals were CAS degree or >98% purity.

3.3 Results and discussion

3.3.1 Mass fluxes, organic carbon fluxes and stable carbon isotope analysis

Settling particulate mass fluxes and organic carbon fluxes determined by sediment traps at the east basin (EM) and west basin (WM) of Lake Superior are shown in Figure 3-2. The settling particulate mass fluxes ranged from 4.41 to 382 mg/m^2/day at EM and 59.7 to 592 mg/m^2/day at WM. These fluxes were considerably lower than values (560 to 1940 mg/m2/day) measured at the same depth in Lake Michigan (Meyers and Eadie, 1993; Eadie et al. 1984); however, the yearly averages were comparable to fluxes in the open ocean at 150m depth. Lake Superior settling particulate mass flux also exhibits greater seasonal variation than the ocean site at this depth (Buesseler et al. 2007). The two open-lake sites have similar seasonal variations, with a considerable increase in mass fluxes in late December and late May. This is consistent with previous settling mass flux measurements (0.001 to 1.2 g/m^2/day) at WM site measured at 145m depth from 2005 to 2008 (Woltering et al 2012), which showed the highest flux occurring in the same two periods as this study. The high settling fluxes are likely due to the winter and spring water column mixing causing enhanced benthic fluxes from local sediment reuspension and downslope sediment transportation in turbidity currents. WM has mass fluxes approximately 4-fold higher than at EM during summer stratification and only slightly higher mass fluxes during the unstratified season (Fig. 3-2). This is likely due to the higher primary production (Sterner 2010) and stronger sediment resuspension at WM relative EM. Thus, the total mass flux profiles at WM and EM suggest that the variations in vertical fluxes result from seasonal variations in primary production and sediment resuspension events.

Organic matter fluxes ranged from 0.64 to 23.1 mgC/m^2/day at EM and 3.72 to 30.8 mgC/m^2/day at WM. These values are comparable to carbonfluxes measurements (Heinen andMcManus et al. 2004) from 1999 to 2000 at 250m water depth (~35

meters above the bottom) at a different site in the western arm of Lake Superior; these literature values varied between 6.0 and 43.2 mgC/m^2/daywith a minimum during winter and a maximum duringspring. However, these values, like the total mass flux values, are much lower than in other Laurentian Great Lakes (Meyers and Eadie, 1993; Eadie et al. 1984) and are comparable or slightly lower than open ocean POM fluxes at 150m depth (Buesseler et al. 2007), though with much larger seasonal variation relative to the ocean. The fact that organic carbon fluxes have similar trends to the bulk particulate settling mass fluxes suggests that the particles originating from sediment resuspension may contribute both organic and mineral fractions to the settling POM pool. Based on modeled yearly water column primary production into POM being 200 to 350 mgC/m^2/day (Sterner 2010), extensive degradation of primary productionhas occurred in the Lake Superior water column;only a small fraction of this POM was able to reach deep water. This is consistent with Baker et al 1991, which shows that 75% of OCsettling from surface waters degrades in transit to the Lake Superior floor. This feature of POC degradation in LakeSuperior is similar to the open-ocean case, where water column degradation oforganic matter is quantitatively much larger than sedimentarydiagenesis. Comparing our POC fluxes to the reported annual average sediment POC burial rate (0.25 mol/m^2/year equivalence to 82 mg/m^2/day, Hales et al. 2008), intensive degradation might have occurred at the sediment-water interface, especially during summer when OC fluxes are much higher and contain more labile components (as discussed in section 3.4.2 and 3.4.3).

OC% and ON% values in sinking material in the hypolimnion of Lake Superior are higher during summer stratification than in other seasons (Fig 3-3a), which is consistent with stronger summer input by primary productivity. The lower organic carbon contents of settling solidsduring unstratified conditions as seen in Fig. 3-3,are likely due to a largercontribution from eroded clays and resuspended sedimentsto the settling flux at that time.

The two sites have similar seasonal variations in terms of C/N ratios and stable carbon and nitrogen isotope values. Settling POM at both sites has similar molar C/N ratios (9.98±0.74 at EM and 9.75±1.22 at WM), suggesting that the dominant POC source is algal or microbial, as opposed to land vascular plant material, which generally has C/N ratios greater than 15. The slightly decreased C/N ratios in summer are consistent with higher inputs from primary production. Except for one sample, the C/N values of all spring-winter samples vary little. This similarity might be due to the lack of a fresh supply of organic matter and extensive degradation over winter and during the mixing event. One exception is that the samples collected around Nov 26th 2009 at both EM and WM exhibit high C and N contents, a higher C/N ratio and more depleted $\delta^{13}C$ values, most likely due to a strong wind and rain event (weather underground archives) that happened in the time period causing high influence by terrestrial inputs. Organic carbon stable isotope ratios change little with seasons at both locations, being -27.9 to -29.7‰ at EM and -27.5 to -29.2‰ at WM. These $\delta^{13}C$ values are similar to those obtained from the plankton tows in Lake Superior (-27~-29‰), suggesting that the settling POM is mainly derived from autochthonous productivity (Meyers and Ishiwatari, 1993; Ostrom et al., 1998).

Although the two sites have similar seasonal variations in terms of organic carbon, nitrogen and isotope contents, settling particulate material at WM contains higher OC and ON contents than EM in the summer season and increases in the OC and ON contents occur after the onset of stratification. This is likely due to stronger primary production at WM relative to EM, based upon chlorophyll concentrations and nutrient levels (Barbiero1 and Tuchman, 2004; Sterner 2011). Compared to the surface sediments (Li, et al 2013 and Fig 4-2), the settling solids are two to four fold more enriched in organic carbon and organic nitrogen than the sediments 30 to 115 m below, suggesting intensive degradation in the deep lake (most likely occurring at the sediment-water interface) and is consistent with differences seen between our POC fluxes and reported annual average sediment POC burial rate (0.25 mol/m^2/year

equivalence to 8.2 mg/m^2/day, Hales et al. 2008). The slightly higher C/N ratios and more enriched $\delta^{13}C$ values in the sediments relative to the settling POM also suggest a greater proportion of microbially reworked OM in the sediments.

3.3.2. Carbohydrate and Amino acid distributions

In addition to bulk parameters such as mass flux and %OC changes, there are also temporal changes in the composition of the organic carbon being delivered, which potentially affect lower water column and benthic heterotrophic activities by microbes, zooplankton and macroorganisms. Particulate carbohydrate carbon normalized to POC (PCHO-C%),reported as a percentage, ranges from 7.0% to 18.8% at EM and from 4% to 19.7% at WM. These are comparable to the PCHO-C%values in the Equatorial Pacific at depths of 105m (18%) to 4000m (5%). Increasing PCHO-C% was seen at both sites from winter-spring to summer, suggesting that higher primary productivity enhanced transportation of carbohydrates to the lake bottom in the warmer, more productive summer season. However, WM and EM (Fig. 3-4a) showed very different spatial and temporal patterns in terms of the total PCHO-C flux. WM showed a steady increase from winter-spring to summer as a primary production response, while a pattern resembling POC mass fluxes was seen at EM site, suggesting an overall impact by sediment resuspension.

For the ten selected samples covering both sites and different seasons, as shown in Fig. 3-5, THAA content varies from 12.9 to 50.4 mg/g of sample; THAA-C accounted for 8.5 to 25.0% of total organic carbon and THAA-N constituted 31.3 to 90.2% of total particulate organic nitrogen (ON). THAA contents, THAA normalized to POC (THAA-C%) and THAA normalized to PON (THAA-N%) values at WM and EM (Fig. 3-5) showed different temporal patterns similar to those with PCHO-C flux. WM showed a steady increase from winter-spring to summer as a primary production response, while a pattern resembling POC mass fluxes was seen at EM site, suggesting influence on amino acids by sediment resuspension. The general

elevations in THAA in summer-settling POM samples at both sites are also consistent with their higher OC and ON contents. The THAA, THAA-C% and THAA-N% values are about two fold higher than those of the ocean at 1357m depth (Gupta and Kawahata, 2000). Considering Lake Superior has comparable primary production to oceans (Sterner, 2010), water depth is likely playing a key role in the preservation of more amino acid in the settling particulate material in Lake Superior. Although total amounts of THAA varied considerably, settling POM samples appeared to be rather similar in terms of the distributions of the individual amino acids (Table 3.1). In all samples (except the sample from the WM 1-14-10 cup), glycine/threonine dominated, with a contribution of up to 41.5 mol%, followed by aspartic acid, histidine and alanine, which contributed 10-20 mol%. Glutamic acid, serine, valine, cystine, leucine, and lysine hydrochloride/proline accounted for 5-10 mol%, and a minor group of arginine, isoleucine, phenylalanine, tyrosine and methionine contributed <5 mol%. This distribution is very similar to that reported for coastal marine sediment samples in Dauwe and Middelburg (1998).

Despite overall similarity between samples, some molar composition differences can be seen (Table 3.1). Due to the overlapping of threonine and glycine, valine and cystine, the Amino Acid based Degradation Index (Dauwe and Middelburg, 1998 and further revised in Dauwe 1999) is not applicable to our data. However, principal component analysis (PCA) based on the Mol % composition of the 17 amino acids in the selected 10 sediment trap samples were applied in the same way as in Dauwe 1999 to investigate the variation of amino acid distribution among samples, as shown in Fig 3-6. Principal component 1 (PC1), which accounts for 75.3% of the variability, separates the samples from EM and WM sites with most EM samples on the negative PC1 side and all WM samples on the positive side of PC1. This suggests distinct amino acid distributions at the two offshore sites, possibly resulting from different settling POM sources (different primary producer community structure) and/or a different extent of degradation at the two sites. Factor coefficients (principle

component loadings) give the relation between the principle components and the original variables (mole percentage of protein amino acids). PC1 has negative coefficients for threonine, glycine, arginine and tyrosine and positive coefficients for all other amino acids; these differences drive the clustering of samples along PC1. Positive correlation can be found between PC1 score and THAA contents for samples from EM (N=5, R^2=0.7864, P=0.0449), with high THAA-content summer samples having more negative PC1 values. However, no correlation is found between PC1 score and the THAA contents of samples from WM (N=5, R^2=0.1801, P=0.4752). This suggests that primary production and amino acid degradation are the main factors affecting amino acid distribution at EM, however, it is likely that other factors such as stronger dilution effects from sedimentary material inputs is affecting the amino acid composition at WM site.

Employment of the sum of carbohydrate, protein and lipid contents has been reported (Navarro and Thompson 1995) as a good estimate of the readily available fraction of POM. While lacking quantitative lipid data (which is generally much smaller that carbohydrate and amino acid concentrations), based upon the PCHO-C%, THAA-C% and THAA-N% variations in this study, I estimate summer POM has 2 two 5 fold higher nutritional values to the benthic consumer than spring-winter POM in Lake Superior at both sites.

3.3.3 Compositional variation of POM as seen by FTIR

3.3.3.1. Infrared absorbance of POM and its 2nd derivative spectra

FTIR spectroscopy was used to characterize settling particulate material collected with sediment traps in Lake Superior at the chemical functional group level. Fig. 3-7 shows FTIR absorbance spectra of individual settling particulate matter samples collected at different times of the year at both EM and WM sites. As reported in previous studies of heterogeneous natural samples with FTIR (Abdulla et al., 2010, Li

et al. 2013; Madejová and Komadel, 2001), a relatively high degree of similarity among samples was observed. This is, in part, due to the overlap of peak responses of multiple functional groups, which broaden FTIR bands and simplify the FTIR spectra. However, peak shifts and peak intensity differences can be seen as a function of sampling time, indicating seasonal changes in POM composition. To resolve overlap bands within each spectrum and to identify exact frequency of peak responses, the 2nd derivative of the FTIR spectra was applied (Smith, 1996; Griffiths and De Haseth, 2007). Below we discuss the main FTIR bands in spectra of all samples based on the peaks resolved by the 2nd derivative spectra (e.g., Fig. 3-8).

All spectra show a broad O-H/N-H absorbance peak centered between 3280 to 3420 cm^{-1}, attributed to the overlap of O-H stretching in organic alcohols, carbohydrate and carboxylic acid compounds or the N-H band of amide or even OH groups bonded to silicates/silica (Pandurangi et al. 1990). The broadness of this peak results from multiple intra-molecular and inter-molecular hydrogen bond interactions. The multiple strong peaks within the 1200-1000 cm^{-1} range (for instance, 1005 cm^{-1}, 1037 cm^{-1} and 1097 cm^{-1} in Fig. 3-8A) are potentially C-O bands from carbohydrates. Carbohydrate occurs in natural organic matter as many different forms of polysaccharides, monosaccharides, oligosaccharides or even conjugation of saccharides with proteins or lipids as glycol-conjugate compounds (Yang et al, 1995; Brandenburg & Seydel, 2002). The C-O bands of these different forms and isomers of carbohydrates appears as a range of frequencies between 1200 to 1000 cm^{-1} due to the difference in C-O bond force constant which is affected by the differences in bond angle and electronic environment. The peaks centered at 1000 to 1100 cm^{-1} could also result from Si-O stretching of biogenic silica/ silicate minerals in settling particulate materials. The intensities (Fig 3-7 and 3-8) of these peaks suggest that polysaccharides/biogenic silica/silicate minerals are the dominant chemical constituents of Lake Superior settling particulate matter.

The compounds containing carbonyl C-O functional groups, including the carboxylic acids and esters, contribute to the small carbonyl absorbance peak centered between 1683 and 1748 cm^{-1}. Combining the carbonyl C-O signal with the C-C-O stretching around 1165 to 1185 cm^{-1}, the presence of aliphatic esters in POM can be confirmed. In addition to aliphatic esters, there is a signal consistent with the presence of the acetyl ester functional group, a possible C-C-O stretching band at 1238 cm^{-1}(Smith, 1999, Celi et al. 1997). But this peak could also be contributed by C-O asymmetric stretching in phenol (Celi et al. 1997) and from C-O vibrations in carbohydrates. Although protein has been considered susceptible towards degradation, the peaks centered around 1651 cm^{-1} (amide I, Silverstein, 1996; Smith, 1999) and 1540 cm^{-1} (amide II, Silverstein, 1996; Widjanarko et al. 2011) confirm the presence of amides, which are the primary building elements of protein and peptides, reaching the hypolimnion of Lake Superior. The large change in dipole moment during the C=O bond stretch gives FTIR the ability to detect small concentrations of amide functional groups (CON^{-}). The vibrations of lignin's aromatic rings, which show up as multiple peaks around 1515 cm^{-1} (Mascarenhas et al., 2000; Raiskila et al. 2007; Derkacheva and Sukhov, 2008) are observed in most POM samples throughout the year at both sites. However, the ~1515 cm^{-1} bands are present as very small contributions to the spectrum (Fig 3-8a, 1518 cm^{-1}). As these bands are fairly weak even in measurements of lignin isolations, the intensity of these bands cannot be applied quantitatively. The potential Si–O–Si asymmetric stretch around 1000 cm^{-1} combined with bands appearing at 3698 and 3620 cm^{-1} (see Fig. 3-8a), which are stretching vibrations of silinol Si–OH from biogenic silica (Smith,1999), confirm the presence of biogenic silica in settling particulate materials.

Thus, throughout the year Lake Superior settling particulate matter from both site EM and WM exhibit strong signals of clay minerals (and some biogenic silica) and recognizable signals from the organic chemical functional groups. Functional groups of carbohydrates, carboxylic acids, aliphatic/acetyl esters, amides/proteins and

phenols/lignins can be identified.

3.3.3.2 Seasonal variations of settling POM based on PCA and FTIR

PCA, a commonly used feature-based classification method (Kvalheim et al., 1985; Sanni et al., 2002), was performed on the data sets comprised of normalized FTIR spectra to investigate the variation among samples at different times of the year at each site. The data matrixes were z-scored and variance scaled before the PCA analysis was performed. Principal components 1 and 2 (PC1 and PC2) account for 76.7% of the variability in the EM data set. PC1 and PC2 account for 75.1% of the variability in the WM data set. As shown in Fig. 3-9, at both EM and WM sites, the winter-spring (Oct-May) POM samples tend to be clustered in negative PC1 space; and in summer, the samples shift toward more positive PC1 values. The separation of samples from different seasons confirms compositional differences of the particulate material as a function of seasonality. At both WM and EM sites, the tight clustering among winter-spring samples suggests higher compositional similarity, which is likely due to remineralization processes leading to a more similar residual POM. In contrast, a more variable composition of summer POM compared to winter-spring POM is revealed by the more scattered distribution of summer samples in the PCA plot. This PCA distribution of Lake Superior POM samples based on FTIR shows that August to September samples drive the PCA 1 variation at both sites.

Differences in the magnitude of the infrared absorbance at characteristic frequencies can be used to compare the amounts of corresponding functional groups present in a group of samples. Fig 3-10 shows seasonality of the primary functional groups within the settling particulate material at both sites based on infrared absorbance intensity changes at 1651cm^{-1} (Amide I C=O stretching), 1540 cm^{-1} (Amide II C=O stretching), 3410 cm^{-1} (O-H stretching of carboxylic acid and carbohydrate), 1736 cm^{-1} (aliphatic ester C=O stretching), 1097 cm^{-1} (carbohydrate/biogenic silica/silicate minerals) and 1005 cm^{-1} (carbohydrate/biogenic silica/silicate minerals). A similar seasonal pattern

of Amide I, Amide II, carboxylic acid, carbohydrate and aliphatic ester was observed, with very small fluctuation in terms of vertical flux of these functional groups in winter-spring season, and a significant increase in summer. Increase in the vertical flux of amides, carboxylic acid, carbohydrate and aliphatic ester after onset of summer stratification, is consistent with significantly elevated lake productivity in summer (Sterner 2010). Positive correlation can be found between amide I peak normalized intensity and THAA contents as obtained with derivative method for samples from both EM (N=5, R^2=0.8037, P=0.0394) and WM (N=5, R^2=0.7825, P=0.0462) sites, with higher THAA content samples having higher FTIR normalized amide I peak intensity (data not shown). However, a weaker correlation (N=10, R^2=0.4310, P=0.0392) was found when data of the two sites are put together. Similar relationships are seen with Amide II. This site specificity is likely due to the small THAA data sets and the different amino acid compositions of OM from different sources at the two different sites.

EM samples were found to be slightly higher in the relative abundance of the Amide I, Amide II, carboxylic acid and aliphatic ester functional groups relative to WM site. This is consistent with our bulk carbon content data in section 3.4.1, which shows higher total organic carbon content of EM samples compared to WM during stratification. As western Lake Superior is more productive than the eastern lake based upon chlorophyll concentrations and nutrient levels (Barbiero1 and Tuchman, 2004; Sterner 2011), these differences in organic carbon contents and organic matter functional groups between EM and WM are likely due to different degrees of dilution with inorganic compounds from mixing events and/or different degradation rates of compounds belonging to the above functional groups in the water column. A different pattern was seen for peaks at 1097 cm^{-1} and 1005 cm^{-1}, both of which represent overlap of signals from carbohydrate and biogenic silica/silicate minerals. The infrared absorbance of summer samples at these two wavelengths decreases relative to winter-spring. Considering that PCHO-C% increases in summer at both sites, the

intensities at 1097 cm^{-1} and 1005 cm^{-1} are therefore likely dominated by biogenic silica/silicate minerals signals. The biogenic silica/silicate minerals in sediments brought up by winter and spring mixing events may continually settle and contribute to the settling particulate matter pool, causing the higher peak intensity at 1097 cm^{-1} and 1005 cm^{-1} in winter-spring relative to summer. From this point of view, the slightly higher intensities at1097 cm^{-1} and 1005 cm^{-1} at WM are consistent with stronger currents and mixing events occurring at WM relative to EM (Bennington et al. 2010). This understanding of the temporal and spatial changes in the quantity and quality of biogeochemically important organic functional groups is potentially helpful to the study of benthic heterotrophic activities by microbes and macroorganisms.

3.4. CONCLUSIONS

Isotopic analysis, C and N contents, wet chemistry carbohydrate and amino acid analysis, and FTIR coupled with PCA were used to characterize settling particulate material and to study the spatial and temporal patterns of organic particulate matter sedimentation in Lake Superior. The origin and biochemical composition of POM were investigated to reveal POM nutritional value to benthic consumers.

A similar seasonal pattern was observed at both sites with the highest mass flux occurring in the unstratified season; however, the most organic rich samples were obtained from the summer stratified season. Processes controlling the type and quantity of sinking solids in the water column of the Lake Superior appear to be resuspension of surficial sediments and primary production.

Increases in PCHO-C%values, THAA contents, THAA-C% and THAA-N% were seen at both sites corresponding to enhanced primary productivity input in summer. However, distinct amino acid distributions as revealed by PCA did not appear related to primary production trends but possibly resulted from differences in OM sources and thedegree of degradation occurring at the two sites. The combination of PCHO-C%

and THAA suggests that summer POM has 2 to 5 fold higher nutritional values to the benthic consumer than spring-winter POM in Lake Superior.

Based on FTIR spectra, clay-minerals/biogenic silica are dominant in all samples obtained through the seasons. Despite the presence of a fully oxygenated water column, which usually facilitates major degradation of organic particles, the settling fluxes also contain a measurable fraction of organic matter, exhibiting functional groups including carbohydrate, carboxylic acid, aliphatic/acetyl ester, amide/protein and phenol/lignin. Principal component analysis of FTIR data from the sediment trap material suggests compositional variation as a function of season, with relatively strong inorganic clay mineral signals dominating in winter-spring and a strong signal from amide, carbohydrate and other organic components in summer. Thus, the relative bioavailability and nutritional values of POM to benthic microbes should be lower in winter than summer, although both the onset of winter and late-spring/early summer exhibited peaks in total mass and POC flux.

Strengths of the FTIR method for quantifying organics in particulate matter are that it produces measurements of organic functional groups, that it does not alter the sample during analysis and that it has relatively low sampling and analytical costs. However, FTIR can lead to overlapping signals for chemical species in POM and sediments; for example, signals at 1200 to 1000 cm^{-1} that could be from carbohydrates, biogenic silica and silicate mineral. Therefore it is good to couple FTIR analyses with extra tests such as the MBTH test for carbohydrate employed in this study for more complete characterization of POM.

Table 3.1. Organic carbon percentage (OC%), organic nitrogen percentage (ON%), molar carbon/nitrogen ratio (C/N ratio), concentration of THAA, THAA-C percentage, THAA-N percentage, and Mol% composition of the 17 THAAs in the selected 10 sediment trap samples covering both sites (EM vs WM) and seasons (winter vs summer). The sampling date listed is the middle day of the entire 11-12 days for each collection of the sample.

Sample date		1-14 2010	4-12 2010	5-26 2010	7-31 2010	8-14 2010	10-20 2009	1-14 2010	4-12 2010	5-26 2010	7-26 2010
Amino Acids* Mole %	ASP	11.4	16.1	11.5	15.2	9.9	18.1	11.3	8.4	12.9	12.4
	GLU	8.2	12.4	8.9	10.4	7.5	13.4	8.1	7.2	9.7	9.6
	SER	9.7	6.8	8.1	9.5	8.1	3.3	10.1	8.2	8.5	9.1
	HIS	10.9	9.9	10.0	10.6	0.9	7.1	21.0	8.2	11.0	11.2
	THR/GLY	16.5	22.0	14.8	26.0	41.5	9.9	2.7	16.0	16.9	18.6
	ALA	17.5	5.0	16.4	6.0	3.1	17.8	19.7	15.6	14.4	19.8
	ARG	0.5	8.7	0.9	11.0	13.0	0.1	0.1	3.7	4.7	0.6
	TRY	0.8	1.1	0.9	1.2	3.1	2.9	0.5	0.5	0.1	0.4
	VAL/CYS	8.3	7.4	10.4	1.7	1.3	5.7	7.6	3.5	3.4	4.8
	MET	2.2	1.9	3.6	1.5	0.0	6.7	0.4	6.2	4.6	2.5
	PHE	0.4	0.6	3.1	0.7	0.8	0.1	4.6	1.3	0.8	0.1
	LLE	0.2	0.3	1.2	0.1	1.1	2.5	4.0	5.0	1.8	1.1
	LEU	3.3	2.0	1.9	1.6	1.9	3.1	1.2	4.3	2.2	1.9
	LYS/PRO	10.1	5.8	8.3	4.6	7.8	9.3	8.8	8.5	8.9	7.9
TOC (%)		6.1	7.6	6.5	6.9	9.6	6.6	5.4	5.7	6.5	8.3
TN (%)		0.7	0.9	0.7	0.8	1.3	0.9	0.7	0.7	0.7	1.0
molar C/N		10.0	9.7	10.8	10.0	9.0	8.9	9.5	9.3	10.6	9.8
THAA (mg/g)		21.1	16.8	12.9	26.9	39.7	18.6	20.3	22.5	28.5	50.4
THAA-C (%)		14.6	9.1	8.5	15.9	17.0	12.0	16.6	17.1	18.4	25.0
THAA-N (%)		52.1	35.7	31.3	67.0	58.9	36.3	56.1	54.1	73.7	90.2

*L-Aspartic Acid (ASP), L(+)-Glutamic acid (GLU), L-Serine (SER), L-histidine (HIS), L-Glycine (GLY), L-Threonine (THR), L-Arginine (ARG), L-Alanine (ALA), L-Tyrosine (TYR), L-Cystine (CYS), L-Valine (VAL), L-Methionine (MET), L-phenylalanine (PHE), L-isoleucine (LLE), L-Leucine (LEU), L-Lysine Hydrochloride (LYS), L-proline (PRO).

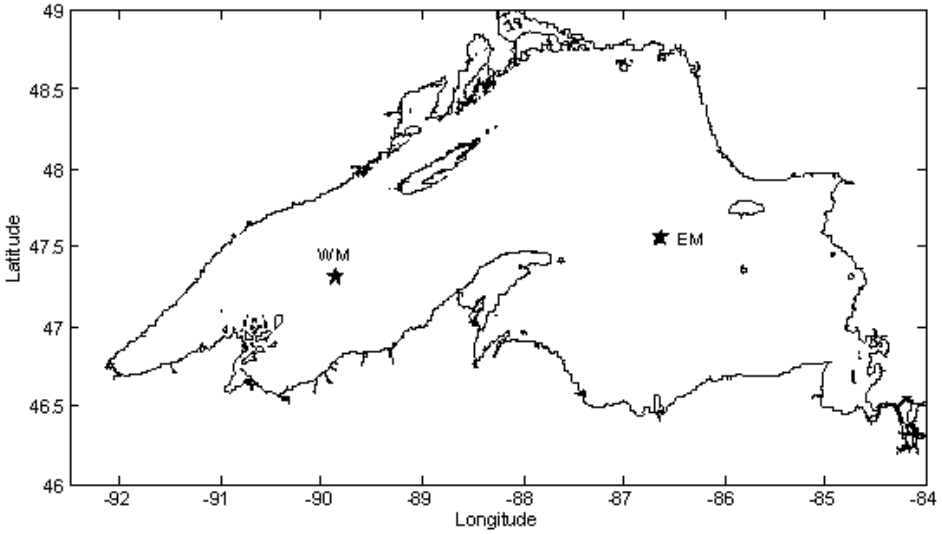

Fig. 3-1. Lake Superior. Stars indicate sampling sites.

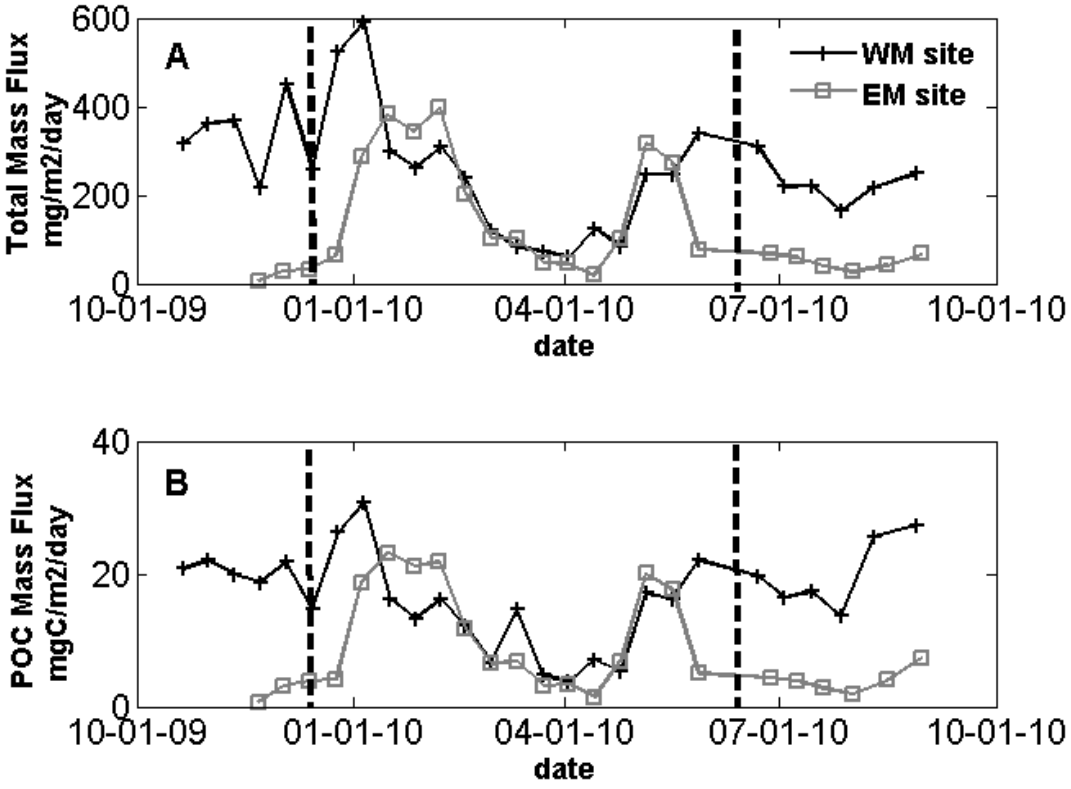

Fig. 3-2 Seasonality of A) total particulate mass fluxes and B) POC mass fluxes in the fall 2009- spring 2010 period in Lake Superior. 3-4 continuous summer trap samples (after June 17th 2010) were averaged to obtain the same resolution as winter trap samples (10-11 days). Black dashed lines indicate onset of fall mixing event (12-10-09) and summer stratification (06-10-10) based upon thermistor data from the EM mooring.

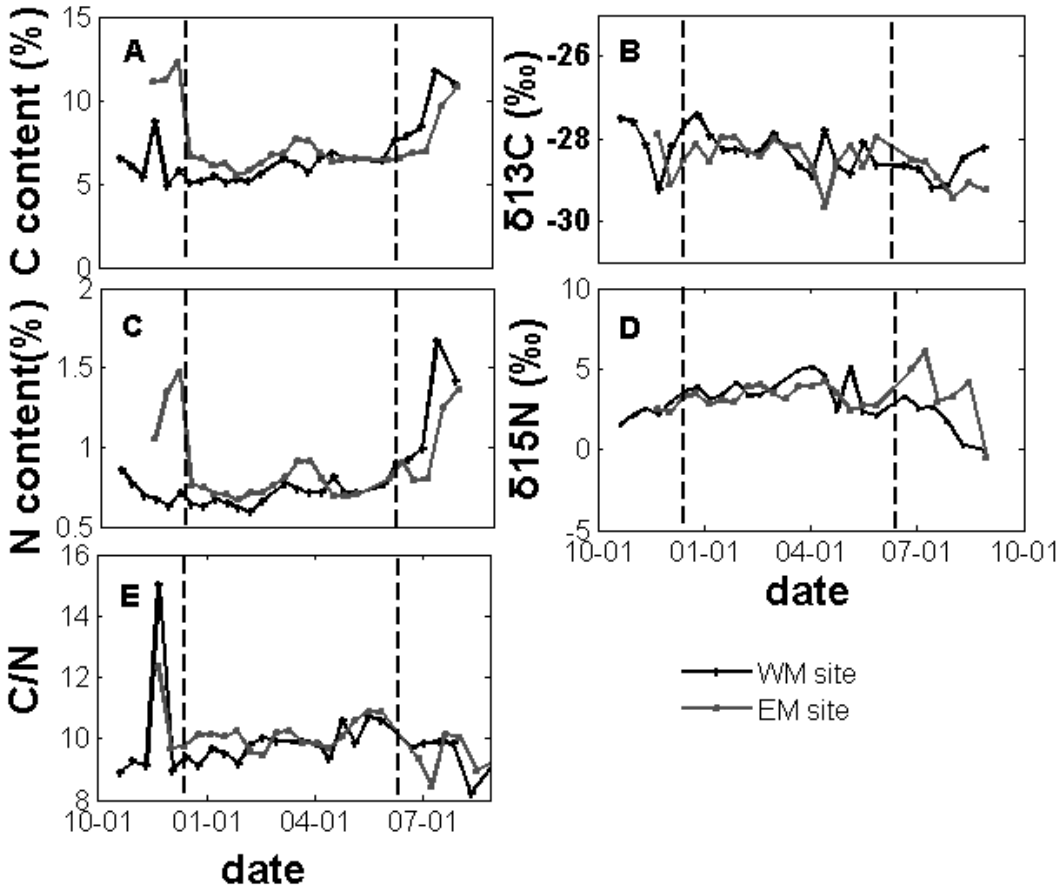

Fig. 3-3. Seasonality of A) Carbon contents in total settling material; B) Stable carbon isotope values; C) Nitrogen contents in total settling material; D) Stable nitrogen isotope values; E) Molar ratio of carbon vs nitrogen. 3 to 4 continuous summer trap samples, which represent settling POM of 3-4 days, were mixed and measured as one sample to match the sampling durations at other seasons. Black dashed lines indicate onsite of spring mixing event (12-10-09) and summer stratification (06-10-10).

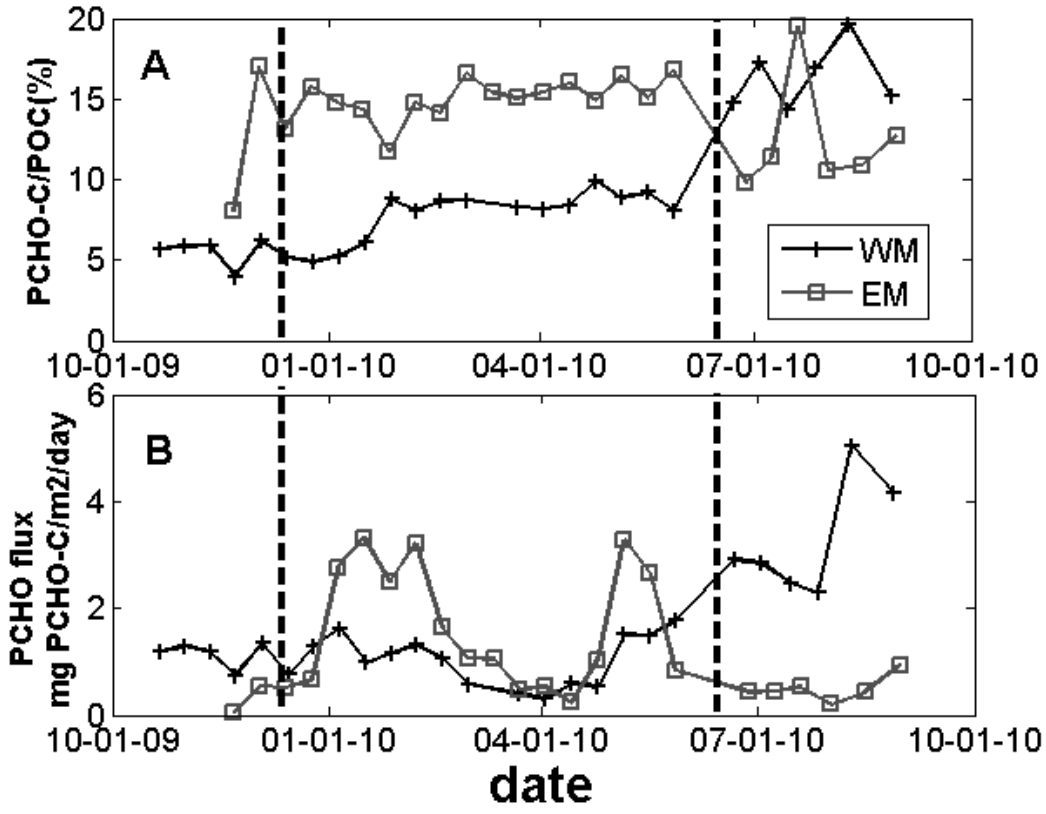

Fig 3-4 A, Seasonal variation of carbohydrate carbon percent in total POC; B, PCHO flux in the fall 2009- spring 2010 period in Lake Superior. Every 3-4 continuous summer trap samples, which represent settling POM of 3-4 days, were mixed and measured as one sample. Black dashed lines indicates onsite of spring mixing event (12-10-09) and summer stratification (06-10-10).

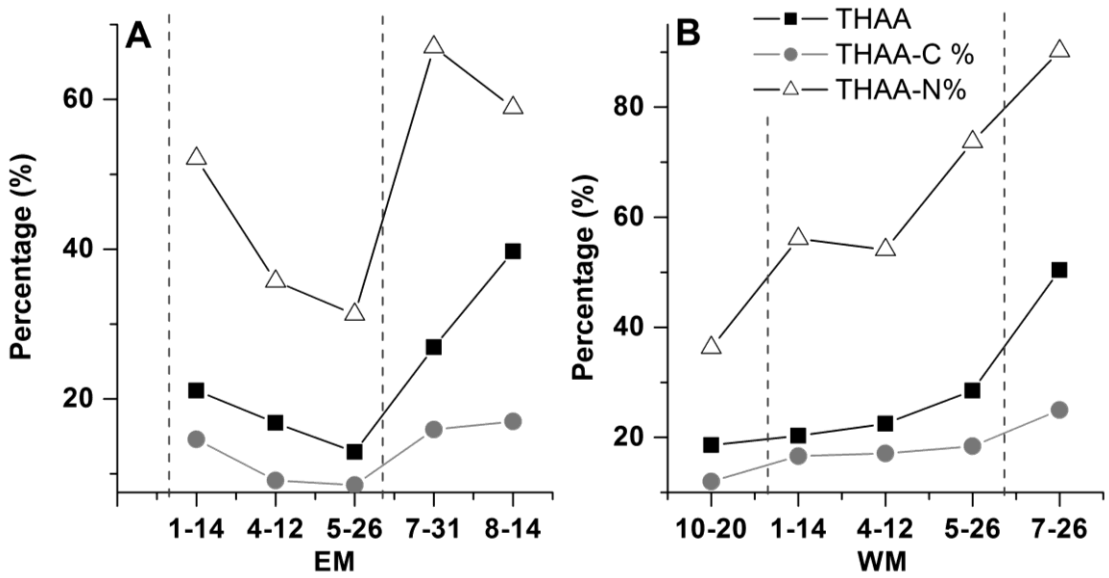

Fig. 3-5 Concentration of THAA, THAA-C percentage, THAA-N percentage of the 5 selected samples from both A) EM and B) WM. Black dashed lines indicate onsite of spring mixing event (12-10-09) and summer stratification (06-10-10).

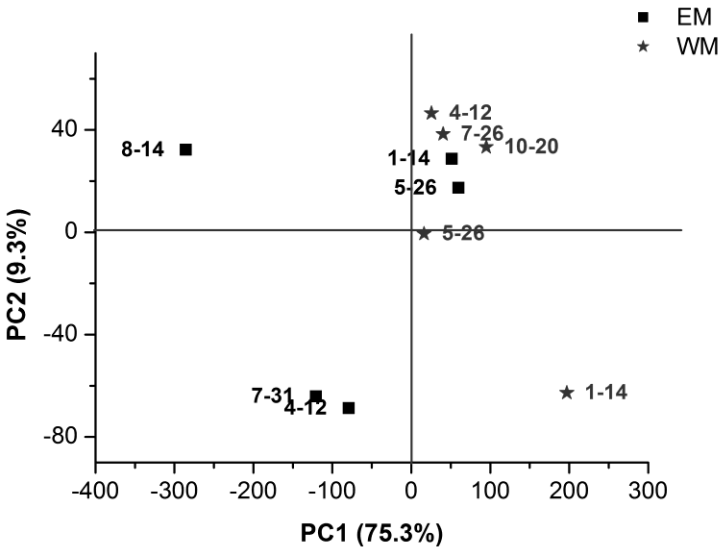

Fig 3-6, PCA projection based on Mol % composition of the 17 THAAs in the selected 10 sediment trap samples. EM samples are shown with filled black squares and WM samples are shown with filled dark gray stars. The sampling dates are indicated in the figure, and represent the middle day of the entire 11-12 days for each collection of the sample. The data matrixes were z-scored and variance scaled before the PCA analysis was performed.

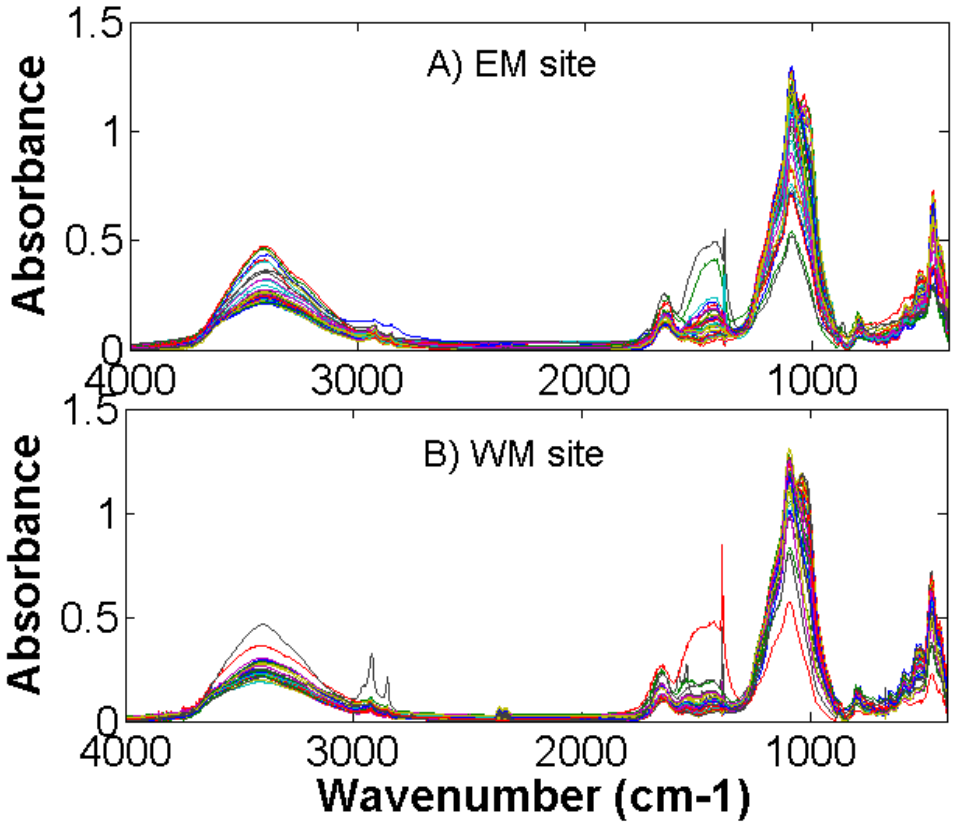

Fig. 3-7 1D FTIR spectra of all settling particulate matter samples collected at different times of the year at A) EM site, B) WM site. The colors indicate different samples. Each spectrum was normalized via total area before comparison to reduce variation from sample loading/processing.

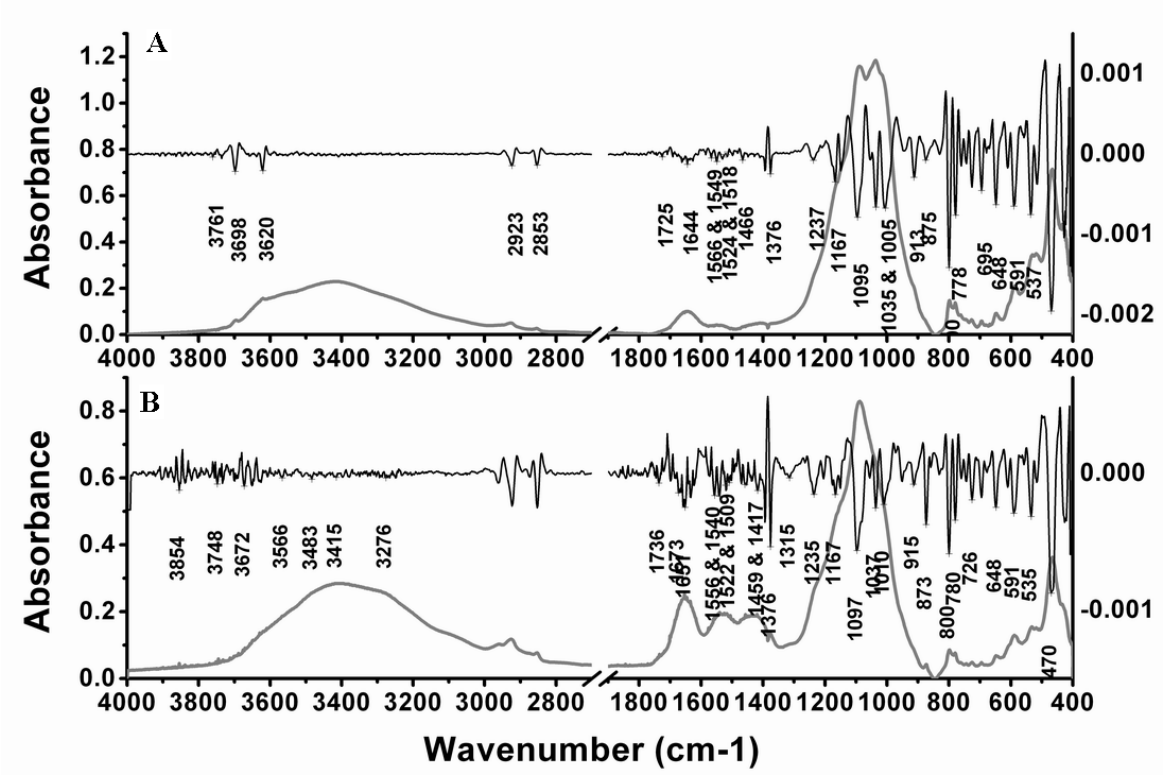

Fig. 3-8 The FTIR spectrum and its 2nd derivative for sinking particulate samples from A. winter (Jan 10th to 21th, 2010) and B. summer (Aug 10th to 15th, 2010) at WM.

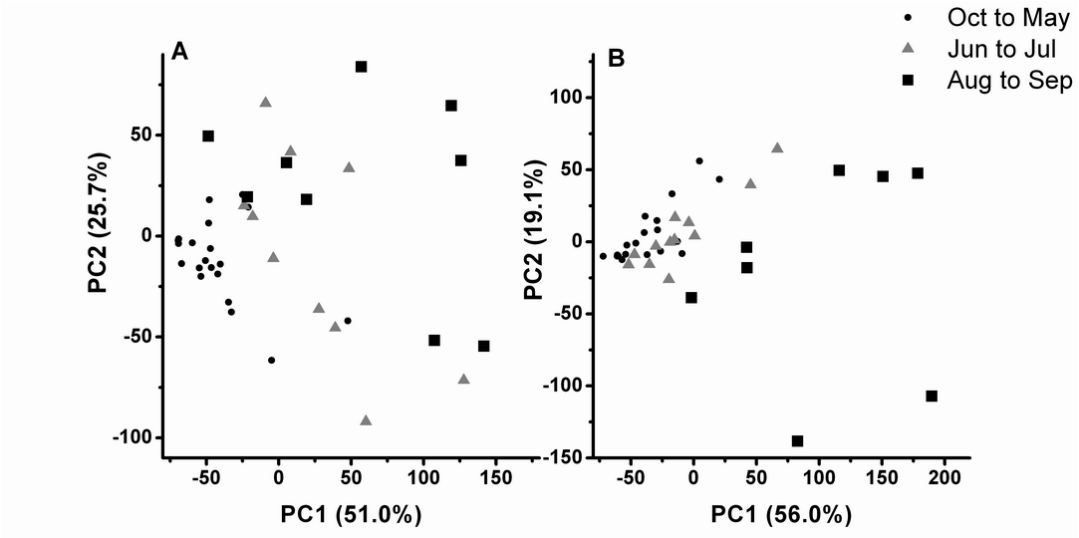

Fig 3-9. PCA projection of normalized FTIR data for A) EM, B) WM.

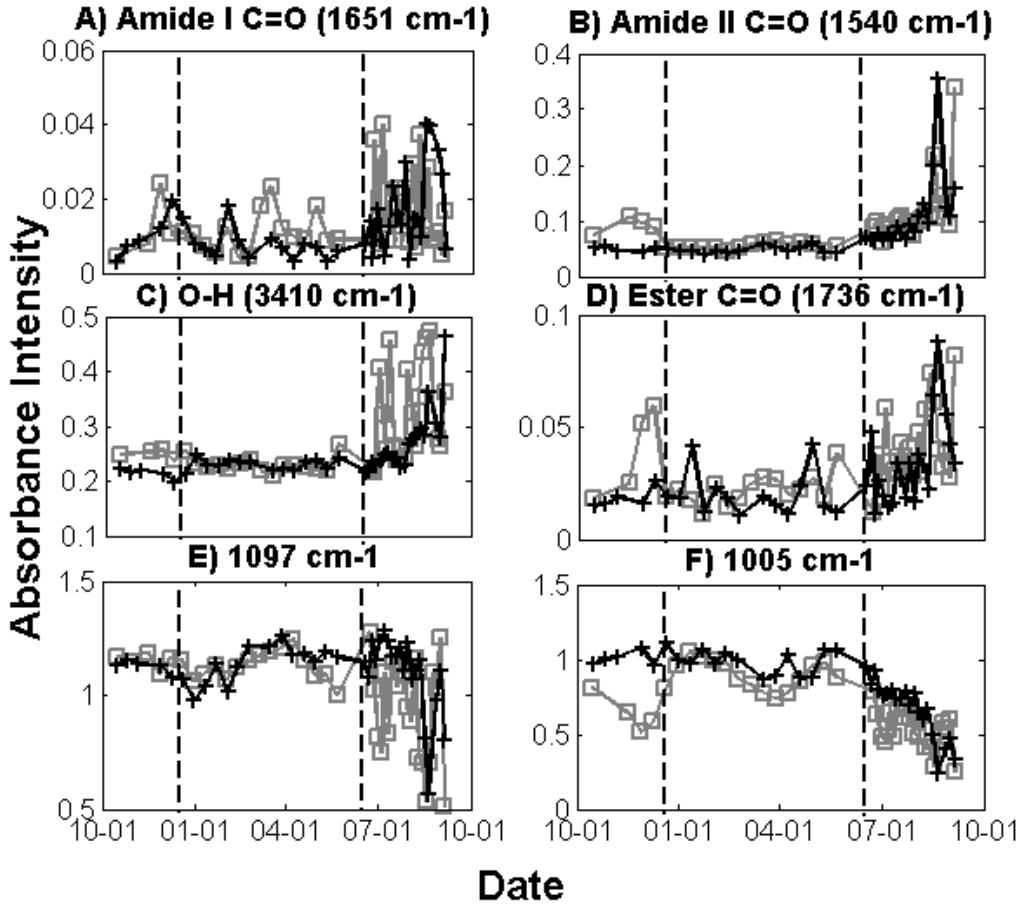

Fig. 3-10 Seasonality of POM compound class distributions in Lake Superior at EM (gray) and WM (black) sites based on normalized absorbance intensity (to total sample absorbance) changes at wavelengths of A) 1651 cm^{-1} representing Amide I C=O stretching, B) 1540 cm^{-1} representing Amide II C=O stretching, C) 3410 cm^{-1} representing O-H stretching of carboxylic acid and carbohydrate, D) 1736 cm^{-1} representing aliphatic ester C=O stretching, E) 1097 cm^{-1} representing overlap of carbohydrate, biogenic silica/silicate minerals, F), 1005 cm^{-1} representing overlap of carbohydrate, biogenic silica/silicate minerals. Each spectrum was normalized via total area before comparison to reduce variation from sample loading/processing. Black dashed lines indicate onsite of the spring mixing event (12-10-09) and summer stratification (06-10-10).

Chapter 4 Diagenetic changes in Lake Superior sediments as seen by FTIR and 2D correlation spectroscopy

Summary

Isotopic and elemental analyses, Fourier-transform infrared spectroscopy (FTIR), principal components analysis (PCA), and two dimensional (2D) correlation analysis, where core depth was used as perturbation, were used to study the diagenesis of organic matter (OM) in Lake Superior sediments. Changes in OM composition were examined at five lake stations over a depth range of 0 to 10 cm. PCA results show that depth-related changes among sites are similar, leading to an increased contribution from inorganic (and possibly refractory aromatic organic) components at each site, and a loss of contribution from other organic components. Synchronous spectra reveal that aliphatic esters and carbohydrates degrade significantly with increasing depth, leading to an increased contribution from clays/ biogenic silica/ inactive carbohydrates. Asynchronous spectra show that, generally, carboxyl groups, including aliphatic ester and amide/protein, degrade first, followed by a group of carbohydrates, and then aromatic compounds and/ or the Si-O framework in clays and biogenic silica. Site dependent compositional variation occurs and appears to be influenced by topography and geology, e.g. the delivery of a larger load of terrestrial inorganic silicate minerals to certain sites and re-suspension/re-deposition, which leads to less intensive down core variation at mid-lake central and eastern-basin sites. The study demonstrates the usefulness of FTIR coupled with PCA and 2D correlation approaches to explore structural changes in sedimentary material during diagenesis.

4.1 Introduction

Early diagenesis of primary organic macromolecules in the oceans is often conceptualized as rapid microbial and chemical destruction of the bio-macromolecules (mainly in the water column) followed by slower condensation

of the metabolic and hydrolysis products to form refractory humic material, which takes place mainly in ocean sediments (Degens, 1967; Kemp and Johnston, 1979). In the Great Lakes, which are much shallower, the role of the sediment-water interface as an area of organic component destruction is likely to be enhanced. In Lakes Ontario and Erie, the most intense microbial activity and the highest bacterial concentrations have been found at the sediment-water interface (Vanderpost, 1972; Dutka et al., 1974). Down core diagenetic alteration of some important paleo-proxies including bulk stable carbon isotopic, stable nitrogen isotopic and C/N ratios, and the concentration of humic substances and some important lipid biomarkers in Great Lakes sediments have been studied (review by Meyers and Ishiwatari, 1993). Also, Kemp and Johnston (1979) used wet-chemistry analyses to investigate the diagenesis of extractable OM in sediments from Lakes Ontario, Erie and Huron. They identified trophic state and water depth as the two controls on the degree of diagenesis of modern sedimentary OM. They also found that the decomposition rate was in the following order: amino acids >> amino sugars > carbohydrates > humic compounds > lipids. Although there have been studies of individual paleo-proxies or of selected extractable fractions like hydrolysable amino acids, amino sugars and carbohydrates, little is known about the composition and transformation of the high molecular weight (MW) entities (both precursors of the extractable material and the portions not amenable to extraction).

With the application of 2D correlation approaches to FTIR data (Abdulla et al., 2010b), more structural information can be extracted from the spectra of complex mixtures such as those in sediments. Noda (1993) developed the concept of generalized perturbation based 2D correlation spectroscopy, which works by spreading the spectral intensity changes within a data set collected across a perturbation (time, temperature, depth) across a second dimension as a function of the perturbation. As pointed out by Noda and Ozaki (2004), by applying 2D correlation spectroscopy, spectral resolution is enhanced by spreading peaks over a second

dimension; the correlations among IR bands facilitate functional group assignments, and the specific sequential order of spectral intensity changes through a data set can be identified through asynchronous analysis. The use of 2D spectroscopy is resolving many ambiguities in natural complex mixtures of compounds with many overlapping peaks (Noda and Ozaki, 2004; Mecozzi et al. 2009a, b, c; Abdulla et al., 2010a, b; Popescu et al., 2010). Using 2D FTIR in conjunction with multivariate statistical methods (such as discriminant analysis, PCA and cluster analysis) can help confirm trends within an FTIR data set and provide additional complementary insight into the distribution of sample compositions.

In this study, isotopic and elemental analysis, FTIR, PCA, and 2D correlation analysis, with core depth as the perturbation, are used to study diagenesis in sediments from Lake Superior. Sedimentary OM is characterized in terms of the functional groups of the principal building blocks of living aquatic organisms (e.g. proteins, carbohydrates, and lipids).

4.2 Materials and methods

4.2.1 Study site and sampling

Lake Superior is the Earth's largest lake by surface area (82,100 km^2), with a maximum depth > 400 m, mean depth 150 m, water residence time 180 yr; it is dimictic, mixing twice annually (Assel, 1986; Herdendorf, 1990; Urban et al., 2005). Organic carbon (OC) deposition in the sediments is ca. 0.48×10^{12} g C yr^{-1} (McManus et al., 2003) to 1.5×10^{12} g C yr^{-1} (Johnson et al., 1982; Klump et al., 1989). Baker et al. (1991) found that < 5% of the organic carbon in surface particulate OC (POC) is transported to the bottom to accumulate in the sediment. Offshore areas have a sedimentation rate (0.01-0.05 cm/yr) close to that of ocean environments and there is minimum bioturbation in the sediment (Evans et al., 1981; Johnson and Eisenreich, 1979; Krezoski, 1989; Jiying et al., 2012). Surface sediments are oxic, with an

average O_2 penetration depth of ca. 7 cm at the mid-lake sites (Li et al., 2012). A lack of limestone in the drainage basin results in remarkably low $CaCO_3$ in the sediment (Matheson and Munwar, 1978).

Multi-cores were collected in May 2010 from five stations in the lake (Fig. 4-1) using an Ocean Instrument multi-corer. The water depth at stations CM, EM, NM, SM and WM was 258 m, 243 m, 218 m, 388 m and 171 m, respectively. From each sampling site one or more cores were extruded and sliced into 0–2 cm, 2–4 cm, 4–6 cm, 6-8 cm and 8-10 cm layers from the sediment-water interface. The slices were put into acid cleaned and combusted (450 °C, ≥ 4 hours) glass jars and stored at -20 °C. Samples were freeze-dried, homogenized and stored at room temperature until further analysis.

4.2.2 Elemental and isotopic analysis

Acid fumigation (Harris et al., 2001) was used to remove carbonate carbon before elemental analysis (EA) and isotope-ratio mass spectrometry (IR-MS). Weighed samples were placed in clean Ag capsules and 50 µl MilliQ water was added to each sample. Samples were then fumed over 12M HCl (6-8 h), oven-dried (60 °C, 4 h) and cooled. For more complete combustion, each sample (in the Ag capsule) was enclosed within a Sn capsule for %C, %N, $\delta^{13}C$ and $\delta^{15}N$ determination with a Costech CNS analyzer interfaced with a ThermoFinnigan Delta-PlusXP stable isotope ratio mass spectrometer.

Radiocarbon measurements were performed at the National Ocean Sciences Accelerator Mass Spectrometry Facility (NOSAMS) at the Woods Hole Oceanographic Institution. Homogenized, acid treated and dried samples were combusted to CO_2, reduced to graphite, and analyzed using accelerator mass spectrometry to determine radiocarbon content. Values are reported as $\Delta^{14}C$ according to the convention of Stuiver and Polach (1977).

4.2.3 FTIR spectral measurement and pre-processing

Spectra were obtained with a Nicolet Magna IR 560 FTIR ESP spectrometer equipped with purge gas generator unit by collecting 200 scans from 4000 to 400 cm^{-1} with resolution of 2 cm^{-1} and using Happ-Genzel apodization. For expelling CO_2 contamination coming from air, 1 lag time (5 min) between closing the analytical chamber and starting analysis was maintained. Freeze-dried, homogenized (but not acid-treated) samples were run as KBr pellets (1 mg sample, 130 mg KBr, homogenized in a mortar and pestle, 1500 psi). The pellet was dried in a dessicator (>6 hrs) before analysis. A pure KBr pellet was analyzed before each sample analysis as a background blank. Spectra were converted to absorbance units and baseline corrected. The second derivatives of these spectra were generated using Origin 7.0 and the 2nd order Savitzky-Golay method with 11 convolution points.

4.2.4 2D correlation and PCA

Before 2D correlation analysis, each spectrum was loaded into MATLAB 7.0 and area-normalized (Abdulla et al., 2010a) to minimize the influence of variable sample loading on the correlation analysis. The PCA noise reduction method proposed by Jung (2004) and applied by Abdulla et al. (2010b) was used to reduce noise prior to 2D correlation analyses. 2D FTIR correlation spectra were constructed for each of the 5 lake sites with core depth (layer) as the perturbation, sorting from the surface sediment layer to depth, in order to study the change in OM composition over this range. The area-normalized, noise-free data sets were imported into a modified version of *2Dshige* software (Kwansei-Gakuin University, Japan, available at *http://sci-tech.ksc.kwansei.ac.jp/~ozaki/*) to generate 2D-correlation spectra.

Besides being used as a noise reduction method, PCA was also used in its more traditional sense of classifying samples, in order to explore the compositional differences and similarities among samples. For classification, the data matrix was

z-scored and variance scaled before the PCA analysis was performed. This minimizes the influence of varying response factors (band intensity differences due to the physical variations in different functional groups) on the PCA groupings. Matlab 7.0 and in-house code were used for processing (Stephens and Minor, 2010).

4.3 Results and discussion

4.3.1 Elemental and isotopic analysis of Lake Superior sediments

The origin, composition and diagenesis of the OM were initially assessed using C and N concentrations and $\delta^{13}C$ values (Fig. 4-2). Consistent down-core $\delta^{13}C$ values (-25.6‰ to -27.9‰) were seen for all stations except SM ($\delta^{13}C$ value of -31.5‰ at 2-4 cm). C/N values ranged between 9.7 and 11.6 (except SM 2-4 cm, C/N of 8.2). Both $\delta^{13}C$ and C/N values are similar to reported values (-26.9‰ to -23.9‰ and 9.1 to 13.4, respectively) for sediments from the western basin and off the Keweenaw Peninsula (Ostrom et al., 1998; Urban et al., 2004) and may indicate that the OM in the sediment is derived from autochthonous productivity (Meyers and Ishiwatari, 1993; Ostrom et al., 1998). However, the C/N values are somewhat higher than reported for Lake Superior phytoplankton, and both the C/N and $\delta^{13}C$ values are also within the range reported for soils (Hoffman et al., 2010). At all sites except SM, which appears unique in its elemental and isotopic composition, C/N values show an initial increase with depth followed by a decrease in the deeper sections. This pattern may represent a slight diagenetic preference for the loss of N vs. C at the very beginning followed by an increase in the proportion of remaining OM from microbial biomass (more enriched in nitrogen-containing compounds, Lehmann et al., 2002) in the deeper part of the core.

In terms of %C, %N and $\delta^{13}C$, down-core trends for EM, CM, and NM are similar, with deep site SM and western-lake site WM exhibiting more extreme changes with depth. The trends indicate site-dependent variation in diagenesis, perhaps related to

water column depth and depositional environment (further discussed in Section 4.3.4.1). While we only have down-core radiocarbon data for two sites (WM and EM), the down-core differences in OM age are more extreme for site WM (Table 4-1), which exhibited the strongest downcore decreases in %C and %N (Fig. 4-2a, b). Radiocarbon data and %C in surface sediments do not, however, appear correlated based on Pearson's linear correlation analysis (N=5, R^2=0.0233, P=0.8064) and may instead reflect varying inputs from sources with different pre-aged OC content.

4.3.2 Insights into sediment OM composition based on 1D FTIR spectroscopy and 2nd derivative spectra

The 1D FTIR spectra from all depths and sites (e.g. Fig. 4-3) are similar to each other. As reported for dissolved OM samples from an Elizabeth River/Chesapeake Bay salinity transect (Abdulla et al., 2010a), the heterogeneity of the samples actually acts to simplify their FTIR spectra, which exhibit broad bands from the overlap of multiple functional groups. Such broadening is also seen in clay analyses by FTIR (e.g., Madejová and Komadel, 2001). However, even in Fig. 4-3, with samples containing a mixture of inorganic and organic compounds, some peak shifts and peak intensity differences can be seen as a function of increasing sediment depth. We therefore applied the 2nd derivative of the FTIR spectra (e.g. Fig. 4-4) to clarify changes in the slope in the original spectra, and thus to identify the number of overlapping bands and the exact frequency of peak response (Smith, 1996; Griffiths and De Haseth, 2007).

Comparison of the 1D FTIR and 2nd derivative spectra of bulk sediment and combusted sediment samples suggest that clays/biogenic silica/carbohydrates are the dominant chemical constituents of Lake Superior surface sediment (Fig 4-4 and Table 4-2). Although optimized combustion conditions (400 °C, 8 hours as suggested by Ball, 1964; Ben-Dor and Banin, 1989) were applied to minimize the loss of structural water and ensure the complete removal of OC, we are aware that any degree of dehydration of clays from combustion might lead to changes in its FTIR spectra,

especially the bands related to crystallized/ absorbed water. However, the comparison of the bulk sediment and combusted sediment spectra (e.g. Fig 4-4a and 4-4b) still shows the strong signal from clay minerals (mainly bands range 1000 to 1200 cm^{-1}) and recognizable signals from organic compounds (mainly bands range 1200 to 1800 cm^{-1}). The relative response factors for different indicator wavenumbers also need to be taken into account. For example, the bands indicating lignin are fairly weak even in measurements of lignin isolates, thus making it difficult to apply them in a quantitative fashion in environmental samples.

From examination of the 1D and 2^{nd} derivative spectra from all five stations and all sediment depths (Table 4-2), Lake Superior sediments of all stations, unsurprisingly, exhibit strong signals of clay minerals (and possibly some biogenic silica) and recognizable signals from the organic chemical functional groups within carbohydrates, carboxylic acids, aliphatic/acetyl esters, amides/proteins and phenols/lignins.

4.3.3 PCA of the FTIR data

PCA, a commonly used feature-based classification method (Kvalheim et al., 1985; Sanni et al., 2002), was performed on the data set comprised of normalized FTIR spectra from all stations and core depths to investigate the variation among samples at different depths from different sites. The data matrix was z-scored and variance scaled before the PCA analysis was performed. PC1 and PC2 account for 79% of the variability in the data set (Fig. 4-5a). For all the stations, the top two to three layers tend to be clustered in negative PC1 space. With increasing depth the samples shift toward more positive PC1 values and the deepest layers are all in positive PC1 space. Positive correlation can be found between PC1 score and radiocarbon age for samples from the same station (e.g. N=3, R^2=0.9789, P=0.0929 for WM), with older layers having more positive PC1 values (data not shown). However, no correlation is found when all the radiocarbon data from Table 4-1 are compared with FTIR-based PC

scores. This is likely due to the lack of down-core radiocarbon values and the differences in pre-aged OM sources in the surface sediment layers at different stations.

In PCA, squaring a loading gives an estimate of the leverage each variable has on the resulting PC. Variables with large leverage can be identified by loading plots (e.g. Fig. 4-5b, a reconstructed loading plot showing loading scaled by instrument response at that wavelength). Plotting the PC1 loadings (Fig. 4-5b) illustrates that samples located on the positive side (Fig. 4-5a) have more refractory character (peaks from 3000 to 3500 cm^{-1} and peaks centered at 600 cm^{-1}, consistent with an enhancement in the proportion of hydrated clays, and perhaps also aromatic organic compounds, in the sample). In contrast, loadings to the negative side of PC1 include the region from 1200 to 1800 cm^{-1}, consistent with carboxylates, aliphatic esters and amide/protein and the region from 1000 to 1200 cm^{-1}, which we attribute to carbohydrates as the clay and silicate peaks in that region should remain relatively stable and thus be subtracted out in the z-scoring step prior to PCA. (The relationships in Fig 4-5a and 4-5b also show that with labile compounds being consumed via diagenesis, the remaining FTIR-amenable material (possibly clays, resistant forms of the original organic mixture, and products from diagenesis) becomes more similar across the lake sites.

There were interesting site-specific variations. SM showed the strongest variation in composition as a function of depth. WM samples from all core depths plotted closer to the ‘deep layer group’, while NM samples appeared less diagenetically altered, as indicated by the top four layers being outside the ‘deep layer group’. The FTIR-PCA-based diagenetic state of the WM sediments agrees with both our 2D correlation FTIR results (see below) and our radiocarbon ages (Table 4-1).

4.3.4 Diagenetic changes with depth as revealed by 2D correlation FTIR

4.3.4.1 2D FTIR synchronous map

2D correlation spectroscopy was performed according to Noda and Ozaki (2004) as described by Abdulla et al., 2010b to extract compositional changes of sediment with depth. Due to its mathematical nature, perturbation based 2D-correlation analysis is especially sensitive to noise. The noise can be the high-frequency noise associated with the instrument's detector and electronic circuits, it can also be low frequency noise and localized noise, such as low-frequency noise caused by instrument drift during the scanning measurements. Noise in the FTIR data could cause artifacts in the 2D treatments, especially for asynchronous maps (Noda and Ozaki, 2004), so we applied the PCA-noise reduction method proposed by Jung et al. (2004) and used by Abdulla et al. (2010b) as the noise filter. The first two principal components contained > 92% of the variation in each data set; reconstructed data sets using these two components were the starting point for 2D correlation studies. The removed spectra appear to consist mainly of noise, exhibiting no recognizable features (Appendix Fig 4-1). To further check that the approach was appropriate, we compared synchronous and asynchronous contour maps with and without noise, as recommended by Abdulla et al. (2010b). As in that study, our synchronous map shows no noticeable differences in the presence or absence of noise; the asynchronous contour maps show some artifacts when using the original noise-containing spectra (data not shown). All 2D correlation results were generated from the noise free spectra.

Spectral data were constructed for each lake site with core depth as the perturbation, sorting from the surface sediment layer to depth. Since previous ^{210}Pb geochronology studies revealed that the offshore area of Lake Superior has a low sedimentation rate (0.01-0.05 cm/yr), minimum influence from wind-generated re-suspension, and minimum bioturbation of only 1-2 cm in the sediment (Evans et al., 1981; Johnson

and Eisenreich, 1979; Krezoski, 1989; Jiying et al., 2012), diagenesis is believed to be the main reason for OM composition changes vs. depth.

The synchronous map shows a symmetric spectrum with respect to the diagonal line. Major auto-peaks spread along the diagonal line represent correlation between a band and itself along a certain perturbation. For example, here the auto-peaks represent variation in FTIR response ("concentration") as a function of increasing depth; the intensity of an auto-peak represents the intensity of the variation. Thus, 2D correlation analysis has the ability to extract only the FTIR responses that change through perturbation out of a complex background, such as a strong stable clay/refractory OM background in the lake sediments in this study. Note that all auto-peaks are positive by definition, indicating a correlation; these correlations could represent either an increase or a decrease in concentration with depth; the direction of change has to be confirmed by comparison of the original spectra.

Taking CM (Fig. 4-6) as an example, 13 distinct auto-peaks are observed in the 2D synchronous correlation spectrum. The greatest change in intensity lies in the multiple bands around 1000 to 1100 cm^{-1}, consistent with Si-O stretching in clay minerals and biogenic silica or C-O stretching in carbohydrates. Considering the general stability of the Si-O bond in clay minerals/ biogenic silica and as evidenced by the disappearance of the main Si-O clay peaks (1065 cm^{-1}, 1095 cm^{-1}, 1037 cm^{-1}) in 2D correlation spectra, any losses indicated by these auto-peaks should mainly result from the diagenesis of labile carbohydrates with a possible minor contribution from biogenic silica dissolution. The band showing the second-greatest change in intensity (~1193 cm^{-1}) is attributed to aliphatic ester or acetyl ester. The band at 1659 cm^{-1} (amide C=O asymmetric stretching) is small, but implies that protein/peptide content changes with diagenesis. The broad auto-peak around 3344 cm^{-1} (an –OH stretch region) indicates changing of phenol, carbohydrate, long chain alcohol and/or carboxylic acid groups over depth. Absorbance and desorption of water to clay minerals, and thus a change in

clay minerology with depth, could also contribute to this band. The peak around 3642 cm^{-1} could be a silinol Si–OH stretch and may indicate the early stages of biogenic silica diagenesis. Thus, the 2D correlation map (Fig. 4-6) implies that in the top 10 cm of the sediment, carbohydrates and aliphatic esters change to the greatest extent, while changes in amide/protein, some combination of phenol/carbohydrate/carboxylic acid/clay minerals (water absorbance and desorption) , as well as biogenic silica, also occur. The changes in carbohydrate (1092 cm^{-1}), aliphatic ester, amide/protein, O-H groups and silinol Si-OH in biogenic silica were confirmed as a decrease by finding depth-related decreases in the peak intensities of the corresponding wavenumbers in the area-normalized 1D FTIR (data not shown). The clay/ biogenic silica/ carbohydrate band at 1003 cm^{-1} is confirmed as an increase, which is likely due to the significant loss of other compounds during digenesis leaving some clays and possibly some non-active carbohydrate/biogenic silica as a greater proportion of total sediment.

In order to identify how these major bands are correlated with each other, the off-diagonal peaks (cross-peaks) in the synchronous map were investigated. Bands represented by X and Y coordinates of positive cross-peaks share the same directional variation with depth, and the relative intensity changes correspond to the relative strength of the change in FTIR response of the functional groups. For CM (Fig. 4-6), 2 sets of functional groups are identified that respond differently with depth. The first set is identified by the positive cross-peaks among Si–OH (3642 cm^{-1}), amide/protein (1659 cm^{-1} and 1530 cm^{-1}), aliphatic ester (1193 cm^{-1}) and carbohydrate/silicate (1092 cm^{-1}); comparison of original spectra shows that this shift is a decrease in proportional response with depth within the sediment. The second set is identified by positive cross-peaks among the clay/ biogenic silica/ carbohydrate band (1003 cm^{-1}), unsaturated C-H (3133 cm^{-1}), methyl C-H (2884 and 2836 cm^{-1}) and the bonds represented by 862 cm^{-1}, 593 cm^{-1} and 536 cm^{-1}; these FTIR bands increase with depth as indicated by their negative cross-peak relationship with the first set of

functional groups (Fig. 4-6). Based on the above cross-peak analysis, peaks at 1092 cm^{-1} and 1003 cm^{-1} represent different carbohydrate and or silicate moieties varying significantly in diagenetic response. The negative correlation of band 1003 cm^{-1} vs. other functional groups (and its increasing in proportion with increasing depth) here is most likely due to the inactive clay minerals and biogenic silica species dominating the signal at this range, and thus is referred to as clay/ biogenic silica/ carbohydrate band in this study.

Although it is hard to assign specific vibration modes to wavenumbers below 1000 cm^{-1}, peaks centered around 800 and 600 cm^{-1} can be attributed to SiO vibrations (quartz, Herbert et al., 1992; Vogel et al., 2008) and to signals from Mg_3OH in chrysotile (Madejová, 2003) and to signals from montmorillonite (620 cm^{-1}, Madejová and Komadel, 2001); these peaks also coincide with those attributed to aromatic vibrations. These peaks show a positive correlation with clay/ biogenic silica/ carbohydrate band (1003 cm^{-1}), unsaturated C-H (3133 cm^{-1}) and methyl C-H (2884 and 2836 cm^{-1}) and a negative correlation with other functional groups (Fig. 4-6). Diagenesis over depth in sediment leads, therefore, to an increase in the relative proportion of clays/biogenic silica and methylated, unsaturated organic and possibly aromatic compounds relative to other functional groups in the sedimentary OM.

The absence of cross-peaks and auto-peaks in bands such as 1700 and 1640 cm^{-1} in 2D FTIR spectra indicates an absence/scarcity of carboxylic acid diagenesis. Since we do find carboxylic acid signals in 1D FTIR, it appears that carboxylic acids are relatively conservative in the sediments. This behavior may be because the more labile portions (such as unsaturated fatty acids) have already been reworked in the water column or because the alterations of fatty acid structures and distributions are too subtle to be seen by FTIR.

As seen in Table 4-3 and (Appendix Fig 4-2) and in the asynchronous study below in

Section 4.3.4.2, the activity of O-H/N-H bands is site dependent. A combination of polymeric alcohol, carboxylic acid, amide, and even water absorbed to clays minerals/ silica as discussed above, could contribute to these bands, and the varying contributions from these compound classes at each station most likely leads to the O-H/N-H activity difference. O-H/N-H bands were found to be positively correlated with inactive clay/carbohydrate bands around 1000 to 1100 cm^{-1} and negatively correlated with other functional groups at SM and CM, the two deepest water sites (388 and 258 m, respectively), while they positively correlated with carbohydrate bands, aliphatic ester and amide/protein at other stations (whose water depths ranged from 171 to 243 m).

NM, SM and WM sediments (Table 4-3 and Appendix Fig 4-2 b,c,d) appear to have a stronger and somewhat different diagenetic response vs. CM and EM. For all 3 of these stations, the correlation coefficient for the auto-peaks is considerably higher than seen for CM and EM. First of all, the clay/ biogenic silica/ carbohydrate bands show negative correlation with other functional groups in the 1100 to 2000 cm^{-1} range, including aliphatic ester bands at all the stations and the amide/protein bands at WM and SM. At NM and WM, the intensity of Si-OH auto-peaks and cross-peaks (around 3629 cm^{-1}) is very low vs. other stations. The diagenetic differences at NM, SM and WM vs. CM and EM could be caused by variation in the sediment source and age, sedimentation rate (Fig. 4-1), water column depth and depositional environment at the sites.

NM differs from all the other sites in its lack of a positive relationship between the aliphatic ester bands and protein and its positive correlation of the aromatic band and aliphatic esters (Table 4-3). It also differs from the other sites in lacking a labile protein signature (there is no autopeak for protein bands at this site, Table 4-3, and Appendix Fig 4-2). These trends indicate increased terrestrial, rather than autochthonous, inputs at this site, which is consistent with circulation patterns in the

lake (Bennington et al., 2010). With diagenesis, the proportion of relatively inactive compounds would increase rapidly as the labile compounds were depleted, resulting in the strong carbohydrate/silicate signal being negatively correlated with other bands (Table 4-3 and Appendix Fig 4-2).

SM has the most distinct 2D synchronous spectrum with a ca.10x greater correlation coefficient than all other stations (as shown by y-axes in the auto-spectra in Fig. 4-6 and Appendix Fig 4-2), which indicates much more intensive variation in compound composition at this site. Core SM was recovered from the deepest location in the lake (Fig. 4-1), where bottom currents are accelerated and erosional features are common (Johnson, 1980). In addition to its differences in FTIR parameters, it also exhibits significantly lower %C and %N relative to the other sites. These differences are likely due to the significantly stronger bottom current scouring away lighter OM-rich sediment. Thus there is most likely a fine layer of very recent organic material that was just deposited (and not yet scoured away) underlain by relatively coarse grained material with highly reworked, refractory OM. Evidence for this is found in the physical properties of this core relative to others: SM has coarser sediment relative to the other cores and SM sediments are yellow (vs. olive gray at other stations), indicating less OM-rich material.

The diagenetic differences at WM are more difficult to explain. WM exhibits stronger changes in %C and %N with depth than NM, CM, and EM (Fig. 4-2) and may be more impacted by the generally higher primary productivity in the western arm of the lake (McManus et al. 2003). However, its surface sediment (0-2 cm) is the oldest among our sample sites (Table 4-1) and may indicate additional sources of pre-aged material at this location.

Another possible scenario to explain the differences in WM, NM and SM vs. EM and CM is the intensive re-suspension believed to occur near EM and CM, as reported by

Zigah et al. (2012) on the basis of radiocarbon distributions in lake particulate OM at these sites. Such re-suspension events could shift much of the OM diagenesis into the water column rather than surface sediment, although if this were the case, we would expect to see lower %C in surface sediment at these sites, rather than the somewhat higher proportion actually measured (Fig. 4-2). A second possibility is that sites EM and CM are areas of deposition for resuspended surface sediment transported from elsewhere in the lake, and thus exhibit less variation down-core than sites more impacted by surface water primary production. Without the intense decomposing of a thin layer of fresh OM at the sediment interface, the clay/ biogenic silica/ carbohydrate region will not show a negative correlation with other functional groups as seen at WM, NM and SM. This scenario is consistent with the correlation coefficients of the auto-spectra (Fig. 4-6 and Appendix Fig 4-2); EM and CM have a 2D correlation coefficient roughly 7-30x smaller than the other stations, indicating much less intense compositional variation in the functional groups, especially the clay/ biogenic silica/ carbohydrate region, as a function of depth. It is also likely that the OM composition of each site is influenced by a varying combination of terrestrial OM/inorganic matter delivery vs. delivery of primary production, as well as differences in transport and depositional processes. The interaction of these processes would be a useful area for further research.

4.3.4.2. 2D FTIR asynchronous map

The asynchronous map supports and extends observations from the synchronous map and PCA analysis. An asynchronous cross-peak between a pair of FTIR bands develops only if the intensities of these two spectral features change out of phase with each other, and thus in our application, show a different depth-scale of diagenetic response. Noda's rule (Noda and Ozaki, 2004) can be applied to the asynchronous data in order to determine the sequential order of the changes between pairs of FTIR bands. The rule basically states that, assuming that features x and y are positively correlated in the synchronous spectrum (see Table 4-3), in an asynchronous spectrum,

a positive cross-peak at x and y indicates a change in feature x before the change in feature y. For the same circumstances, a negative cross-peak at x, y indicates that feature x's change lags behind that of feature y. This sign rule is reversed when the synchronous correlation intensity at the same coordinates is negative (again see Table 4-3). Because through diagenesis, the variation patterns of different functional groups in Lake Superior sediment are presumably monotonic, Noda's rule is reliable and is used here to identify the relative order of response of different functional groups to diagenesis.

For example, CM (Fig. 4-7a), exhibits positive asynchronous cross-peaks for the following species on the x-axis relative to a y of 1003 cm^{-1}: 3633 cm^{-1}, 1658 cm^{-1}, 1537 cm^{-1},1193 cm^{-1}, 1092 cm^{-1}. These, coupled with the presence of negative synchronous peaks at the same coordinates (Table 4-3 and Appendix Fig 4-3), indicate that the intensity of the clay/ biogenic silica/ carbohydrate band at 1003 cm^{-1} changes predominantly before the change in amide/protein (1658 cm^{-1}, 1537 cm^{-1}), aliphatic ester (1193 cm^{-1}), another group of carbohydrates (1092 cm^{-1}) and Si-O-H bands in biogenic silica (3633 cm^{-1}). It was shown above that this clay/ biogenic silica/ carbohydrate band increases in relative intensity with increasing depth most likely indicating its persistence as other species are removed via diagenesis (although its own generation within the sediments cannot be disproved). Using Noda's rule and a comparison of the actual FTIR spectra indicates the following order of diagenetic susceptibility (removal) at site CM from shallowest to deepest: carboxyl groups (including aliphatic ester and amide/protein)> carbohydrates > aromatic compounds and the Si-O framework in clay/ biogenic silica. O-H/N-H groups are found changing before aliphatic ester, amide/protein and the carbohydrates indicated by 1092 cm^{-1}. The Si-OH bond in biogenic silica (3621cm^{-1}) also changes (decrease in relative concentration at CM) before the O-H/N-H bonds resulting from polymeric alcohols/carboxylic acid/amide or absorbed water and carbohydrates. This order of response is based upon data in Table 4-3 and Fig 4-7 (see Appendix 4-4 for further

details).

Similar trends were observed for EM (Appendix Fig4-2) except that preferential changes in all carbohydrate peaks occur before changes in O-H/N-H groups and Si-OH bonds. This indicates that the activity of O-H/N-H bonds in polymeric alcohol/carboxylic acid/amide/silicate bands/adsorbed water, as well as Si-OH bonds in biogenic silica are site dependent; in another words, the compounds which contribute to the O-H/N-H bands in each station are different, leading to the O-H/N-H activity differences. Also, the diagenetic status of biogenic silica may be different among stations as well.

Therefore, for CM and EM stations the general sequential order of OM diagenesis in sediment is that carboxyl groups (including aliphatic ester and amide/protein) are the first to exhibit losses, followed by a group of carbohydrates, while clay minerals/ Si-O framework in biogenic silica and the aromatic compounds exhibit greater stability and thus increase in relative FTIR response. The activity of O-H/N-H bonds in polymeric alcohols/carboxylic acid/amide/adsorbed water bands as well as Si-OH bands in biogenic silica are site dependent.

NM, SM and WM show a similar diagenetic tendency for all the other functional groups (with slight variation in peak positions) as compared to CM and EM, except for the clay/ biogenic silica/ carbohydrate bands (as shown in Fig. 4-7b for WM and Appendix Fig 4-3, for the other sites). At NM, SM and WM, the change in clay/ biogenic silica/ carbohydrate bands (1100 to 1000 cm^{-1}) appears to occur after all other functional groups. This could be due to the intense decomposing of a thin layer of fresh OM at the sediment surface of these sites vs CM and EM, and the dominance of inactive clay or relatively stable OM moieties (perhaps terrestrially-derived structural carbohydrates). With the diagenetic loss of total OM with depth, the relative proportion of these refractory components would increase, as also shown by synchronous spectra for NM, SM and WM (see above and Fig. 4-6).

The compositional differences characterized by a domination of inactive clays/ biogenic silica/ stable carbohydrate at these sites could be caused by the differences in sediment source, sedimentation rate, water-column depth and depositional environment, such as intensity of sediment re-suspension. It is possible that the wind-driven prevailing circulation in the lake contributes more terrestrial material at certain times of the year to NM, carrying a relatively large amount of non-active clay minerals and refractory carbohydrate. Adding to this likelihood is the relative closeness of NM to several large inflows including the Nipigon River, Pigeon River, Pic River and Aguasabon River systems as well the site's location relative to the Slate Islands. For SM, as discussed above, the refractory nature of the sediment is most likely due to a local acceleration of bottom currents in the deep trough, inhibiting the accumulation of fine-grained sediment, leaving coarser sediment with refractory, reworked OM. For WM, the clay/ biogenic silica/ carbohydrate response may result from the age of the surface sediments (Table 4-1); the WM sediment core exhibits an age range of 940 to 7910 yr BP in the top 10 cm. These ages are significantly greater than those at EM (235 and 1530 yr BP for the 0-2 and 8-10 cm slices, respectively). As WM surface-sediment OM is older, the labile carbohydrates may already have been degraded or transported elsewhere.

The diagenesis trends seen in Lake Superior are consistent with previous studies of OM diagenesis in both marine and lacustrine sediments. For example, sediments from the southern Cape coastline of South Africa analyzed by pyrolysis–gas chromatography mass spectrometry show that selective preservation/degradation drives the major down-core variability in OM composition (Carr et al., 2010). The lower half of the core, older than 12,000 yr, was characterized by suites of low-MW aromatic pyrolysis products; surface sediments were characterized by products derived from fresh emergent or terrestrial vegetation, including lignin monomers, plant-derived fatty acids and long -chain *n*-alkanes. A ^{13}C-NMR study of sediment

diagenesis in Jellyfish Lake, an anoxic marine lake in Palau (Orem et al., 1991) revealed that the major post-deposition change in sedimentary OM was carbohydrate biodegradation, whereas, lignin and aliphatic substances were preserved.

4.4 Conclusions

Isotopic analysis, C and N content and FTIR coupled with PCA and 2D correlation analyses were used to study the composition of and diagenesis of Lake Superior sediments. A dominant contribution of clay-minerals/ biogenic silica along with common organic matter functional groups (carbohydrate, carboxylic acid, aliphatic/acetyl ester, amide/protein and phenol/lignin) were identified; their diagenetic changes were studied as well.

The stable carbon isotopic values and C/N ratios at all sites (Fig. 4-2) are consistent with primarily microbial organic matter, either from an autochthonous or soil microbial source. The %C concentrations in the sediments ranged from just over 4% to approximately 1% and decreased with depth at all sites, showing the strongest degree of change at WM (and a high degree of change in SM as well, though we have incomplete data for that site).

PCA analysis of the FTIR data (Fig. 4-5) shows that, with increasing depth, carboxylates, aliphatic esters, amide/protein, and carbohydrates decrease and the remaining FTIR amenable material becomes more similar across the lake sites. The greatest spread along PC 1 with depth occurs for site SM, followed by site WM, as would be consistent with the degree of change in %C in the surface sediments across sites (Fig 4-2).

2D correlation analysis, by spreading FTIR spectra into a second dimension, increased the resolution, separating overlapping bands and providing more detailed information about band positions and changes in band intensity with diagenesis. As

with the PCA analysis, 2D correlation analysis (Fig 4-6, Table 4-3) shows that chemical composition of the sediments changes with depth. Aliphatic ester functional group and some carbohydrates appear most susceptible to diagenesis. Slight shifts in wavenumbers indicate changes within these compound classes as a function of location in the lake. Asynchronous spectra (Fig. 4-7) can provide a sequential order of early stage OM diagenesis. In general: carboxyl groups including those in aliphatic ester and amide/protein change first, followed by a group of carbohydrates and then aromatic compounds and/or clay minerals and/or the Si-O framework of biogenic silica. This is consistent with bulk information showing initial losses of nitrogen relative to carbon (which could be due to rapid diagenetic changes in protein concentrations).

In addition to general diagenetic trends in Lake Superior sediment, we do see some spatial variability in surface sediment composition. NM, SM and WM have distinct down-core compositional variations relative to EM and CM. We believe NM to be affected by increased terrestrial input, SM to be affected by local acceleration of bottom currents in the deep trough and WM to be affected by the geological nature of the sediment or sediment resuspension. In addition, down-core variability in the lake may be related to variation in sedimentation rates. Coupling FTIR analysis on deeper cores along with estimated sedimentation rates for each core would be a useful approach for further study.

Table 4-1. $\Delta^{14}C$ and corresponding age (in radiocarbon years) of sedimentary particulate matter with porewater removed by centrifuging before freeze-drying. Precisions are based on error of standards or multiple analyses.

Stations	Sediment depth (cm)	Water column depth (m)	$\Delta^{14}C$ (‰)	Age (radiocarbon years B.P.)
CM	0-2	258	-19.6	100±20
NM	0-2	218	-22.6	125±20
SM	0-2	388	-36.6	240±15
EM	0-2	243	-35.7	235±15
EM	4-6		-126.2	1030±20
EM	8-10		-179.5	1530±15
WM	0-2	171	-116.8	940±15
WM	4-6		-595.8	7220±35
WM	8-10		-620.3	7720±35

Table 4-2. Bands used for compound identification of Lake Superior sediment samples (surface layer) with FTIR 2nd derivative spectra

Compound classes	Vibration mode	CM	EM	NM	SM	WM
		Representing Band Position (cm^{-1})				
Carboxylic acid [a~d]	C=O stretching in COOH (1710±15), +	1712	1716	1710	1716	1717
	Asym. stretching of -COO- (1600±40), +	1612 1630	1577	1633*	1619	1617
	Sym. stretching of -COO- (1405±45), +	1414	1406	1413	1400	1407
	O-H in-plane bending (1418±22), +	1426	1418	1432	1434	1417
Amide [a,d,e,f]	Amide I C=O stretching (1650±20), ++	1649 1658	1646 1655	1633* 1643	1652 1662	1653
	Amide II C=O stretching (1550±20), +	1554	1540	1551	1542	1559
Ester [a, d]	Aliphatic, C=O stretching (1740±10), +	1739	1734	1730	1748	1734
	Aliphatic, C-C-O stretching (1185±25), +++	1176	1175	1177	1176	1174
	Acetyl, C-C-O stretching (1240±5), ++	1238	1237	1238	1237	1240
Lignin [h~j]	vibrations of aromatic rings (1515±5), +	1515	1515	1512	1520	1519
Carbohydr-ateand Clay/ Biogenic silica	*O-H stretching ~3400, ++	3399	3405	3400	3388	3392
	Si–OH stretching, ++	3697 3621	3700 3620	3697 3621	3699 3620	3700 3621
	*C-O asym. stretching (1100±100), +++ or Si-O asym. stretching (1000±100), +++	913 1007 1038 1095 1165	913 1008 1038 1095 1164	913 1007 1039 1095 1165	913 1007 1037 1079 1164	913 1004 1037 1096 1165

References: a, Smith,1999; b, MacCart y & Rice, 1985; c, Celi et al. 1997; d, Silverstein, 1996; e, Harisa and Severcanb, 1999; f, Widjanarko et al. 2011; g, Pandurangi et al. 1990; h, Mascarenhas and Arbuckle, 2000; i, Raiskila et al. 2007; j, Derkacheva and Sukhov, 2008; relative response in the 1-D spectrum is indicated with +++ for intense, ++ for moderate, and + for weak; note that the relative response was the similar for all samples. *The signal at 1643 cm^{-1} could be from H-O-H bending of water molecules adsorbed to clays (e.g., Madejová, 2003). 1165 cm^{-1} is found to be signal from quartz (Ramachandran and Beaudoin, 2008). The very broad band around 3400 cm^{-1} can be attributed to the overlap of OH groups bonded to clays, O-H stretching of phenol, carbohydrate and carboxylic acid compounds and the N-H band in amide. The C-O asymetric stretching from carbohydrates and Si-O asymmetric stretching from clay/ biogenic silica overlaps at 1000 to 1000 cm^{-1} range.

Table 4-3. Compound class correlation relationship (varying with depth) as indicated by 2D synchronous FTIR cross-peaks.

Compound class* (CM)	A	B	C	D	E	F	G
A (1193)		+	+	-	-	+	-
B(1659, 1530)	+		+	-	-	+	-
C(1092)	+	+		-	-	+	-
D(1003)	-	-	-		+	-	+
E (3344)	-	-	-	+		-	+
F (3642)	+	+	+	-	-		-
G(3133, 539)	-	-	-	+	+	-	

Compound class* (EM)	A	B	C	D	E	F	G
A (1217, 1725)		+	+	-	+	-	-
B (1658, 1537)	+		+	-	+	N#	-
C(1087, 1040)	+	+		-	+	-	-
D(988)	-	-	-		-	+	+
E (3404)	+	+	+	-		-	-
F (3629)	N	N	-	+	-		+
G (586)	-	-	-	+	-	+	

Compound class* (NM)	A	B	C	D	E	F	G
A(1250, 1730)		N	-	-	+	N	+
B (none)	N		N	N	N	N	N
C(1087)	-	N		+	-	N	-
D(1031)	-	N	+		-	N	-
E (3402)	+	N	-	-		N	+
F (none)	N	N	N	N	N		N
G (622, 567)	+	N	-	-	+	N	

Compound class* (SM)	A	B	C	D	E	F	G
A (1224)		+	N	-	-	-	-
B (1544)	+		N	-	-	-	-
C(none)	N	N		N	N	N	N
D(1013)	-	-	N		+	+	+
E (3427)	-	-	N	+		+	+
F (3621)	-	-	N	+	+		+
G (590)	-	-	N	+	+	+	

Compound class* (WM)	A	B	C	D	E	F	G
A (1210)		+	N	-	N	N	-
B (1653, 1559)	+		N	-	N	N	-
C(none)	N	N		N	N	N	N
D(1012)	-	-	N		N	N	+
E (none)	N	N	N	N		N	N
F (none)	N	N	N	N	N		N
G (531)	-	-	N	+	N	N	

* A, Aliphatic Ester;
B, Amide/ protein;
C, Carbohydrate;
D, Clay/ Biogenic silica/ Carbohydrate;
E, OH/NH groups;
F, Biogenic silica/silicate;
G, Clay/ Inorganic / Aromatic compound.
N indicates no identifiable cross-peak

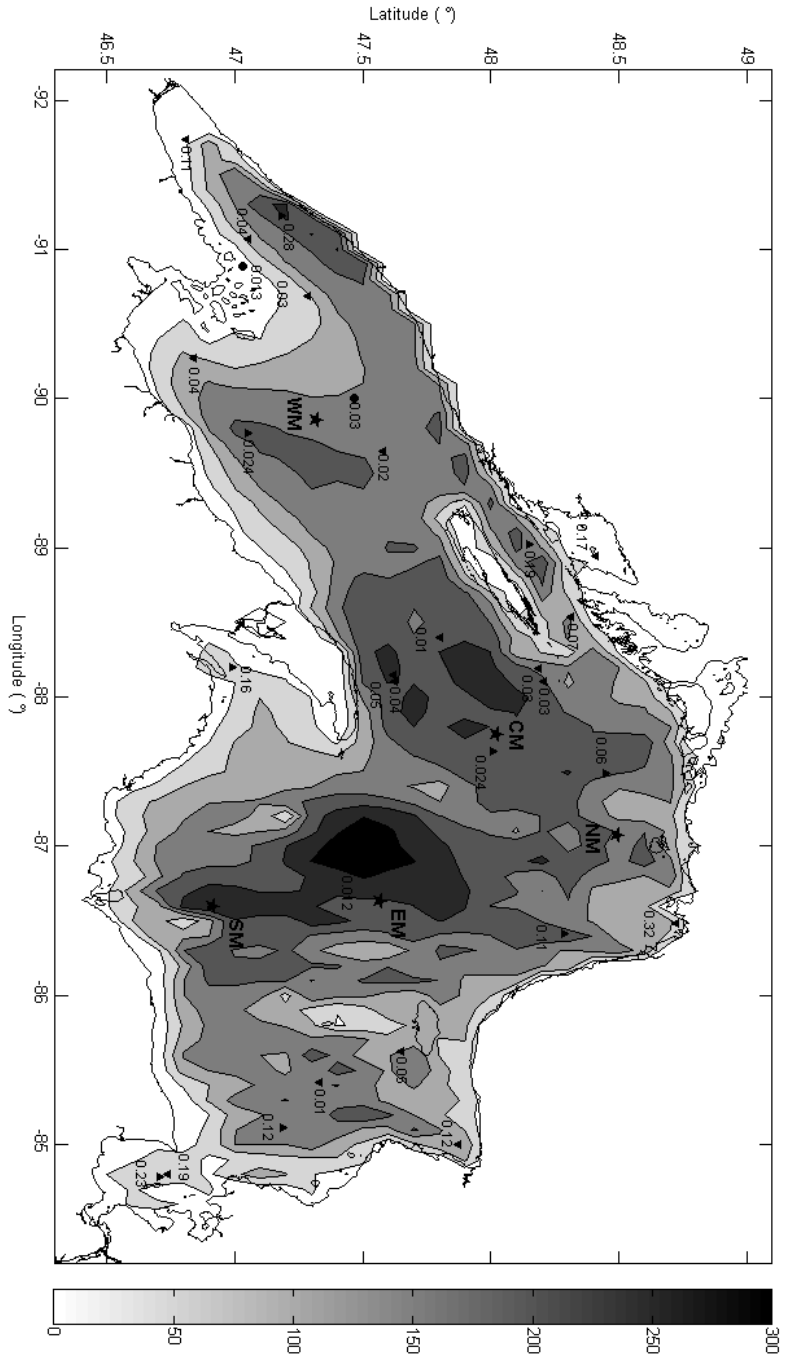

Fig. 4-1. Map of Lake Superior. Sampling sites (CM, EM, NM, SM and WM) are shown with stars. Sedimentation rates from previous studies are included for reference: Down triangles were obtained with the ^{210}Pb method and are from Evans (1981); up triangles are from Kemp et al. (1978) using the pollen method; circles are from Bruland et al. (1975) and were obtained from ^{210}Pb and pollen methods.

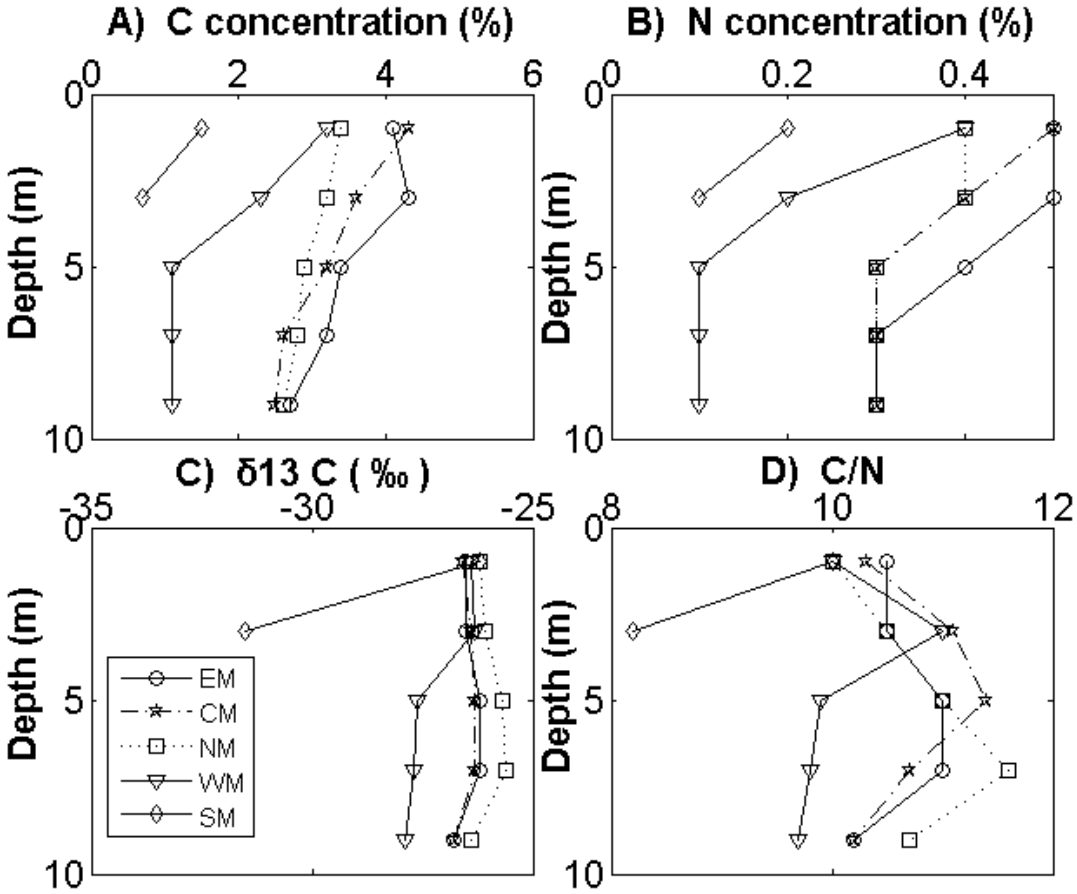

Fig. 4-2. Elemental and isotopic analysis results from Lake Superior sediments, showing down core trends in a) C% (wt./wt.), b) N% (wt./wt.), c) $\delta^{13}C$ and d) atomic C/N ratio.

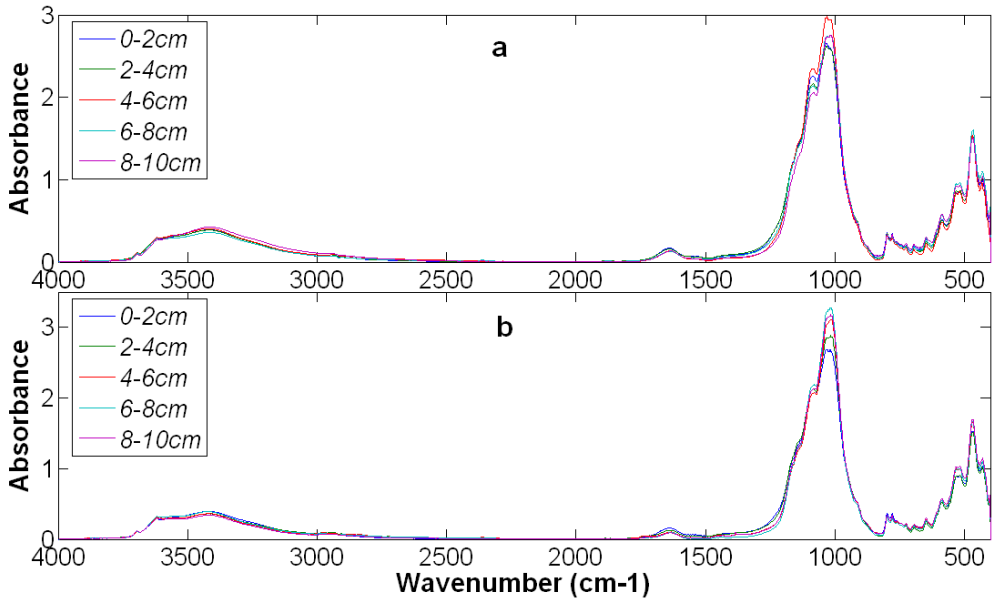

Fig. 4-3. 1D FTIR spectra of sediments at different depths at a) CM and b) WM stations. Each spectrum was normalized via total area as described in text before comparison to reduce variations from sample loading/processing.

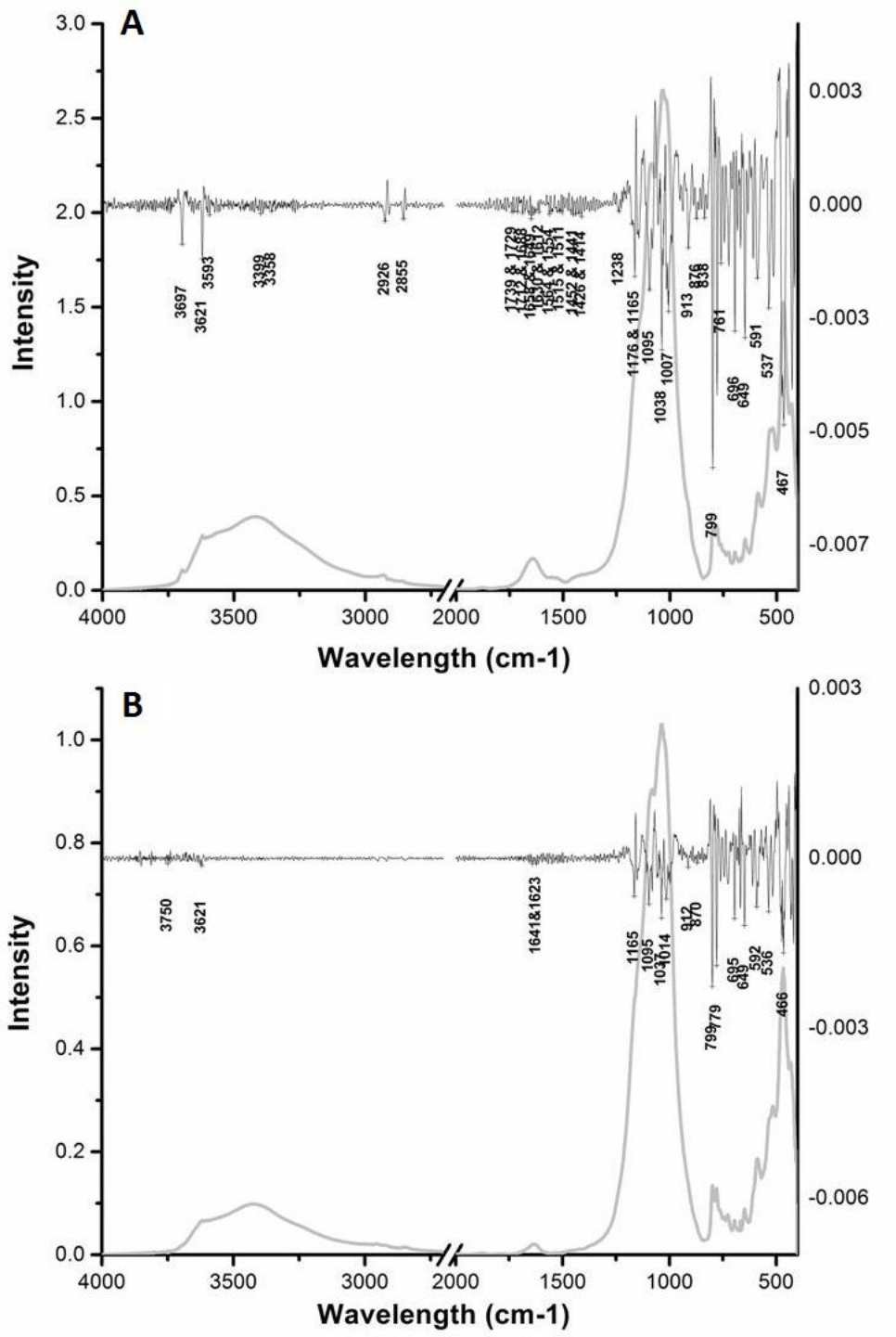

Fig. 4-4. 1D FTIR spectrum and 2nd derivative for the top 2 cm of the a) bulk sediment and b) combusted sediment samples at the CM station. The combustion conditions of 400 °C, 8 hours as suggested by Ball, 1964; Ben-Dor and Banin, 1989 were applied to minimize the loss of structural water and ensure the complete removal of OC.

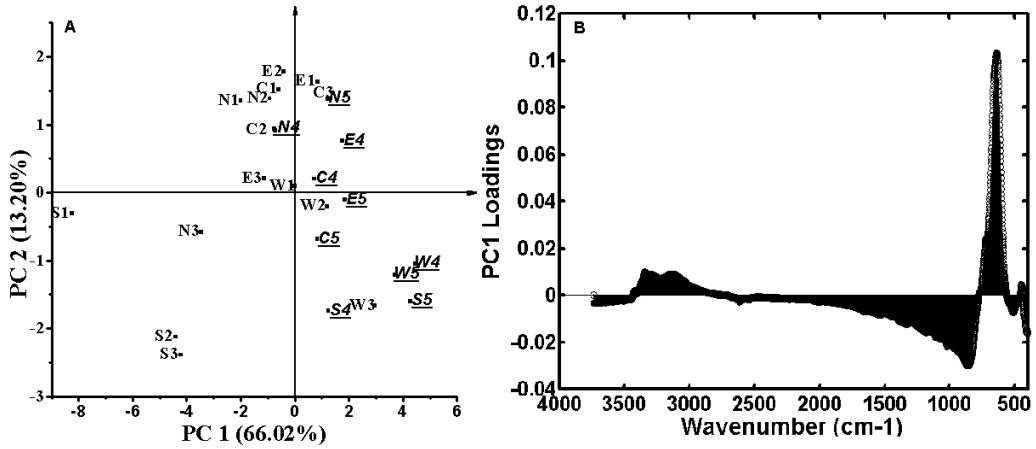

Fig. 4-5. PCA projection (a) and corresponding PC1 loading plot (b) for normalized FTIR data. For Fig. 5a, samples are named as the first station letter (see Table 4-1) plus a number indicating depth within the sediment core: 1, 0-2 cm; 2, 2-4 cm; 3, 4-6 cm; 4, 6-8 cm; 5, 8-10 cm. Deepest layers are shown with bold italic font and underlining.

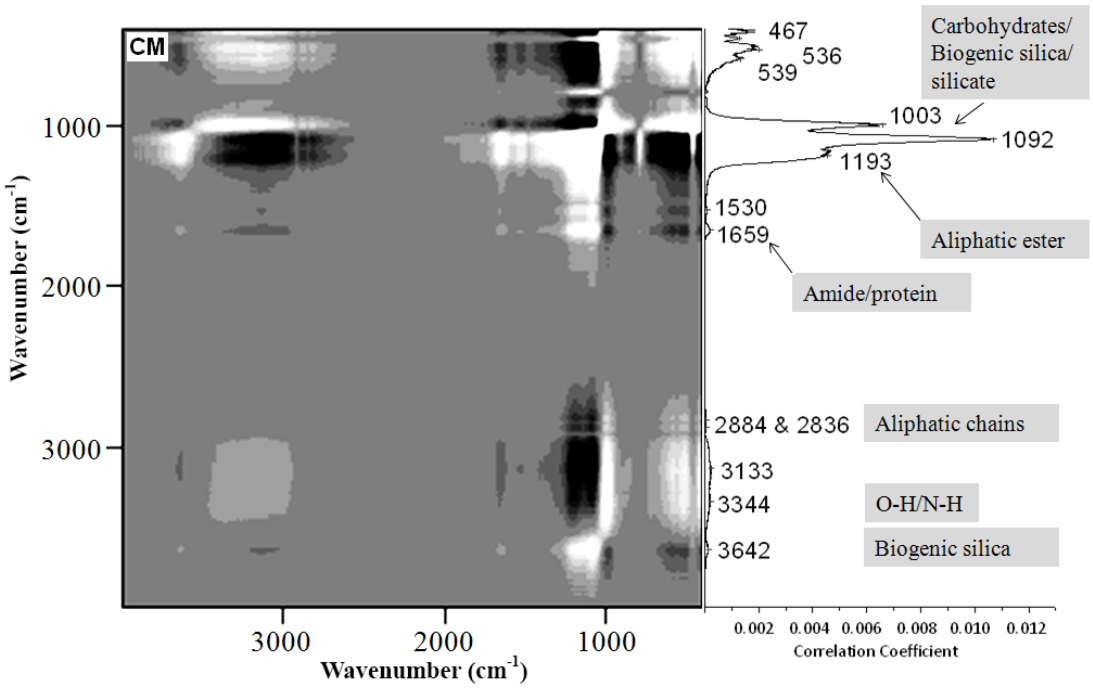

Fig. 4-6. Synchronous 2D correlation spectrum down-core for CM station. The spectral data set was constructed sorting from the shallowest depth to the deepest. The data set was normalized and PCA reconstructed before 2D correlation analysis (see text for further details). For ease of identification of peaks the slice through auto-peak diagonal is plotted to the right of each 2D correlation spectrum. White indicates positive correlation; black indicates negative correlation.

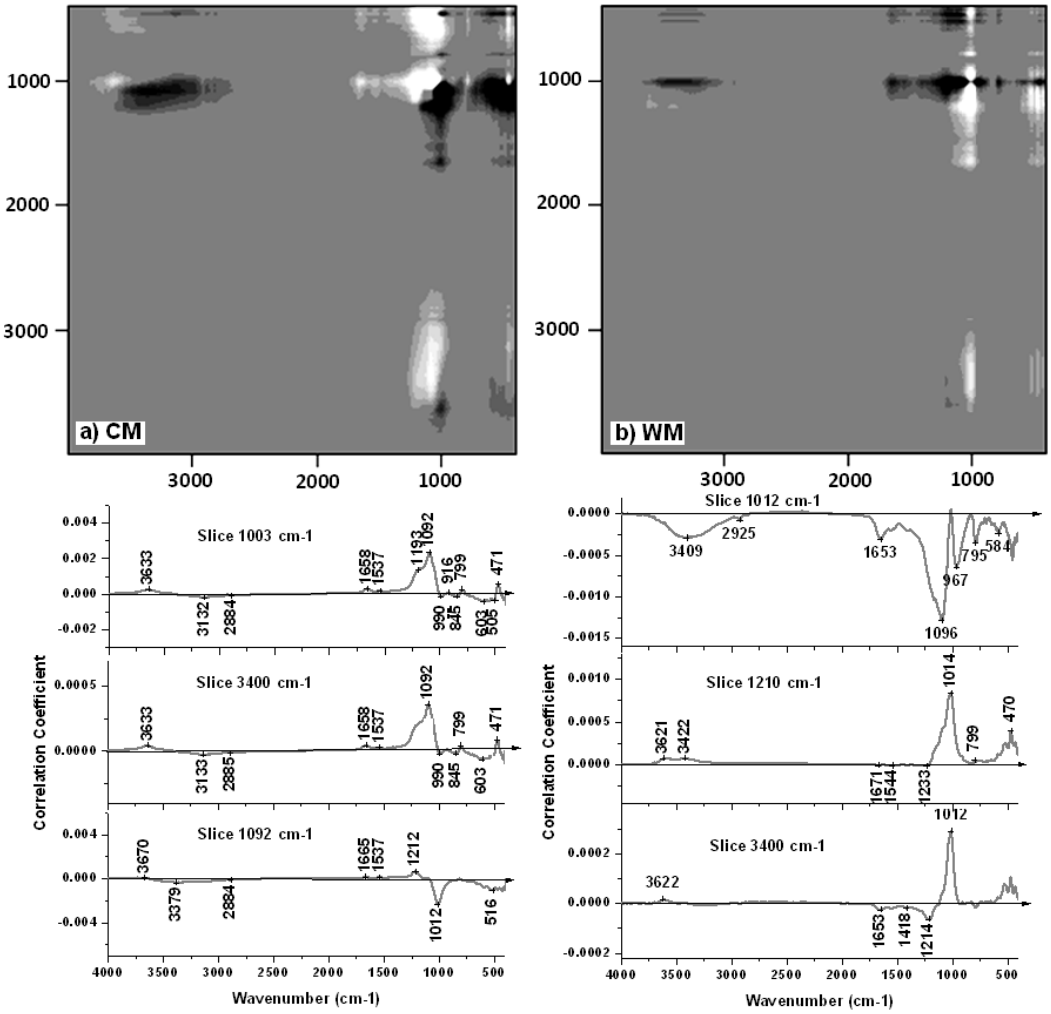

Fig. 4-7. Asynchronous 2D correlation spectrum for a) CM and b) WM. Each spectral data set was constructed sorting from the shallowest depth to the deepest. The data set was normalized and PCA reconstructed before 2D correlation analysis. For ease in identification of peaks, horizontal slices (y is constant) across the region of interest are plotted below each 2D correlation spectrum.

Chapter 5: Summary of conclusions and future work

The composition of DOM, settling POM and sedimentary OM in Lake Superiorand its relationship with organic matter source and dynamics were studied with the combination of advanced spectroscopic techniques, TOC analysis,and natural abundancestable and radiocarbon signatures. Results were used to infer the source, function, reactivity and biogeochemical cycles of the different carbon pools in Lake Superior at a range of temporal and spatial scales.

The combination of DOC analyses, stable and radiocarbon signatures and UV/visible spectrometry parameters on the bulk dissolved organic matter indicates that Lake Superior offshore water is oligotrophic, low in dissolved organic carbon content, and very clear. The DOM is primarily modern (post-bomb) and autochthonous in origin, with molecular features beinglow in aromatic components,primarily non-humic, hydrophilic and low molecular weight. Different SPE resins (SDB-XC vs C18) perform differently on the isolation of DOM. XC disks lead to greater DOC and CDOM recoveries as well as less fractionation in composition relative to initial water samples as determined by DOC mass balances and UV-Visible spectrophotometry parameters including $SUVA_{254}$, E2/E3 and spectral slope. We discover the preferential recovery of higher molecular weight and aromaticity material with both SPE resin types, with SDB-XC SPE providing less deviation from ‘init’ water samples.FT-ICR-MS data shows molecular-level similarities and differences among ‘eR’ obtained with different extractions disks. The ‘eR’ of different extraction resinsshared approximately 70% of compounds identified by FT-ICR-MS. The lignin-CRAM like fraction (a small fraction of which contains N and P) was found to be the major component at both WM and BR sites. Formulae in other functional groups including lipid, protein, amino-sugar, carbohydrate, and condensed hydrocarbon regions were also found and a portion of the formulae contain N and P in addition to C, H, and O. Comparing the two resin types, SDB-XC ‘eR’ has similar

percentages of CHO compounds, a higher proportion of CHOS, CHONP, CHONSP compounds, and lower proportion of CHON, CHONS and CHOP compounds than C18 ‘eR’. CA and PCA analysis, which are commonly used statistical measurements of sample similarity, confirm that the greatest variance in the sample set is driven by sample location, rather than the difference in extraction techniques.To get a comprehensive understanding of the DOM chemical composition and reactivityas well as its variations with sources and dynamics in Lake Superior, future work should include the investigation of SPE DOM samples from sites across the entire Lake Superior with ESI FT-ICR MS and should expand current work to a comparison of DOM from surface and deep water samples collected in both western and eastern basins during both stratified and mixed water-column conditions.

Settling POM and itsspatial and temporal sedimentation patterns, origin and biochemical compositionwere investigatedto reveal POM nutritional value to benthic consumers and to infer the POC cycling in Lake Superior. A similar seasonal pattern was observed at both sites with the highest mass flux occurring in the unstratified season; however, the most organic rich samples were obtained from the summer stratified season. Processes controlling the type and quantity of sinking solids in the water column of the Lake Superior appear to be resuspension of surficial sediments and primary production.Increases in PCHO-C%values, THAA contents, THAA-C% and THAA-N% were seen at both sites corresponding to enhanced primary productivity input in summer. However, distinct carbohydrate and amino acid distributions between EM and WM reveal possible differences in OM sources and thedegree of degradation occurring at the two sites. The combination of PCHO-C% and THAA suggests that summer POM has 2 to 5 fold higher nutritional value to the benthic consumer than spring-winter POM in Lake Superior. Based on FTIR spectra, clay-minerals/biogenic silica are dominant in all samples obtained through the seasons, with a measurable fraction of organic matter including carbohydrate, carboxylic acid, aliphatic/acetyl ester, amide/protein and phenol/lignin. Principal component analysis

of FTIR data from the sediment trap material suggests compositional variation as a function of season, with relatively strong inorganic clay mineral signals dominating in winter-spring and a strong signal from amide, carbohydrate and other organic components in summer. This further supports our wet chemistry results indicating that the relative bioavailability and nutritional values of POM to benthic microbes are lower in winter than summer. To better understand the dynamics of settling POC in the lake, future work includes investigation of the mean ages and potential source distribution of the sinking POC pool. A better constrainton primary production and its seasonal variations will also enhance ourunderstanding of the settling particulate material dynamics and help us distinguish export from the surface lake vs sediment resuspension. Also, the riverine particulate organic matter input should be assessed in a variety of spatial and temporal scales across the lake to better constrain terrestrial influence on the lake's settling- POM biogeochemistry.

The composition and diagenesis of Lake Superior sedimentary OM were investigated with the combination of FTIR, stable and radiocarbon signatures. A dominant contribution from clay-minerals/ biogenic silica along with a distinct contribution from common organic matter functional groups (carbohydrate, carboxylic acid, aliphatic/acetyl ester, amide/protein and phenol/lignin) are identified. The %C and %N concentrations in the sediments decreased with depth at all sites with various degrees of change at different sites. PCA analysis of the FTIR data shows that, with increasing depth, carboxylates, aliphatic esters, amide/protein, and carbohydrates decrease and the remaining FTIR amenable material becomes more similar across the lake sites. 2D correlation analysis shows that the chemical composition of the sediments changes with depth, with aliphatic esters and some carbohydrates appearing most susceptible to diagenesis.Asynchronous spectra can provide a sequential order of early stage OM diagenesis. In general: carboxyl groups including those in aliphatic ester and amide/protein change first, followed by a group of carbohydrates and then aromatic compounds and/or clay minerals and/or the Si-O framework of biogenic

silica. In addition to general diagenetic trends in Lake Superior sediment, we do see some spatial variability in surface sediment composition. NM, SM and WM have distinct down-core compositional variations relative to EM and CM. We believe NM to be affected by increased terrestrial input, SM to be affected by local acceleration of bottom currents in the deep trough and WM to be affected by the geological nature of the sediment or sediment resuspension. Since down-core variability in the lake may be related to variation in sedimentation rates, future work includes research coupling FTIR analysis on deeper cores along with better estimation of sedimentation rates for each core.

Comparing DOM vs settling POM and sedimentary OM, DOM in Lake Superior is generally younger (turnover time ~60 years) than sedimentary organic matterbased on existing natural abundance radiocarbon data; although lacking of radiocarbon data for settling POM, we estimate it to vary considerably over a year due to the variable contribution from its two main sources, sediment resuspension vs primary production, which exhibit distinct age differences. The average $\delta^{13}C$ and C/N values of the three carbon pools are similar and revealing the possible overlap of the primarilyautochthonousand terrestrial plant inputs. Settling particles are two to four fold more enriched in organic carbon and organic nitrogen than the sediments 30 to 115 m below, suggesting intensive degradation occurring at the sediment-water interface. The differences in trap and sedimentary samples are consistent with differences seen between our POC fluxes (0.64 to 23.1 $mgC/m^2/day$ at EM and 3.72 to 30.8 $mgC/m^2/day$ at WM)and reported annual average sediment POC burial rates (0.25 $mol/m^2/year$, equivalent to 8.2 $mg/m^2/day$, Hales et al. 2008). The slightly higher C/N ratios and more enriched $\delta^{13}C$ values in the sediments relative to the settling POM indicates preferentialremineralization/mobilization of N and microbial reworking of OM in the sediments.

Biogeochemical dynamics of OM in aquatic systemsprovide key insights

forunderstanding carbon cycling in these systems, and thus have relevance to the local andglobal climate. This thesis work determined the detailedcomposition and dynamics of the major fractions of OM in Lake Superior. The results show the importance of in-lake and terrestrial influenceson different carbon pools and may be used to determine how episodic events and anthropogenic activities may alter the above processes and eventually affect C storage and cycling.

REFERENCES

Abdulla H.A.N., R.F. Dias, and E.C. Minor. 2009. Understanding the enhanced aqueous solubility of styrene by terrestrial dissolved organic matter using stable isotope mass balance and FTIR. *Organic Geochemistry* 40, 547-552.

Abdulla H.A.N., E.C. Minor, R.F. Dias, and P.G. Hatcher 2010a. Changes in the compound classes of dissolved organic matter along an estuarine transect: A study using FTIR and 1^{3}C NMR. *Geochimica et Cosmochimica Acta.* 74, 3815-3838.

Abdulla H.A.N., E. C. Minor, and P.G. Hatcher. 2010b. Using Two-Dimensional Correlations of ^{13}C NMR and FTIR To Investigate Changes in the Chemical Composition of Dissolved Organic Matter along an Estuarine Transect. *Environ. Sci. Technol.* 44, 8044-8049.

Abdulla, H.A.N., R.L.Sleighter, P.G.Hatcher. 2013. Two Dimensional Correlation Analysis of Fourier Transform Ion Cyclotron Resonance Mass Spectra of Dissolved Organic Matter: A New Graphical Analysis of Trends. *Anal. Chem.* 85, 3895-3902.

Aluwihare L.I., D.J. Repeta, and R.F. Chen. 1997. A major biopolymeric component to dissolved organic carbon in surface sea water. *Nature.* 387, 166-169.

Aravena R. and L.I. Wassenaar. 1993. Dissolved organic carbon and methane in a regional confined aquifer: Carbon isotopic evidence for associated subsurface sources. *Applied Geochemistry*. 8, 483-493.

Austin J. and S. Colman. 2008. A century of temperature variability in Lake Superior. *Limnol. Oceanogr*. 53, 2724-2730.

Assel, R.A. 1986. Fall and winter thermal structure of Lake Superior. *Journal of Great Lakes Research* 12, 251-262.

Baas, M., R. Pancos, B. Geel van, and J.S. Sinninghe Damsté. 2000. A comparative study of lipids in sphagnum species. *Organic Geochemistry*, 31, 535-541.

Baker J. E. and S. J. Eisenreich. 1989. PCBs and PAHs as Tracers of Particulate Dynamics in Large Lake. *Journal of Great Lakes Research.* 15, 84-103.

Baker J.E., S.J. Eisenreich, and B. J. Eadie. 1991. Sediment trap fluxes and benthic recycling of organic carbon, polycyclic aromatic hydrocarbons, and polychlorobiphenyl congeners in Lake Superior. *Environ. Sci. Technol*. 25, 500-509.

Ball, D.E. 1964. Loss-on-ignition as an estimate of organic matter and organic carbon in non-calcareous soils. *Journal of soil science* 15, 84-92.

Barbiero1, R.P, M.L. Tuchman. 2004. The Deep Chlorophyll Maximum in Lake Superior. J. Great Lakes Res. 30 (Supplement 1), 256–268.

Barros, G.V., L.A. Martinelli, T.M. Oliveira Novais, J. H.B. Ometto, and G. M. Zuppi. 2010. Stable isotopes of bulk organic matter to trace carbon and nitrogen dynamics in an estuarine ecosystem in Babitonga Bay (Santa Catarina, Brazil). *Science of the Total Environment*, 408, 2226-2232.

Ben-Dor, E, A. Banin 1989. Determination of organic matter content in arid-zone soils using a simple “loss-on-ignition” method. *Communications*

in Soil Science and Plant Analysis 20, 1675-1695.

Benner, R. In: *Biogeochemistry of Marine Dissolved Organic Matter;* Hansell, D.A., C.A. Carlson, Eds. Academic Press, Boston, 2002, 69-70.

Benner, R., B. Biddanda, B. Black, and M. McCarthy. 1997. Abundance, size distribution, and stable carbon and nitrogen isotopic compositions of marine organic matter isolated by tangential-flow ultrafiltration. *Mar. Chem*. 57: 243–263.

Bennington, V., G.A. McKinley, N. Kimura, C.H. Wu. 2010. General circulation of Lake Superior: Mean, variability, and trends from 1979 to 2006. *Journal of Geophysical Research*, 115, C12015, doi:10.1029/2010JC006261.

Bloesch, J. and U. Uehlinger. 1990. Epilimnetic carbon flux and turnover of particle size classes in oligo-mesotrophic Lake Lucerne, Switzerland. *Arch. Hydrobiol*. 118, 403-419.

Blough, N.V., R. Del Vecchio. 2002. Chromophoric DOM in the coastal environment, p. 509-546. In Hansell, D.A., and C.A. Carlson [eds.] *Biogeochemistry of marine dissolved organic matter*. Academic Press.

Brandenburg, K. and U. Seydel. 2002. Vibrational spectroscopy of carbohydrates and glykoconjugates. *Handbook of Vibrational Spectroscopy*. John Wiley & Sons, Chichester. UK, 3481-3507.

Brincat, D., K.Yamada, R. Ishiwatari, H. Uemur, and H. Naraoka. 2000. Molecular-isotopic stratigraphy of long-chain n-alkanes in Lake Baikal Holocene and

glacial age sediments. *Organic Geochemistry*. 31, 287-294.

Bruland, K.W., M. Koide, C. Bowser, L.J. Maher, E.D. Goldberg. 1975. ^{210}Pb and pollen geochronologies on Lake Superior Sediments. *Quaternary Research* 5, 89-98.

Buesseler, K.O. , A.N. Antia, M. Chen, S.W. Fowler, W.D. Gardner, O. Gustafsson, K. Harada, A.F. Michaels, M.Rutgers van der Loeff, M. Sarin, D.K. Steinberg, T. Trull. 2007. An assessment of the use of sediment traps for estimating upper ocean particle fluxes. *Journal of Marine Research*. 65, 345-416.

Burdige D.J. 2007. Preservation of Organic Matter in Marine Sediments: Controls, Mechanisms, and an Imbalance in Sediment Organic Carbon Budgets? *Chem. Rev.* 107, 467-485.

Burdige, D.J., A. Skoog, K. Gardner. 2000. Dissolved and particulate carbohydrates in contrasting marine sediments. *Geochimica et Cosmochimica Acta*, 64(6), 1029-1041.

Berner, R. A.1989. Biogeochemical cycles of carbon and sulfur and their effect on atmospheric oxygen over Phanerozoic time. In: *The long term stability of the Earth system* (ed. E. J. Barron). 1, 97–122.

Carr, A.S., A. Boom, B.M. Chase, D.L. Roberts, Z.E. Roberts. 2010. Molecular fingerprinting of wetland organic matter using pyrolysis-GC/MS: an example from the southern Cape coastline of South Africa. *Journal of Paleolimnology* 44, 947-961.

Canuell, E.A., J. E. Cloern, D. B. Ringelberg, J. B. Guckert, and G. H. Rau. 1995. Molecular and isotopic tracers used to examine sources of organic matter and its incorporation into the food webs of San Francisco Bay. *Limnol. Oceanogr*. 40, 67-81.

Carlson, C.A., H.W. Ducklow, and A.F. Michaels. 1994. Annual flux of dissolved organic carbon from the euphotic zone on the northwestern Sargasso Sea. *Nature*. 371, 405-408

Celi, L., M. Schnitzer and M. Nègre. 1997. Analysis of carboxyl groups in soil humic acids by a wet chemical method, Fourier transform infrared spectrometry and solution-state ^{13}C nuclear magnetic resonance, a comparative study. *Soil Science* 162, 189-197.

Charlton M.N. and D.R.S. Lean. 1987. Sedimentation, Resuspension, and Oxygen Depletion in Lake Erie (1979). *Journal of Great Lakes Research*. 13, 709-723.

Cline, J. D. and I. R. Kaplan. 1975. Isotopic fractionation of dissolved nitrate during denitrification in the eastern tropical north Pacific Ocean. *Mar. Chem*. 3, 271-299.

Cole, J.J., N.F. Caraco, G.W. Kling, and T.K. Kratz. 1994. Carbon dioxide supersaturation in the surface waters of lakes. *Scienc.e* 265, 1568-1570.

Cotner, J., B. Bopaiah, W. Makino, and E. Stets. 2004. Organic carbon biogeochemistry of Lake Superior. *Aquatic Ecosystem Health and Management*. 4, 451-464.

Cowie G. L. and J.I. Hedges. 1992. The role of anoxia in organic matter preservation in coastal sediments: relative stabilities of the major biochemicals under oxic and anoxic depositional conditions. *Org. Geochem*. 19, 229-234.

D'Andrilli, J., J. P. Chanton, P. H. Glaser, and W.T. Cooper. 2010. Characterization of

dissolved organic matter in northern peatland soil porewaters by ultra high resolution mass spectrometry. *Organic Geochemistry*, 41.791-799.

Dauwe, B., J.J. Middelburg. 1998.Amino acids and hexosamines as indicators of organic matter degradation state in North Sea sediments. Limnol. Oceanogr., 43, 782-798.

Dauwe, B. 1999. Linking diagenetic alteration of amino acids and bulk organic matter reactivity. *Limnol. Oceanogr*, 44, 1809-1814.

Davis J. and R. Benner. 2005. Seasonal trends in the abundance, composition and bioavailability of particulate and dissolved organic matter in the Chukchi/Beaufort Seas and western Canada Basin. *Deep-Sea Research*. 52, 3396-3410.

Degens, E.T. 1967. Diagenesis of organic matter, In: Larsen, G., Chilingar, G.V., (Eds.) *Diagenesis in Sediments*. Elsevier, Amsterdam, pp. 345-390.

Degens, E.T., V. Ittekkot. 1985. Particulate organic carbon an overview. In: Degens, E.T., S.K. Kempe, and R. Herrera. (editor). *Transport of Carbon and Minerals in Major World Rivers*. Mitt. Geol. Palaont. Inst. Univ. Hamburg. 58, 7-27.

Derkacheva O. and D. Sukhov. 2008. Investigation of Lignins by FTIR Spectroscopy. *Macromol. Symp*.265, 61–68.

Deuser, W.G., E.H. Ross, and R.F. Anderson. 1981. Seasonality in the supply of sediment to the deep Sargasso Sea and implications for the rapid transfer of matter to the deep ocean. *Deep Sea Research.* 28, 495-505.

Dittmar T., R.J. Lara, and G. Kattner. 2001. River or mangrove? Tracing major organic matter sources in tropical Brazilian coastal waters. *Mar. Chem.* 73, 253-71.

Dittmar, T., B. Koch, H. Hertkorn, G. Kattner. 2008. A simple and efficient method for solid phase extraction of dissolved organic matter (SPE-DOM) from seawater. *Limnology and Oceanography*: Methods 6: 230-235.

Druffel, E.R.M., P.M. Williams, J.E. Bauer, and J.R. Ertel. 1992. Cycling of dissolved and particulate organic matter in the open ocean. Journal of Geophysical Research 97(C10): 15,639-15,659.

Duce, R.A. and E.K. Duursma. 1977. Input of organic matter to the ocean. *Mar. Chem.* 5, 319-339.

Dutka, B.J., J.B. Bell, D.L.S. Liu. 1974. Microbiological examination of offshore Lake Erie sediments. *Journal of the Fisheries Research Board of Canada* 31, 299-308.

Eadie, B.J., R.L Chambers, W.S. Gardner, and G.L. Bell. 1984. Sediment trap studies in Lake Michigan: resuspension and chemical fluxes in the southern basin. *J. Great Lakes Res*. 10, 307-321.

Eglinton, G. and R.J. Hamilton. 1967. Leaf epicuticular waxes. *Science*. 156, 1322-1334.

Eppley R.W. and B.J. Peterson. 1979. Particulate organic matter flux and planktonic new production in the deep ocean. *Nature*. 282, 677-680.

Evans, J.E., T.C. Johnson, E.C. Alexander, Jr., R.S. Lively, Eisenreich, S.J. 1981. Sedimentation rates and depositional processes in Lake Superior from ^{210}Pb Geochronology. *Journal of Great Lakes Research* 7, 299-310.

Farquhar G.D., J.R. Ehleringer, and J.T. Hubick. 1989. Carbon isotope discrimination and photosynthesis. *Annual Review of Physiology and Molecular Biology*. 40, 503-537.

Ficken, K.J., B. Li., D.L. Swain, G. Elinton. 2000. An n-alkane proxy for the sedimentary input of submerged/floating freshwater aquatic macrophytes. *Organic Geochemistry.* 31, 745-749.

France, R.L. 1995. Differentiation between littoral and pelagic food webs in lakes using stable carbon isotopes. *Limnology and Oceanography* 40: 1310–1313.

Frank, M.P. and R.W. Powers. 2007. Simple and rapid quantitative high-performance liquid chromatographic analysis of plasma amino acids. *Journal of Chromatography B.* 852, 646-649.

Freudenthal, T., T. Wagner, F. Wenzhofer, M. Zabel, and G. Wefer. 2001. Early diagenesis of organic matter from sediments of the eastern subtropical Atlantic: Evidence from stable nitrogen and carbon isotopes. *Geochimica et Cosmochimica Acta*. 65, 1795-1808.

Gälman V., J. Rydberg, S.S. de-Luna, R. Bindler and I. Renberg. 2008. Carbon and nitrogen loss rates during aging of lake sediment: changes over 27 years studied in varved lake sediment. *Limnol Oceanogr*. 53, 1076-82.

Gearing, P., F.E. Plucker, and P.L. Parker. 1977. Organic carbon stable isotope ratios of continental marine sediments. *Mar. Chem.* 5, 251-266.

Grey J. and R.I. Jones. 2001. Seasonal changes in the importance of the source of organic matter to the diet of zooplankton in Loch Ness, as indicated by stable isotope analysis. *Limnol. Oceanogr.* 46, 505-513.

Griffiths P.R. and J.A. De Haseth. 2007. *Fourier Transform Infrared Spectroscopy*. Wiley-Inter science, New Jersey.

Gupta,L.P.,H.Kawahata. 2000.Amino acid and hexosamine composition and flux of sinking particulate matter in the equatorial Pacific at 1753ºE longitude. *Deep-Sea Research* I, 47,1937-1960.

Hales, B., W. Cai, G.B. Mitchell, C.L. Sabine, and O. Schofield [eds.] 2008: North American Continental Margins: A Synthesis and Planning Workshop. Report of the North American Continental Margins Working Group for the U.S. Carbon Cycle Scientific Steering Group and Interagency Working Group. U.S. Carbon Cycle Science Program, Washington, DC, 110 pp.

Hansell, D.A., Carlson, C.A. (2001) Marine Dissolved Organic Matter and the Carbon Cycle. *Oceanography* 14, 41-49.

Harisa, P.I., F. Severcanb. 1999. FTIR spectroscopic characterization of protein structure in aqueous and non-aqueous media. *Journal of Molecular Catalysis B: Enzymatic* 7, 207-221.

Harris, D., W.R. Horwáth, C. Van Kessel. 2001. Acid fumigation of soils to remove carbonates prior to total organic carbon or carbon-13 isotopic analysis. *Soil Science*

Society of America Journal 65, 1853-1856.

Hedges, J.I.1992. Global biogeochemical cycles: progress and problems. *Mar. Chem.* 39, 67-93.

Hedges, J.I., G. Eglington, P. Hatcher, D.L. Kirchman, C. Arnosti, S. Derenne, R.P. Evershed, I. Kogel-Knabner, J.W. de Leeuw, R. Littke, W. Michaelis, and J. Rullkotter. 2000. The molecularly uncharacterized component of nonliving organic matter in natural environments. *Organic Geochemistry*, 31, 945-958.

Hedges J.I., R.G. Keil, and G.L. Cowie. 1992. Sedimentary diagenesis: organic perspectives with inorganic overlays. *Chemical Geology*. 107, 487-492.

Hedges, J.I. and D.C. Mann. 1979. The lignin geochemistry of marine sediments from the southern Washington coast. *Geochimica et Cosmochimica Acta*. 43, 1809-1818.

Hedges, J.I. and J.M. Oades. 1997. Comparative geochemistries of soils and sediments. *Organic Geochemistry*. 27, 319-361.

Helms, J.R., Stubbins, A., Ritchie, J.D., Minor, E.C., Kieber, D.J., Mopper, K. (2008) Absorption spectral slopes and slope ratios as indicators of molecular weight, source, and photobleaching of chromophoric dissolved organic matter. *Limnol. Oceanogr.* 53(3), 955–969.

Heinen E.A.,J. McManus.2004. Carbon and Nutrient Cycling at the Sediment-water Boundary in Western Lake Superior. *J. Great Lakes Res.* 30 (Supplement 1):113-132.

Henrichs S.M. 1992. Early diagenesis of organic matter in marine sediments: progress and perplexity. *Mar. Chem*. 39, 119-149.

Herbert T.D. 2001. Review of alkenone calibrations (culture, water column, and sediments). *Geochem. Geophys. Geosyst.* 2, 2000GC000055.

Herbert, T.D., B.A. Tom and C. Burnett. 1992. Precise major component determinations in deep-sea sediments using Fourier Transform Infrared Spectroscopy. *Geochim. Cosmochim. Acta* 56, 1759-1763.

Herdendorf, C. E. 1982. Large lakes of the world. *Journal of Great Lakes Research*. 3, 379-412.

Hernes, P.J., J.I. Hedges, M.L. Peterson, S.G. Wakeham and C. Lee. 1996. Neutral carbohydrate geochemistry of particulate material in the central equatorial Pacific. *Deep-Sea Res* II. 43:1181-1204.

Hernes, P.J., M.L. Peterson, J.W Murray, S.G. Wakeham, C Lee, and J.I Hedges. 2001. Particulate carbon and nitrogen fluxes and compositions in the central equatorial Pacific. *Deep-Sea Res*. Part I 48, 1999-2023.

Hertkorn, N, Benner, R., Frommberger, M., Schmitt-Kopplin, Ph., Witt, M., Kaiser, K., Kettrup, A., Hedges, J. I. (2006) Characterization of a major refractory component of marine dissolved organic matter. *Geochim. Cosmochim. Acta* 70, 2990–3010.

Hertkorn, N., M. Frommberger, M. Witt, B.P. Koch, Ph. Schmitt-Kopplin, E.M. Perdue. 2008. Natural Organic Matter and the Event Horizon of Mass Spectrometry. *Analytical Chemistry.* 80, 8908-8919.

Hockaday, W.C., Purcell, J.M., Marshall, A.G., Baldock, J.A., Hatcher, P.G. (2009) Electrospray and photoionization mass spectrometry for the characterization of organic matter in natural waters: a qualitative assessment. *Limnol. Oceanogr.*: Methods 7, 81-95.

Hoffman, J.C., G.S. Peterson, A.M. Cotter, J.R. Kelly. 2010. Using stable isotope mixing in a Great Lakes coastal tributary to determine food web linkages in young fishes. *Estuaries and Coasts*, DOI: 10.1007/s12237-010-9295-0.

Hughey, C.A., C.L. Hendrickson, R.P. Rodgers, and A.G. Marshall. 2001. Kendrick Mass Defect Spectrum: A Compact Visual Analysis for Ultrahigh-Resolution Broadband Mass Spectra. *Anal. Chem*. 73, 4676-4681.

Johnson, T.C. 1980. Late-glacial and postglacial sedimentation in Lake Superior based on seismic-reflection profiles. *Quaternary Research* 13, 380-391.

Johnson, T.C., S.J. Eisenreich. 1979. Silica in Lake Superior: mass balance considerations and a model for dynamic response to eutrophication. *Geochimica et Cosmochimica Acta* 43, 7-92.

Johnson, T.C., J.E. Evans, S.J. Eisenreich. 1982. Total organic carbon in Lake Superior USA, Canada: sediments comparisons with hemi pelagic and pelagic marine environments. *Limnol. Oceanogr*. 27, 481-491.

Johnson, K.M. and M.J. Sieburth. 1977. Dissolved carbohydrates in seawater. I. A precise spectrophotometric analysis for monosaccharides. *Mar. Chem.*, 5, 1-13.

Jung, Y.M. 2004. Principal component analysis based two-dimensional correlation

spectroscopy for noise filtering effect. *Vibrational Spectroscopy* 36, 267-270.

Kemp A.L.W. and L.M. Johnston. 1979. Diagenesis of Organic Matter in the Sediments of Lakes Ontario, Erie, and Huron. *Journal of Great Lakes Research*. 5, 1-10

Keough, J.R., M.E. Sierszen, and C.A. Hagley. 1996. Analysis of a Lake Superior coastal food web with stable isotope techniques. *Limnol. Oceanogr*. 41, 136–146.

Keough, J.R., C.A. Hagley, E. Ruzycki, and M.E. Sierszen. 1998. $\delta^{13}C$ composition of primary producers and role of detritus in a freshwater coastal ecosystem. *Limnol. Oceanogr*. 43, 734-740.

Kerner, M., H. Hohenburg, S. Ertl, M. Reckermann, and A. Spitzy. 2003. Self-organization of dissolved organic matter tomicellelike microparticles in river water. *Nature*. 422, 150-154.

Kim, S., Kramer, R.W., Hatcher, P.G. (2003) Graphical method for analysis of ultrahigh-resolution broadband mass spectra of natural organic matter, the Van Krevelen Diagram. *Analyt. Chem.* 75, 5336-5344.

Kirchman, D.L., Y. Suzuki, C. Garside, and H.W. Ducklow. 1991. High turnover rates of dissolved organic carbon during a spring phytoplankton bloom. *Nature.* 352, 612-614.

Klump, J.V., R. Paddock, C.C. Remsen, S. Fitzgerald, M. Boraas, P. Anderson, 1989. Variations in sediment accumulation rates and the flux of labile organic matter in eastern Lake Superior basins. *J. Great Lakes Res. 15,* 104–122.

Koprivnjak, J.-F., P.H. Pfromm, E. Ingall, T.A. Vetter, P. Schmitt-Koplin, N. Hertkorn, M. Frommberger, H. Knicker, E.M. Perdue. 2009. Chemical and spectroscopic characterization of marine dissolved organic matter isolated using coupled reverse osmosis-electrodialysis. *Geochimica et Cosmochimica Acta* 73: 4215-4231.

Krezoski, J.R.1989. Sediment reworking and transport in eastern Lake Superior: In situ rare earth element tracer studies. *Journal of Great Lakes Research* 15, 26-33.

Kruger, B.R., B.J.Dalzell, E.C. Minor. 2011. Effect of organic matter type and salinity on dissolved organic matter isolation via ultrafiltration and solid phase extraction. *Aquat. Sci* DOI: 10.1007/s00027-011-0189-4.

Kujawinski, E.B.2002. Electrospray ionization Fourier transform ion cyclotron resonance mass spectrometry (ESI FT-ICR MS): Characterization of complex Environmental mixtures. *Environ. Forensics* 3, 207-216

Kujawinski, E.B., M.D. Behn. 2006. Automated analysis of electrospray ionization Fourier-transform ion cyclotron resonance mass spectra of natural organic matter. *Anal. Chem.* 78, 4363-4373.

Kujawinski, E.B., K.Longnecker, N.V.Blough, R.Del Vecchio, L.Finlay, J.B.Kitner, S.J. Giovannoni. 2009. Identification of possible source markers in marine dissolved organic matter using ultrahigh resolution mass spectrometry. *Geochim. Cosmochim. Acta* 73, 4384-4399.

Kvalheim, O.M., D.W. Aksnes, T. Brekke, M.O. Eide, E. Sletten. 1985. Crude oil characterization and correlation by principal component analysis of ^{13}C nuclear magnetic resonance spectra. *Analytical Chemistry* 57, 2858-2864.

Lam, B., A.Baer, M.Alaee, B.Lefebvre, A.Moser, A. Williams,A.J. Simpson. 2007. Major Structural Components in Freshwater Dissolved Organic Matter. *Environ. Sci. Technol* 41 (24), 8240–8247.

Lee, C. 1988. Amino Acid and Amine Biogeochemistry in Marine Particulate Material and Sediments. IN *Nitrogen Cycling in Coastal Marine Environments.* Edited by T. H. Blackburn and J. Sørensen. John Wiley & Sons Ltd.

Lee, C., and C. Cronin. 1982.The vertical flux of particulate organic nitrogen in the sea: decomposition of amino acids in the Peru upwelling area and the equatorial Atlantic. *J. Mar. Res*. 40, 227-51.

Lee, C., and C. Cronin. 1984. Particulate amino acids in the sea: effects of primary productivity and biological decomposition. *J. Mar. Res*. 42, 1075-97.

Lehmann, M.F., S.M. Bernasconi, A. Barbieri, J.A. McKenzie. 2002. Preservation of organic matter and alteration of its carbon and nitrogen isotope composition during simulated and in situ early sedimentary diagenesis. *Geochimica et Cosmochimica Acta* 66, 3573-3584.

Lewis C.A., S.J. Rowland, D. Walton, A.C. Aplin, and M.L. Coleman. 1993. Quantitative Assessment of Changes Occurring in Organic Matter during Early Diagenesis [and Discussion]. *Physical Sciences and Engineering*. 344, 101-111.

Li, J., D. Miklesh, M. Kistner, D.E. Canfield, S. Katsev. 2012. Carbon mineralization and oxygen dynamics in sediments with deep oxygen penetration, Lake Superior. *Limnology & Oceanography* 57, 1634-1650.

Li, H., E.C. Minor, P.K. Zigah. 2013. Diagenetic changes in Lake Superior sediments as seen from FTIR and 2D correlation spectroscopy. *Organic Geochemistry* 58, 125-136.

Lindroth P., K. Mopper. 1979. High Performance Liquid Chromatographic Determination of Subpicomole Amounts of Amino Acids by Precolumn Fluorescence Derivatization with o-Phthaldialdehyde. *Analytical Chemistry,* 51, 1667-1674.

Loh, A. N., J. E. Bauer, and E. A. Canuel. 2006. Dissolved and particulate organic matter source-age characterization in the upper and lower Chesapeake Bay: A combined isotope and biochemical approach. *Limnology and Oceanography,* 51, 1421-1431.

MacCarthy, P., J.A. Rice. 1985. Spectroscopic methods (other than NMR) for determining functionality. In: Aiken, G., MCknight, D., Wershaw, R., MacCarthy, P. (Eds.). *Humic Substances in Soil, Sediment, and Water: Geochemistry, Isolation and Characterization*, John Wiley and Sons, New York, NY, pp. 527-559.

Madejová, J. 2003. FTIR techniques in clay mineral studies. *Vibrational Spectroscopy* 31, 1–10.

Madejová, J., P. Komadel. 2001. Baseline studies of the clay minerals society source clays: infrared methods. *Clays and Clay Minerals* 49, 410–432.

Mannino, A. and H. R. Harvey. 2000a. Biochemical composition of particles and dissolved organic matter along an estuarine gradient: Sources and implications for DOM reactivity. *Limnol. Oceanogr*. 45, 775-788.

Mannino, A. and H.R. Harvey. 2000b. Terrigenous dissolved organic matter along an estuarine gradient and its flux to the coastal ocean. *Organic Geochemistry*. 31, 1611-1625.

Mantoura, R.F.C. and E.M.S. Woodward. 1993. Conservative behavior of riverine dissolved organic carbon in the Severn Estuary: chemical and geochemical implications. *Geochimica et Cosmochimica Acta*. 47, 1293-1309.

Mascarenhas, J.D., G.A. Arbuckle. 2000. Characterization of plant carbohydrates and changes in leaf carbohydrate chemistry due to chemical and enzymatic degradation measured by microscopic ATR FTIR spectroscopy. *Society for Applied Spectroscopy* 54, 681- 686.

Masiello, C.A. and E.R.M. Druffel. 2001. Carbon isotope geochemistry of the Santa Clara River. *Global Biogeochem. Cycles.* 15, 407-416.

Matheson, D.H., M. Munawar. 1978. Lake Superior basin and its development. *Jounal of Great Lakes Research* 4, 249-263.

Mayzaud, P., J.P. Chanut, and R.G. Ackman. 1989. Seasonal changes in the biochemical composition of marine particulate matter with special reference to fatty acids and sterols. *Mar. Ecol. Prog. Ser.* 56, 189-204.

Mead, R.N., K.M.Mullaugh, G.Brooks Avery, R.J.Kieber, J.D.Willey, D.C. Podgorski .2013. Insights into dissolved organic matter complexity in rainwater from continental and coastal storms by ultrahigh resolution Fourier transform ion cyclotron resonance mass spectrometry. *Atmos. Chem. Phys.* 13, 4829–4838.

McManus, J., E.A. Heinen, M.M. Baehr. 2003. Hypolimnetic oxidation rates in Lake Superior: role of dissolved organic material on the lake's carbon budget. *Limnol. Oceanogr.* 48, 1624-1632.

Mecozzi, M., F. Moscato, M. Pietroletti , F. Quarto, F. Oteri, and A.M. Cicero. 2009a. Applications of FTIR spectroscopy in environmental studies supported by two dimensional analysis. *Global NEST Journal*. 11, 593-600.

Mecozzi M. and E. Pietrantonio. 2006. Carbohydrates proteins and lipids in fulvic and humic acids of sediments and its relationships with mucilaginous aggregates in the Italian seas. *Mar. Chem.* 101, 27-39.

Mecozzi M., E. Pietrantonio, and M. Pietroletti. 2009b. The roles of carbohydrates, proteins and lipids in the process of aggregation of natural marine organic matter investigated by means of 2D correlation spectroscopy applied to infrared spectra. *Spectrochimica Acta Part A.* 71, 1877-1884.

Mengerink, Y. , D. Kutlán , F. Tóth, A. Csámpai, I. Molnár-Perl. 2002. Advances in the evaluation of the stability and characteristics of the amino acid and amine derivatives obtained with the o-phthaldialdehyde / 3-mercaptopropionic acid and o-phthaldialdehyde /N-acetyl-L-cysteine reagents High-performance liquid chromatography–mass spectrometry study. *Journal of Chromatography* A. 949, 99-124.

Meyers P.A. and B.J Eadie. 1993. Sources, degradation and recycling of organic matter associated with sinking particles in Lake Michigan. *Org. Geochem.* 20, 47-56.

Meyers P.A. and R. Ishiwatari. 1993. Lacustrine organic geochemistry-an overview of

indicator of organic matter sources and diagenesis in lake sediments. *Org. Geochem.* 20, 867-900.

Meyers P.A., M.J. Leenheer, and R.A. Bourbonniere. 1995. Diagenesis of Vascular Plant Organic Matter Components during Burial in Lake Sediments. *Aquatic Geochemistry.* 1, 35-52.

Minor, E.C., J.J. Boon, H.R. Harvey, and A. Mannino. 2001. Estuarine organic matter composition as probed by direct temperature-resolved mass spectrometry and traditional geochemical techniques. *Geochimica et Cosmochimica Acta*. 65, 2819-2834.

Minor, E.C., T.I. Eglinton, J.J. Boon, R. Olson. 1999. A protocol for the characterization of oceanic particles via flow cytometric sorting and direct temperature-resolved mass spectrometry. *Anal. Chem.* 71, 2003-2013.

Minor, E.C., Steinbring, C.J., Longnecker, K., Kujawinski, E.B. (2012) Characterization of dissolved organic matter in Lake Superior and its watershed using ultrahigh resolution mass spectrometry. *Org. Geochem.* 43,1–11.

Minor E.C. and P.S. Nallathamby. 2004. Cellular vs. detrital POM: a preliminary study using fluorescent stains, flow cytometry, and mass spectrometry. *Mar. Chem.* 92, 9-21

Minor E.C. and B. Stephens. 2008. Dissolved organic matter characteristics within the Lake Superior watershed. *Organic Geochemistry 39, 1489*-1501.

Mopper, K., A. Stubbins, J.D. Ritchie, H.M. Bialk, P. G. Hatcher. 2007. Advanced Instrumental Approaches for Characterization of Marine Dissolved Organic Matter:

Extraction Techniques, Mass Spectrometry, and Nuclear Magnetic Resonance Spectroscopy. *Chem. Rev*. 107, 419-442.

Moreira-Turcq P.F. and J.M Martin. 1998. Characterization of fine particles by flow cytometry in estuarine and coastal Arctic waters. *Journal of Sea Research*. 39, 217-226.

Murphy E.M., S.N. Davis, A. Long, D. Donahu, and A.J. Jull. 1989. Characterization and isotopic com- position of organic and inorganic carbon in the Milk River Aquifer. *Water Resources Research*. 25, 1893-1905.

Navarro, J.M., R.J. Thompson, 1995. Seasonal fluctuations in size spectra, biochemical composition and nutritive value of the seston available to suspension feeding bivalve in a subartic environment. *Mar. Ecol. Prog. Ser.* 125, 95–106

Nebbioso A, A. Piccolo. 2013. Molecular characterization of dissolved organic matter (DOM): a critical review. *Anal. Bioanal. Chem.* 405(1),109-24.

Noda, I. 1993. Generalized two-dimensional correlation method applicable to infrared, Raman, and other types of spectroscopy. *Appl. Spectrosc*. 47, 1329-1336.

Noda I. and Y. Ozaki. 2004. *Two-Dimensional Correlation Spectroscopy: Applications in Vibrational and Optical Spectroscopy*. John Wiley And Sons Ltd (United States).

Orem, W.H., W.C. Burnett, W.M. Landing, W.B. Lyons, W. Shower. 1991. Jellyfish Lake, Palau: Early diagenesis of organic matter in sediments of an anoxic marine lake. *Limnology and Oceanography* 36, 526-543.

Ostrom N.E, D.T. Long, E.M. Bell, and T. Beals. 1998. The origin and cycling of particulate and sedimentary organic matter and nitrate in Lake Superior. *Chemical Geology*. 152, 13-28.

Pakulski J.D., R. Benner. 1992. An improved method for the hydrolysis and MBTH analysis of dissolved and particulate carbohydrates in seawater. *Marine Chemistry*, 40, 143-160

Pandurangi, R.S., M.S. Seehra, B.L. Razzaboni and P. Bolsaitist. 1990. Surface and Bulk Infrared Modes of Crystalline and Amorphous Silica Particles: A Study of the Relation of Surface Structure to Cytotoxicity of Respirable Silica. *Environmental Health Perspectives*, 86, 327-336.

Pedersen T.F. and S.E. Calvert. 1990. Anoxia vs. productivity: what controls the formation of organic-carbon rich sediments and sedimentary rocks? *Am Assoc Petrol Geol Bull.* 74, 454-66.

Peuravuori, J., Pihlaja, K. 1997.Molecular size distribution and spectroscopic properties of aquatic humic substances. *Anal. Chim. Acta* 337, 133-149.

Plante, C.J. and Jumars P.A. 1992. The microbial environment of marine deposit-feeder guts characterized via microelectrodes. *Microb. Ecol.* 23, 257-277.

Plante, C.J. and A.G. Shriver. 1998. Patterns of differential digestion of bacteria in deposit feeders: A test of resource partitioning. *Mar. Ecol. Prog. Ser.* 163, 253-258.

Popescu C., M. Popescu, and C. Vasile. 2010. Characterization of fungal degraded lime wood by FT-IR and 2D IR correlation spectroscopy. *Microchemical Journal*. 95,

377-387

Putschew A., B.M. Scholz-bottcher, and J. Rullkotter. 1996. Early diagenesis of organic matter and related sulphur incorporation in surface sediments of meromictic Lake Cadagno in the Swiss Alps. *Org. Geochem.* 25, 379-390.

Raiskila, S., M. Pulkkinen, T. Laakso, K. Fagerstedt, M. Löija, R. Mahlberg, L. Paajanen, A.-C. Ritschkoff, P. Saranpää. 2007. FTIR spectroscopic prediction of Klason and acid soluble lignin variation in Norway spruce cutting clones. *Silva Fennica* 41, 351-371.

Raimbault, P., N. Garcia, and F. Cerutti. 2008. Distribution of inorganic and organic nutrients in the South Pacific Ocean-evidence for long term accumulation of organic matter in nitrogen depleted waters. *Biogeosciences*. 5, 281-298.

Ramachandran, V.S., J.J. Beaudoin. 2008. *Handbook of Analytical Techniques in Concrete Science and Technology: Principles, Techniques and Applications*. Noyes Publications / William Andrew Publishing, LLC, Norwich, New York, United States.

Raymond, P. A. and J. E. Bauer. 2001. Riverine export of aged terrestrial organic matter to the North Atlantic Ocean. *Nature*. 409, 497-500.

Reeves, A.D. and M.R. Preston. 1989. The composition of lignin in estuarine suspended particulates and the distribution of particulate lignin in estuaries as determined by capillary gas chromatography of cupric oxide oxidation products. *Estuarine Coastal Shelf Sci.*. 29, 583-599.

Repeta D.J., T.M. Quan, L.I. Aluwihare, and A. Accardi. 2002. Chemical

characterization of high molecular weight dissolved organic matter in fresh and marine waters. *Geochim. Cosmochim. Acta*. 66, 955-962.

Saino, T. and A. Hattori. 1980. ^{15}N abundance in oceanic suspended particulate matter. Nature, 283, 752–754.

Sanni, O.D., M.S. Wagner, D. Briggs, D.G. Castner, J.C. Vickerman. 2002. Classification of adsorbed protein static ToF-SIMS spectra by principal component analysis and neural networks. *Surface and Interface Analysis* 33, 715-728.

Schmidt, M., R. Bozt, D. Rickert, G. Bohrmann, S.R. Hall, S. Mann. 2001. Oxygen isotopes of marine diatoms and relations to opal-A maturation. *Geochimica et Cosmochimica Acta* 65, 201-211.

Schmidt, F., M. Elvert, B.P.Koch, M.Witt, K. Hinrichs. 2009. Molecular characterization of dissolved organic matter in pore water of continental shelf sediments. *Geochim. Cosmochim. Acta* 73, 3337–3358.

Schimmelmann, A., M.D. Lewan, and R.P. Wintsch. 1999. D/H isotope ratios of kerogen, bitumen, oil, and water in hydrous pyrolysis of source rocks containing kerogen types I, II, and III. *Geochimica et Cosmochimica Acta*. 63, 3751-3766.

Sholkovitz E.R. and D. Copland. 1981. The coagulation, solubility and adsorption properties of Fe, Mn, Cu, Ni, Cd, Co and humic acids in a river wate. *Geochimica et Cosmochimica Acta*.45, 181-189.

Silverstein R.M. and F.X. Webster. 1996. *Spectrometric identification of organic compounds*. John Wiley & Sons, Inc.

Simjouw, J. P., E. C. Minor, K. Mopper. 2005. Isolation and characterization of estuarine dissolved organic matter: Comparison of ultrafiltration and C-18 solid-phase extraction techniques. *Mar. Chem.* 96, 219-235.

Sleighter, R. L. and P.G. Hatcher. 2008. Molecular characterization of dissolved organic matter (DOM) along a river to ocean transect of the lower Chesapeake Bay by ultrahigh resolution electrospray ionization Fourier transform ion cyclotron resonance mass spectrometry. *Mar. Chem.* 110, 140-152.

Smith B.C. 1996. *Fundamentals of Fourier Transform Infrared Spectroscopy*, CRC Press, Boca Raton, Florida.

Smith B. C. 1999. *Infrared Spectral Interpretation: A Systematic Approach*. CRC Press, Boca Raton, Florida.

Stedmon, C.A., S.Markager, H. Kaas. 2000. Optical properties and signatures of chromophoric dissolved organic matter (CDOM) in Danish coastal waters. *Estuar. Coast. Shelf Sci.* 51, 267–278.

Steinbring C. J. 2010, M.S. Thesis. *High-resolution electrospray ionization mass spectrometry for molecular level characterization of dissolved natural organic matter in the Lake Superior watershed*. University of Minnesota.

Stenson, A.C., W.M.Landing, A.G.Marshall,W.T. Cooper. 2002. Ionization and fragmentation of humic substances in electrospray ionization Fourier transform ion cyclotron resonance mass spectrometry. *Analyt. Chem.* 74, 4397-4409.

Sterner, R.W., T.M. Smutka, R.M.L. McKay, X. Qin, E. T. Brown, and R.M. Sherrell. 2004. Phosphorus and trace metal limitation of algae and bacteria in Lake Superior. *Limnology and Oceanography*. 49, 495-507.

Sterner, R.W. 2010.In situ-measured primary production in Lake Superior. Journal of Great Lakes Research. 36, 139-149.

Sterner, R.W. 2011. C:N:P stoichiometry in Lake Superior: freshwater sea as end member. *Inland Waters*, 1,29-46

Strand, M. 2005. Trophic ecology of the Lake Superior wave zone: a stable isotope approach. *Hydrobiologia*. 544, 271-278.

Stephens, B.M. and E.C. Minor. 2010. DOM characteristics along the continuum from river to receiving basin: a comparison of freshwater and marine transects. *Aquatic Sciences*: doi: 10.1007/s00027-010-0144-9.

Stuiver, M., H.A. Polach. 1977. Discussion: reporting of ^{14}C data. *Radiocarbon* 19, 355–363.

Sweeney R. E. and I.R. Kaplan. 1980. Natural abundances of ^{15}N as a source indicator for near shore marine sedimentary and dissolved nitrogen. *Mar. Chem.* 9, 81-94.

Talbot M. R. and T. Laerdal. 2001. The late Pleistocene-Holocene palaeolimnology of Lake Victoria East Africa based upon elemental and isotopic analyses of sedimentary organic matter. *J Paleolimnol*. 23, 141-64.

Thunell R.C., D.M. Sigman, F. Muller-Karger, Y. Astor, and R. Varela. 2004. Nitrogen

isotope dynamics of the Cariaco Basin, Venezuela. *Global Biogeochemical Cycles* 18, GB3001, doi: 10.1029/ 2003GB002185.

Thurman, E.M., and R.L. Malcolm. 1981. Preparative isolation of aquatic humic substances. E*nvironmental Science and Technology* 15(4): 463-466.

Urban, N.R., X. Lu, Y. Chai, D.S. Apul. 2004. Sediment trap studies in Lake Superior: Insights into resuspension, cross-margin transport, and carbon cycling. *Jounal of Great Lakes Research* 30, 147-161.

Urban, N.R., M.T. Auer, S.A. Green, X. Lu, D.S. Apul, K.D. Powell, L. Bub. 2005. Carbon cycling in Lake Superior. *Journal of Geophysical Research* 110, C06S90, doi:10.1029/2003JC002230.

Vanderpost, J. M. 1972. Bacterial and physical characteristics of Lake Ontario sediment during several months. *Proceedings 15th Conference of Great Lakes Research* 198-213.

Vander Zanden, M.J., and J.B. Rasmussen. 2001. Variation in $\delta^{15}N$ and $\delta^{13}C$ trophic fractionation: Implications for aquatic food web studies. *Limnol. Oceanogr.* 46. 2061-2066.

Vetter, T. A., E. M. Perdue, E. Ingall, J.-F. Koprivnjak, and P.H.Pfromm. 2007. Combining reverse osmosis and electrodialysis for more complete recovery of dissolved organic matter from seawater. *Sep. Purif. Technol*. 56:383–387.

Voß M. and U. Struck. 1997. Stable nitrogen and carbon isotopes as indicator of

eutrophication of the Oder River (Baltic Sea). *Mar. Chem.* 59, 35-49.

Vogel, H., P. Rosen, B. Wagner, M. Melles, P. Persson. 2008. Fourier transform infrared spectroscopy, a new cost-effective tool for quantitative analysis of biogeochemical properties in long sediment records. *J. Paleolimnol.* 40, 698-702.

Wakeham, S.G., C. Lee, J.I. Hedges, P.J. Hernes, and M.L. Peterson. 1997. Fate of major biochemicals in water column particles and sediments of the central Equatorial Pacific Ocean. *Geochimica et Cosmochimica Acta*. 61, 5363-5369.

Warnken, K.W., W. Davison, H. Zhang, J. Galceran, and J. Puy. 2007. In situ measurements of metal complex exchange kinetics in freshwater. *Environ. Sci. Technol*. 41(9): 3179-3185.

Weishaar J.L., G.R.Aiken, B.A.Bergamaschi, M.S.Fram, R.Fujii, K. Mopper. 2003. Evaluation of Specific Ultraviolet Absorbance as an Indicator of the Chemical Composition and Reactivity of Dissolved Organic Carbon. *Environ. Sci. Technol.* 37, 4702-4708.

Wetzel, R.G. 2001. *Limnology: Lake and River Ecosystems,* third edition. Academic Press, San Diego.

Whittle, K.J. 1977. Marine organisms and their contribution to organic matter in the ocean. *Mar. Chem.* 5, 381-411.

Widjanarko S.B., A. Nugroho and T. Estiasih. 2011. Functional interaction components of protein isolates and glucomannan in food bars by FTIR and SEM studies. *African Journal of Food Science* 5, 12-21.

Williams, P.J., B. Le. 2000. Heterotrophic Bacteria and the dynamics of dissolved organic material, p. 153-200. In D.L. Kirchman [ed.] Microbial ecology of the oceans. New York (NY): Wiley-Liss, Inc.

Williams, P.M. and E.R.M. Druffel. 1987. Radiocarbon in dissolved organic matter in the central North Pacific Ocean. *Nature*. 330, 246-248.

Williams, P.M. and L.I. Gordon. 1970. Carbon-13: Carbon-12 ratios in dissolved and particulate organic matter in the sea. *Deep-Sea Research*. 17, 19-27.

Woltering, M, J.P. Werne, J.L. Kish, R.Hicks, J.S. Sinninghe Damste´,S. Schouten. 2012. Vertical and temporal variability in concentration and distribution of thaumarchaeotal tetraether lipids in Lake Superior and the implications for the application of the TEX86 temperature proxy. *Geochimica et Cosmochimica Acta* 87, 136-153.

Wu, Z., R.P. Rodgers, and A.G. Marshall. 2004.Two- and Three-Dimensional van Krevelen Diagrams: A Graphical Analysis Complementary to the Kendrick Mass Plot for Sorting Elemental Compositions of Complex Organic Mixtures Based on Ultrahigh-Resolution Broadband Fourier Transform Ion Cyclotron Resonance Mass Measurements. *Anal. Chem.* 76, 2511-2516.

Yang D., D. Castro, I. EI-Sayed, M. EI-Sayed, R. Saxon and Y. Nancy. 1995. A Fouriertransform infrared spectroscopic comparison of cultured human fibroblast and fibrosarcoma cells. *SPIE* 2389, 543-550.

Zigah P.K., E.C. Minor, J.P. Werne, and S.L. McCallister. 2011. Radiocarbon and

stable carbon isotopic insights into provenance and cycling of carbon in Lake Superior. *Limnol. Oceanogr.*, 56(3), 867-886.

Zigah, P.K., E.C. Minor, J.P. Werne and S.L. McCallister. 2012. An isotopic ($\Delta^{14}C$, $\delta^{13}C$, and $\delta^{15}N$) investigation of particulate organic matter and zooplankton biomass in Lake Superior and across a size-gradient of aquatic systems. *Biogeosciences Discuss.* 9, 4399-4439.

Zigah, P. K., E. C.Minor, J.P. Werne. 2012. Radiocarbon and stable-isotope geochemistry of organic and inorganic carbon in Lake Superior. *Global Biogeochem. Cycles* doi:10.1029/2011GB004132.

Zigah, P.K. 2012. Thesis. Sources, biogeochemical cycling, and fate of organic matter in Lake Superior: an investigation using natural abundance radiocarbon and stable isotopes. University of Minnesota.

Zigah, P.K., E.C. Minor, H.A.N. Abdulla, J.P. Werne, P.G. Hatcher.2014.An investigation of size-fractionated organic matter from Lake Superior and a tributary stream using radiocarbon, stable isotopes and NMR. *Geochimica et Cosmochimica Acta*. 127: 264-284.

Appendix

Appendix. Table 2-1 The calibrants used for the peak calibration.

Compound	Formular mass	Compound	Formular mass
$C_{13}H_{19}O_4$	239.1289	$C_{27}H_{25}O_{14}$	573.125
$C_{16}H_{23}O_4$	279.1602	$C_{27}H_{21}O_{16}$	601.0835
$C_{14}H_{13}O_8$	309.0616	$C_{29}H_{37}O_{14}$	609.2189
$C_{16}H_{19}O_8$	339.1085	$C_{28}H_{35}O_{15}$	611.1981
$C_{17}H_{21}O_9$	369.1191	$C_{30}H_{27}O_{16}$	643.1305
$C_{19}H_{23}O_{10}$	411.1297	$C_{31}H_{23}O_{16}$	650.0913
$C_{24}H_{33}O_8$	449.2181	$C_{34}H_{35}O_{16}$	699.1931
$C_{21}H_{25}O_{12}$	469.1352	$C_{33}H_{35}O_{18}$	719.1829
$C_{25}H_{33}O_{10}$	493.2079	$C_{35}H_{43}O_{18}$	751.2455
$C_{28}H_{41}O_8$	505.2807	$C_{46}H_{43}O_{17}$	877.3288
$C_{24}H_{29}O_{14}$	541.1563		

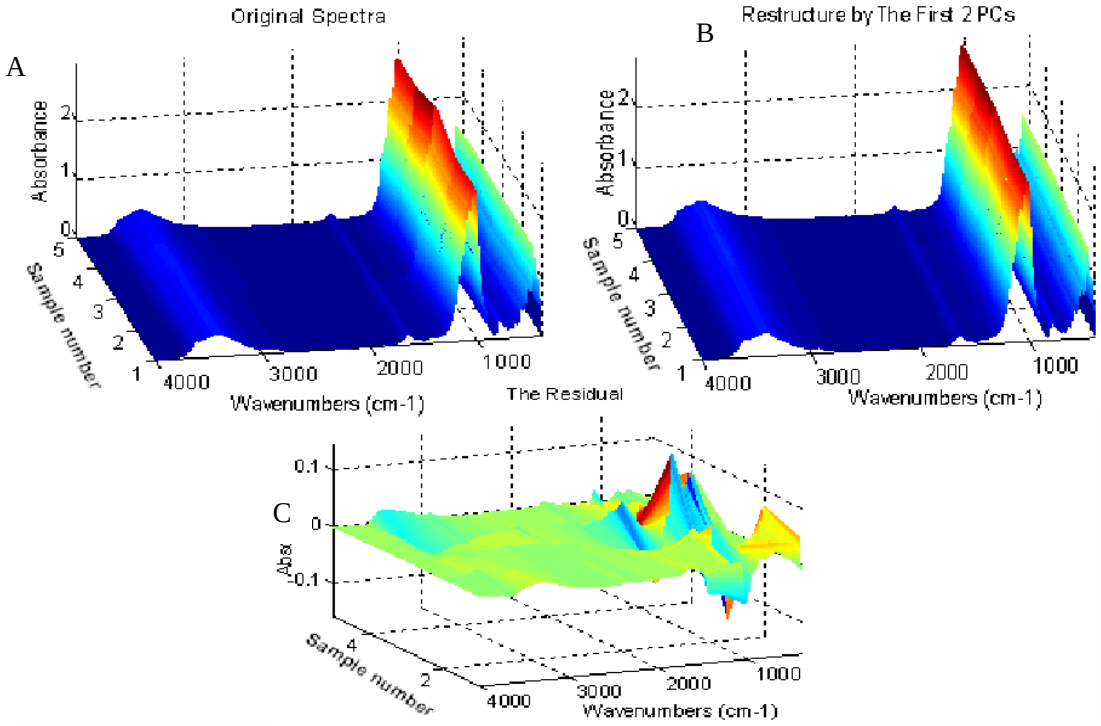

Appendix. Fig 4-1 A) Original spectral of the CM data set sorting from surface sediments to depth, B) PCA reconstruction with the first two principle components, C) the residual noise features. Note that the first 2 PCs retain the main features of the data set, while eliminating the noise shown in Appendix. Fig 4-1C.

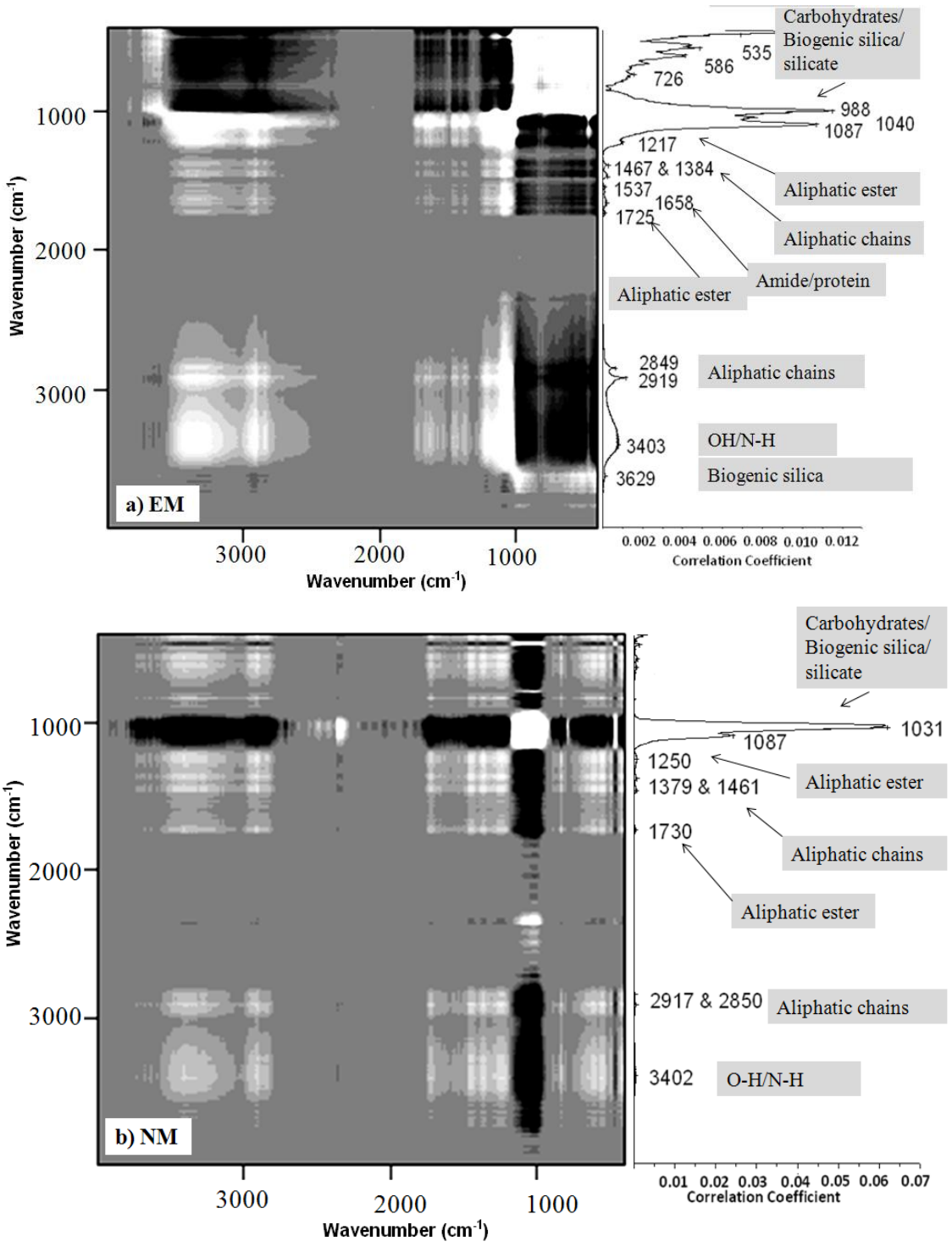
a) EM
Wavenumber (cm-1)
1000
2000
3000
3000
2000
1000
Wavenumber (cm-1)
Carbohydrates/
Biogenic silica/
silicate
535
586
726
988
1087
1040
1217
1467 & 1384
Aliphatic ester
1537
1658
1725
Aliphatic chains
Amide/protein
Aliphatic ester
2849
2919
Aliphatic chains
3403
OH/N-H
3629
Biogenic silica
0.002 0.004 0.006 0.008 0.010 0.012
Correlation Coefficient
b) NM
Wavenumber (cm-1)
1000
2000
3000
3000
2000
1000
Wavenumber (cm-1)
Carbohydrates/
Biogenic silica/
silicate
1031
1087
1250
Aliphatic ester
1379 & 1461
1730
Aliphatic chains
Aliphatic ester
2917 & 2850
Aliphatic chains
3402
O-H/N-H
0.01 0.02 0.03 0.04 0.05 0.06 0.07
Correlation Coefficient

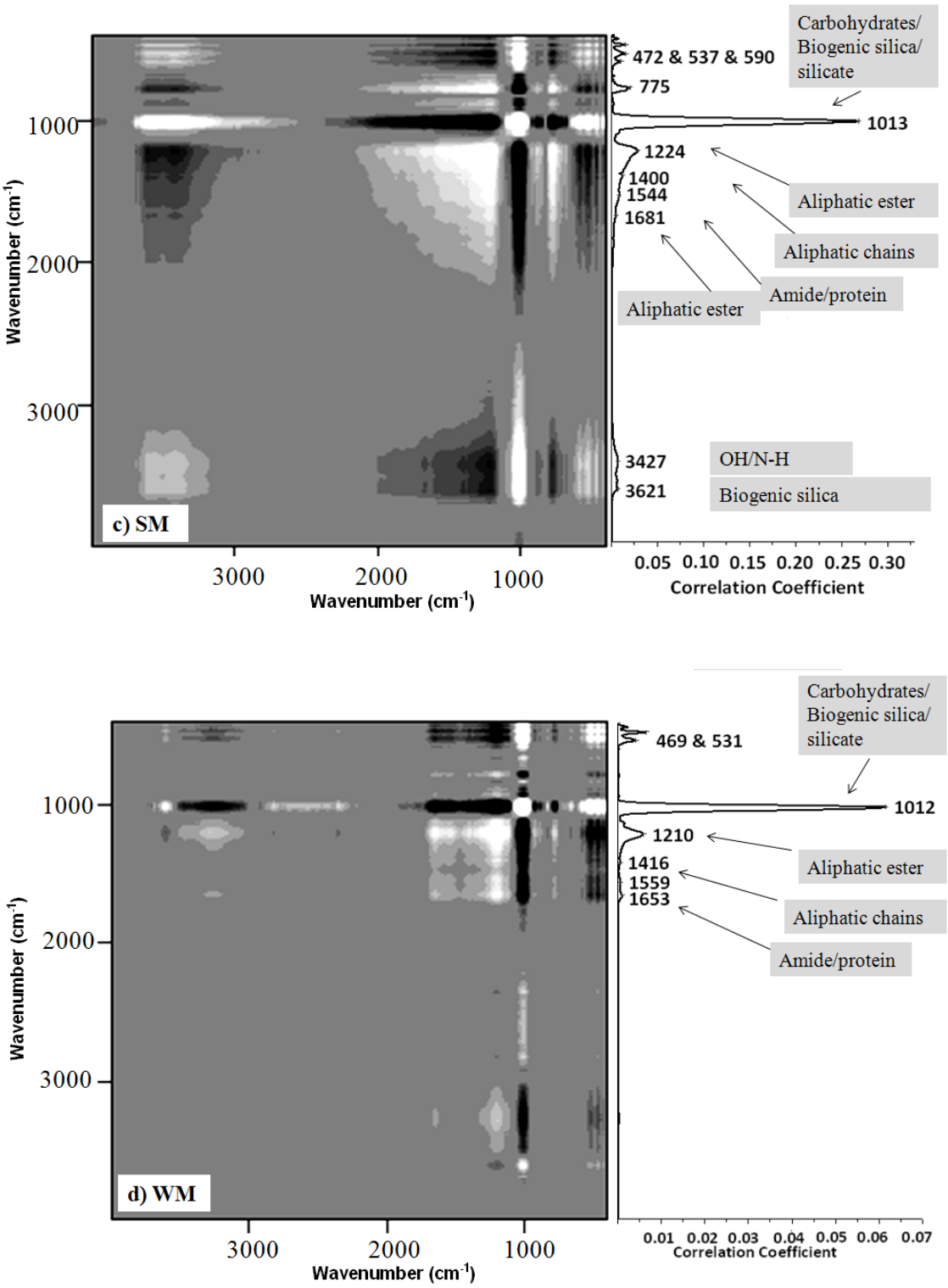

Appendix. Fig 4-2 The synchronous 2D correlation spectrum down-core for stations a) EM, b) NM, c) SM and d) WM. The spectral data set for each station was constructed sorting from the surface sediments to depth. The data set was normalized and PCA reconstructed before 2D correlation analysis (see text for further details). For ease in identification of peaks the slice through auto-peak diagonal is plotted to the right of each 2-D correlation spectrum. White indicates positive correlations; black indicates negative correlations.

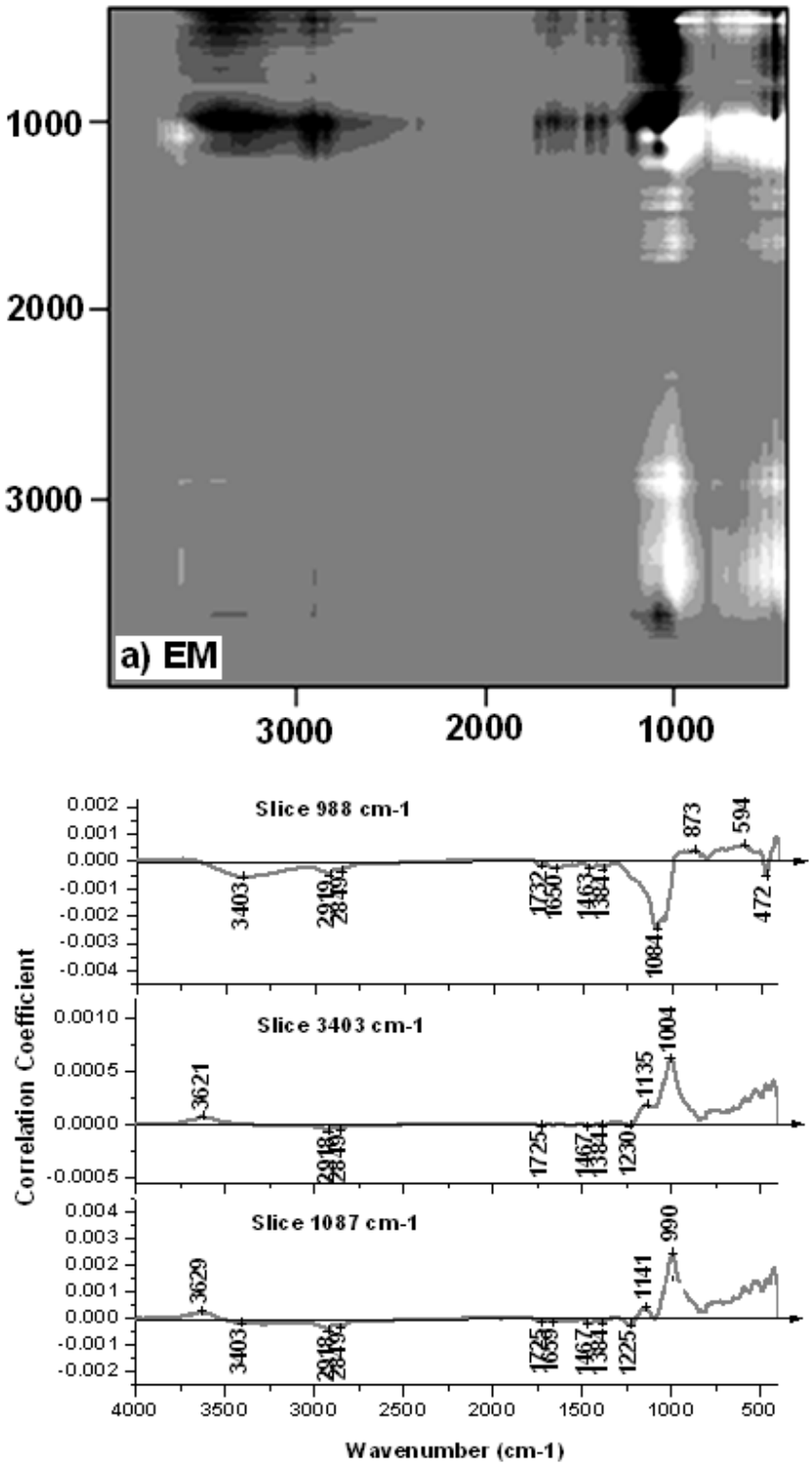
a) EM
1000
2000
3000
3000
2000
1000
Slice 988 cm-1
Slice 3403 cm-1
Slice 1087 cm-1
Correlation Coefficient
Wavenumber (cm-1)
4000
3500
3000
2500
2000
1500
1000
500

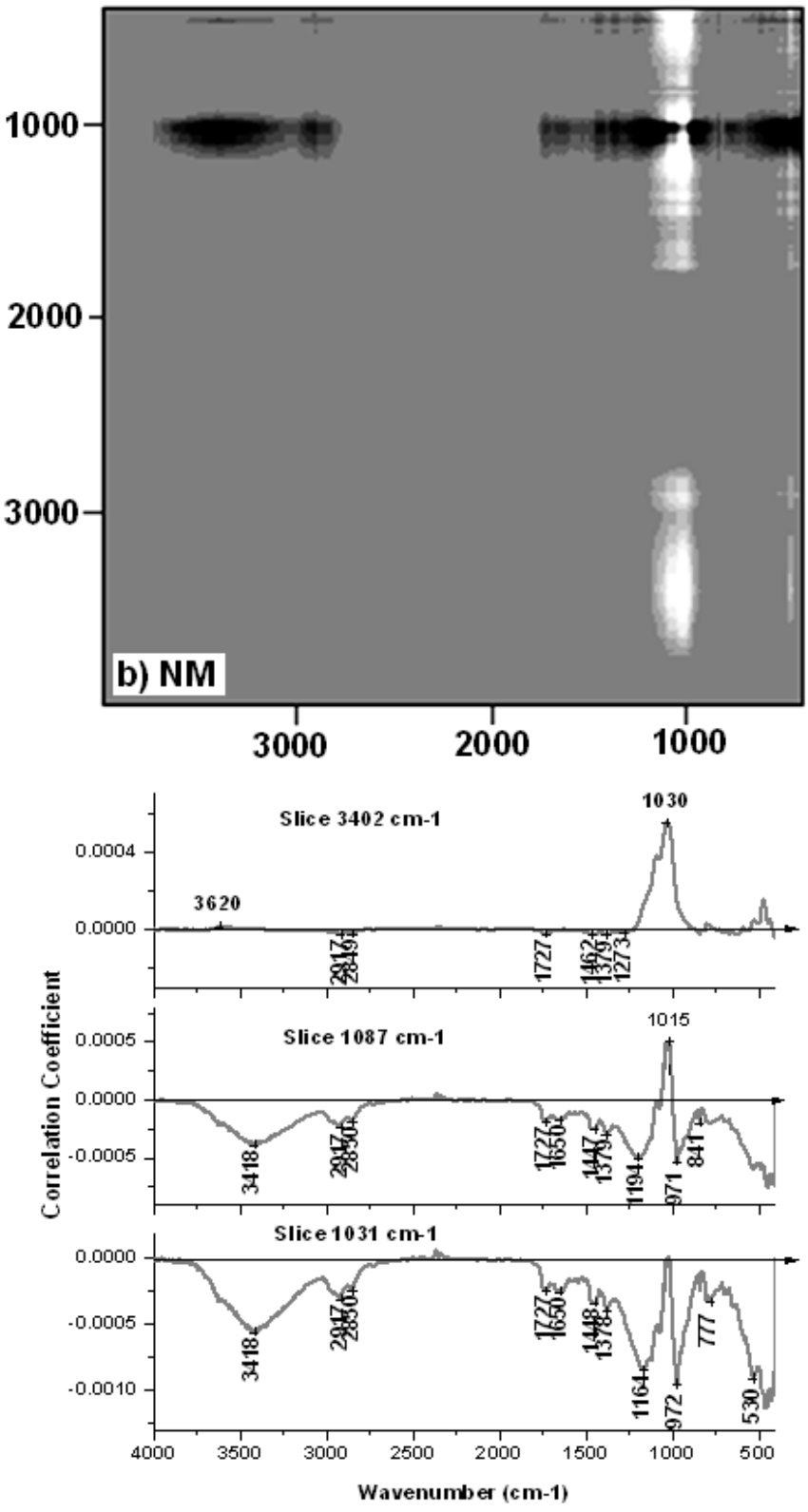
1000
2000
3000
b) NM
3000
2000
1000
Slice 3402 cm-1
1030
0.0004
0.0000
3620
2917
2849
1727
1462
1379
1273
Slice 1087 cm-1
1015
0.0005
0.0000
-0.0005
3418
2917
2850
1727
1650
1447
1379
1194
971
841
Slice 1031 cm-1
0.0000
-0.0005
-0.0010
3418
2917
2850
1727
1650
1448
1378
1164
972
777
530
Correlation Coefficient
4000
3500
3000
2500
2000
1500
1000
500
Wavenumber (cm-1)

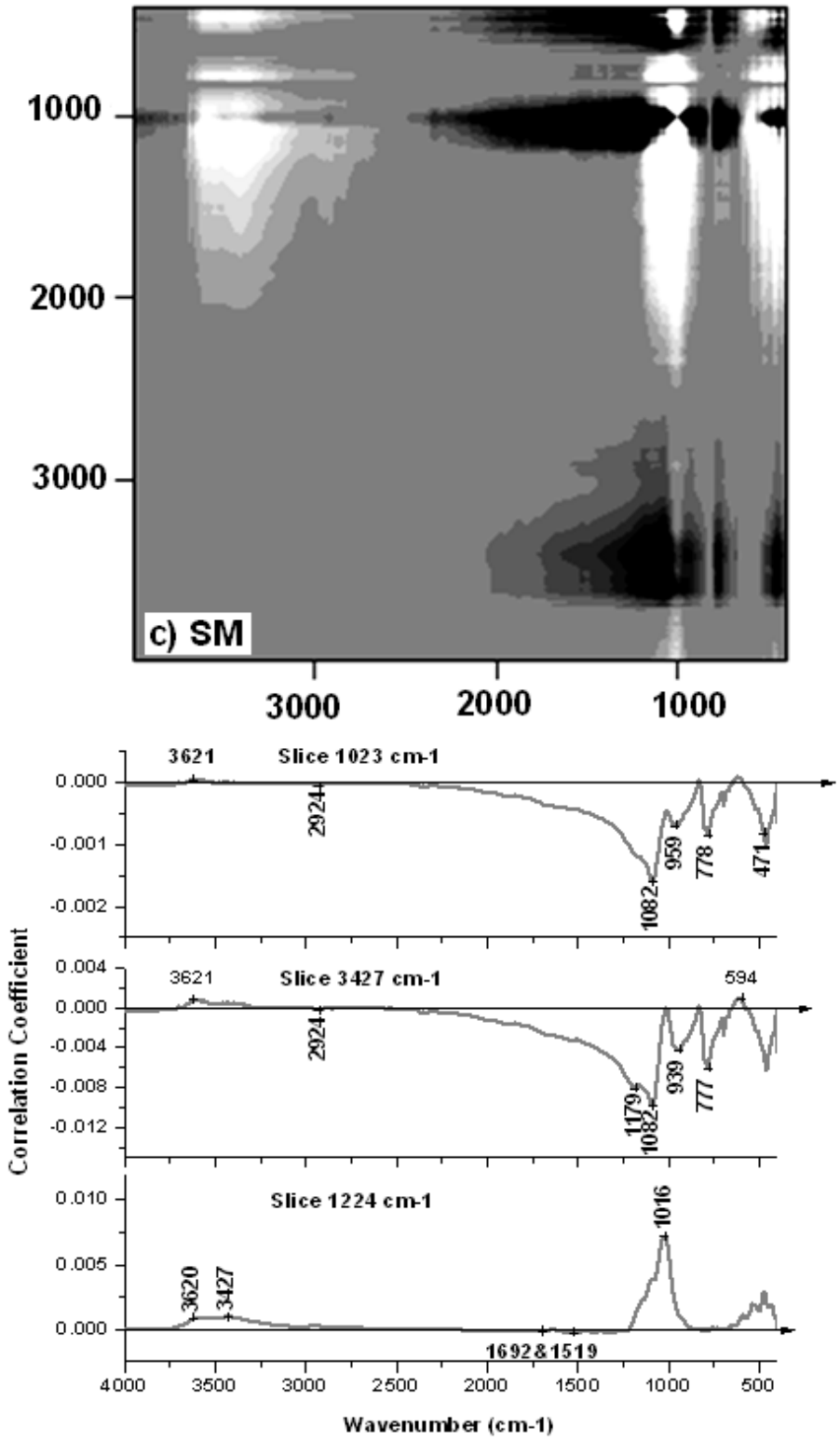

Appendix. Fig 4-3 The asynchronous 2D correlation spectrum for a) EM, b) NM and c) SM. The spectral data set of each station was constructed sorting from surface sediments to depth. The data set was normalized and PCA reconstructed before 2D correlation analysis. For ease in identification of peaks, the horizontal slices (v2 to be constant) across the region of interest are plotted bellow each 2-D correlation spectrum.

Appendix. 4-4 “Further information on asynchronous relationships and Noda’s rule as applied to diagenetic sequences”:

Diagenetic sequence at site CM:

Carboxyl groups (including aliphatic ester and amide/protein) > carbohydrates > aromatic compounds and the Si-O-Si framework in biogenic silica/silicate is based upon the following peaks (x, y); (592 cm^{-1}, 1092 cm^{-1}), (1012 cm^{-1}, 1092 cm^{-1}), (1212 cm^{-1},1092 cm^{-1}), (1537cm^{-1}, 1092 cm^{-1}) , (1665 cm^{-1}, 1092 cm^{-1}), (593cm^{-1}, 1193 cm^{-1}), (862cm^{-1}, 1193 cm^{-1}).

That O-H/N-H groups change before aliphatic ester, amide/protein and the carbohydrates indicated by 1092 cm^{-1} is based on cross-peaks at (3379 cm^{-1},1092 cm^{-1}), (1658 cm^{-1}, 3400 cm^{-1}), (1537 cm^{-1}, 3400 cm^{-1}) and (1193 cm^{-1}, 3400 cm^{-1}).

The Si-OH bond in biogenic silica also changes before the O-H/N-H bonds as revealed by peak (3633 cm^{-1}, 3400 cm^{-1}) and (3670 cm^{-1}, 1092 cm^{-1}).

Diagenetic sequence at site EM:

Preferential changes in all carbohydrate peaks before O-H/N-H groups and Si-OH bond are revealed by cross-peaks at (1004 cm^{-1}, 3403 cm^{-1}), (1135 cm^{-1}, 3403 cm^{-1}), (3621 cm^{-1}, 3403 cm^{-1}), and (3629 cm^{-1}, 1087 cm^{-1}).